Failure paths for levees

Final

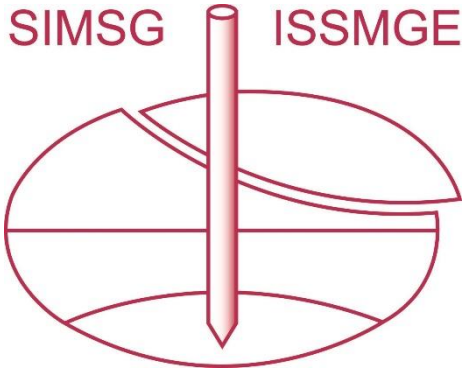

February 2022

PREPARED BY
Technical Committee on
Geotechnical Aspects of Dikes and Levees
(TC201)

Authors Part A and editors Part B and C:
Meindert Van (Deltares, The Netherlands)
Esther Rosenbrand (Deltares, The Netherlands)
Remy Tourment (INRAE, France)
Philip Smith (RoyalHaskoning DHV, United Kingdom)
Cor Zwanenburg (Deltares, The Netherlands)

Citation: Van, M.A., Rosenbrand, E., Tourment, R., Smith, P. and Zwanenburg, C. Failure paths for levees. International Society of Soil mechanics and Geotechnical Engineering (ISSMGE) – Technical Committee TC201 'Geotechnical aspects of dikes and levees', February 2022. Download (TC201 Dykes and Levees | ISSMGE)

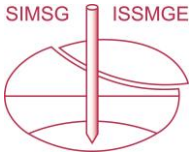
SIMSG
ISSMGE

Preface

On a yearly basis the international federation of Red Cross and Red Crescent Societies produces a world disasters report[1], which provides an overview of the impact of natural hazards on our lives. Each year, floods are the most occurring events. From this overview we learn that for example, in 2019 27% of the reported disasters were related to flooding, affecting 69 countries, killing 1586 people and displacing more than 10 million people[2]. In India alone 8 events in 2019 caused inundation of 1.2 million km^2. A historical overview, given in the world disasters report, shows a continuous increase in reported floods over time, with 151 floods reported in the period of 1960 to 1969, while between 2000 and 2009 1499 floods were observed. With the predicted sea level rise and increase in rain intensity due to climate change, it is to be expected that these numbers will continue to rise in the near future.

These numbers are impressive and show the importance of safety against flooding. An important observation in the world disasters report is that although the number of reported flood events is steadily increasing over the years, the number of people affected by floods is decreasing since 2000s. Although this might be attributed to various factors, the world disaster report concludes that increased investment in disaster reduction is one of those factors. A basic disaster reduction measure is found in building water retaining structures such as dikes and levees. At many places in the world impressive networks have been built over the years, while at other places building of such a network has just begun. An essential aspect in the designing dikes and levees is the understanding of the different failure mechanisms and how these mechanisms interact. However, a good understanding of failure mechanisms is also relevant for maintenance of existing structures and upgrading of existing structures to the latest understanding of design load conditions. Finally, a good understanding of failure mechanisms is relevant when transferring knowledge and experience from one location to another, where different load or sub soil conditions might be relevant.

Failure paths form an efficient way to depict the different ways a construction can fail, and how different failure mechanisms can interact and strengthen each other. Failure paths are powerful tools in explaining the events in case of a failed construction, or in assessing the safety of a design of a new dike or in assessing the safety of an existing structure under a change in loading conditions, for example due to climate change.

This report collects experiences of dike and levee failures, discusses different failed cases and summarises these experiences in failure paths that can generally be used in forensic engineering, design and maintenance of dikes and levees for different loading conditions, climate zones and engineering traditions. The inventory, which formed the basis of the report, showed that knowledge on the application of failure paths for water retaining structures was fragmentized and different definitions were used in different engineering traditions. To overcome these differences this report starts with a set of clear definitions. We hope that the definitions in this report will be followed in the engineering world and as such contribute to exchanging experiences without misunderstandings.

The report is a production of the International Society of Soil Mechanics and Geotechnical Engineering, Technical committee 201, Geotechnical Aspects of Dikes and Levees, ISSMGE-TC201. This TC brings together practitioners and academics in the field of dikes and levees around the world. With this report we hope to set a step forward in sharing our experiences and

[1] World Disasters Report 2020 | IFRC

[2] 2019-IDMC-GRID.pdf (internal-displacement.org)

knowledge and hope that application of the thoughts and ideas in this report may lead to new experiences, further development of the use of failure paths in dike design and finally assists in further reducing the number of people being affected by floods.

Cor Zwanenburg
Chair ISSMGE-TC201

Acknowlegdements

This report represents a collaborative effort to which members of the International Society of Soil Mechanics and Geotechnical Engineering, Technical committee 201, Geotechnical Aspects of Dikes and Levees and of the EWG-IE (ICOLD European Club Working Group on Internal Erosion of Dams, Dikes and Levees and their Foundations) contributed with case histories and examples of failure path analysis. The effort was coordinated by Meindert Van (Deltares), Esther Rosenbrand (Deltares), Remy Tourment (INRAE, France), Philip Smith (Royal Haskoning DHV), and Cor Zwanenburg (Deltares). They authored Part A of the report and reviewed and edited the contributions in Part B and Part C. Ligaya Wopereis (Deltares) played an important role in giving the report to its current appearance.

Contents

1 Introduction

1.1 Background and Aim

Flooding can occur when water passes over, through or beneath a flood retention structure. Typically, the most dangerous flooding is caused by a catastrophic breach as this can lead to an uncontrolled release of water through the flood defence under conditions of a high hydraulic load. The main objective of the design, assessment and maintenance of levees is usually to avoid a situation where breach and consequential flooding occurs. When a breach occurs, it has often been caused by a combination of events or a sequence of events (possibly over an extended period of time) which may have caused deterioration, damage and eventually failure of the structure. Such a sequence of events is called a failure path (or also a failure scenario or failure mode).

For the assessment (either performance assessment or risk assessment) or design of levees, a range of possible failure paths must be considered. Different mechanisms can be distinguished which contribute to the damage and deterioration of a levee, such as slope sliding, or internal erosion. The exceedance of the limit state for an individual mechanism often is not enough to result in flooding of the predicted area. For instance, a slope instability may occur, but if there is enough residual strength in the levee, additional mechanisms need to develop before flooding occurs. Failure paths allow for the consideration of this additional strength in the analyses of the levee.

Various institutions worldwide provide guidelines for working with failure paths (e.g., the International Levee Handbook, and the USBR best practice guidelines, and other examples in the (inter)national literature). The level of detail in the failure paths and the terminology varies among different countries, and among practitioners from different technical backgrounds. This can complicate the discourse.

In cases where a breach has occurred, a forensic analysis can be undertaken to determine the causes of the failure and to construct the failure path that led to the flooding. In those cases, it is not unusual for breaches to have been the result of a combination of mechanisms, which may have happened simultaneously, and which could also have affected each other. These interactions are complex and difficult to anticipate in design and assessment.

The aim of this report is to facilitate the international discourse on the application of failure path analysis and address the possible interactions among different mechanisms. The focus is on levees, although many effects may be similar for embankment dams. The failure paths considered are cases where the initiating event is a high-water load, and the final event is flooding of the protected area. Other initiating events may occur, such as earthquakes, but these are beyond the current scope.

1.2 Approach

The basis for this report is a compilation of case histories, and of failure paths used for assessment and design. These contributions were provided by members of the ISSMGE-TC201, ICOLD TC LE and the EWG-IE. The information was used to construct a framework in the form of a failure tree. This contains the mechanisms and failure paths from different contributions at a high level of abstraction and shows possible interactions among mechanisms.

By breaking down the chain of events that together cause flooding into discrete mechanisms that can be analysed, this approach is intended to facilitate the back analysis of the complex combination of events that causes flooding.

The use of the framework is illustrated by indicating the failure paths from the case histories in the tree. As site specific characteristics often play an important role, the important characteristics which affected the occurrence of the different mechanisms in the failure tree were compiled in a table.

1.3 Report structure

Part A provides an overview of the key concepts in this report and presents the proposed failure tree and overview of important aspects per event in the tree. The section finishes with a discussion and recommendations.

Part B contains the collection of the contributed failure paths for case studies, these failure paths are illustrated in the framework. Part C contains the collection of contributed failure paths that are used for assessment and design. A glossary of key terms used is added at the end of the report.

2 Part A: Overall failure tree key characteristics

2.1 Terminology and key concepts

Terminology relating to levee failures and failure mechanisms can differ amongst practitioners from different countries or from different fields of expertise. For instance, the term failure may be used to describe the 'inability to achieve a defined performance threshold for a given function, in particular for flood defence' in the International Levee Handbook (CIRIA, French Ministry of Ecology, and USACE 2013). However, it can also be used to describe the physical collapse or disintegration of a significant part of a structure. Therefore, the definition of key terms used in the report are included in the Glossary.

In this section we present the concepts of failure paths and the different failure mechanisms as they are used in this report.

In the context of this report, the initiating event is a high-water event. Other initiating events may occur in practice, for instance earthquake loading, however, this is outside of the scope of the report. The term failure is reserved for failure of the levee to retain water, resulting in flooding of the protected area. This differs from the exceedance of the limit state for a specific mechanism, which may indicate failure of a component of the levee whereas the levee itself still fulfils the function of retaining water.

A mechanism is a physical process (mechanical, chemical, hydraulic, geotechnical, etc.) that can lead to degradation, damage or collapse of (a part of) a structure. Often in the literature the name of a mechanism is used as synonymous to a failure path containing this mechanism, while in different contexts/countries the details of these paths can be quite different.

In this report, a failure path is considered as an entire sequence of events by which an initial event, the high-water loading, leads to flooding of the protected area. A failure path consists of a sequence of events and mechanisms as illustrated below:

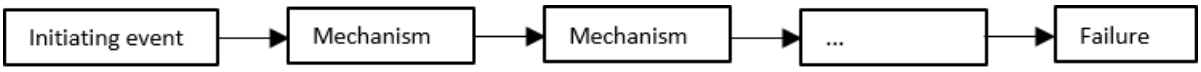

Figure 2.1 Illustration of a generic failure path consisting of an initiating event that causes a sequence of mechanisms to occur leading to failure.

Although the term failure path suggests a linear sequence of events, different mechanisms may occur simultaneously in time and influence each other. The term failure tree, which indicates the presence of branches, describes such situations. A failure tree may also be used to show different parallel failure paths which might or might not occur as illustrated below:

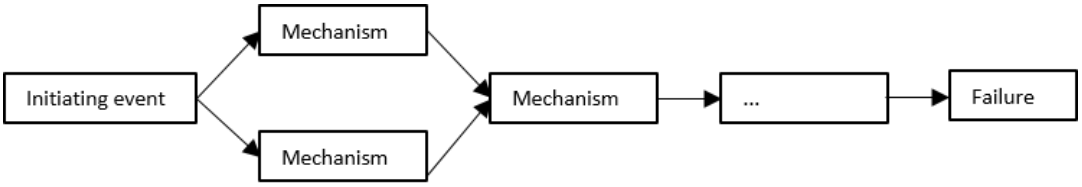

Figure 2.2 Illustration of a generic failure tree consisting of an initiating event that can cause individual events to occur in parallel.

The back analysis of a case of failure can result in insight in the failure path or scenario that led to the flooding. A failure tree may be used for design, in order to assess the different possible mechanisms and failure paths that can lead to the failure.

Event tree analysis and fault tree analysis are methods that are often encountered when considering failure paths. Event trees are typically used for design to identify possible failure paths, whereas fault tree analysis may typically be used as part of a back-analysis to establish how different mechanisms combined to trigger a failure. A brief summary of these methods, based on the ILH (CIRIA, French Ministry of Ecology, and USACE 2013), is provided below.

Event tree analysis starts from an initial event, to infer resulting mechanisms or scenarios that can lead to failure. This results in a tree built up of nodes, connected by branches, where the nodes represent the uncertain scenarios. The scenarios and contributing factors can be associated with a probability in order to compute a probability of failure. Expert analysis can be used to evaluate the scenarios.

Fault tree analysis starts from failure and conducts a back analysis to find the underlying causes. The aim is to identify the original causes that led to the event. Causes can be combined, through AND gates, or may be independent, OR gates. Fault trees consist of different levels that correspond to failure of a function or component, which can result from different causes.

In the international literature there is much knowledge on the individual mechanisms. Below is an overview of the mechanisms that are considered in this report. Note that some mechanisms can be further subdivided into a higher level of detail. For instance, external erosion on the water side can be subdivided into different mechanisms depending on the type of revetment. As the objective of the current report is to provide an overview on a high level of abstraction, those distinctions are not made here. When those mechanisms are relevant in the analysis, these will need to be considered in more detail.

Seepage or increase of pore water pressure in foundation or in embankment body
During long-lasting high-water events (flood, high tide), depending on the permeability of the material, an increase in pore water pressure causes seepage through the foundation and/or the embankment body, see Figure 2.3 (Tourment, et al., 2019).

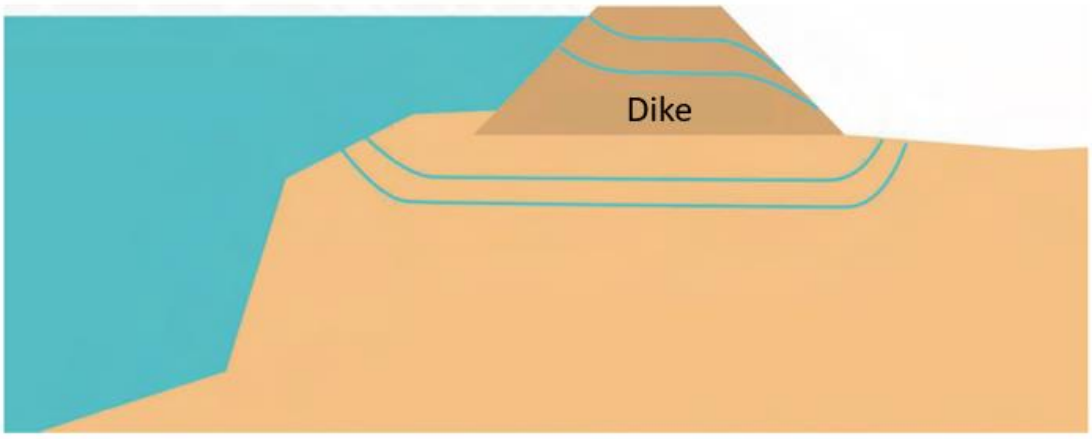

Figure 2.3 Seepage or increase of pore water pressure in foundation or in embankment body taken from (Tourment, et al., 2019).

External erosion water side

External erosion water side refers to erosion at the surface of a levee due to hydraulic loading on the water side slope of the levee (see Figure 2.4). The loading can refer to frontal or oblique external forces such as wave run-up (current), wave impact as well as to lateral forces such as the current of the river. Wind forces (depending on the surface material), aging of surface materials and/or localized turbulence can also play a role.

This mechanism is initiated when the load exceeds the resistance of the surface material (soil particles, grass, etc.) of the levee. The consequence is that erosion forms either a scour which undermines the foundation or embankment body and can, if it continues long enough, lead to collapse of the levee.

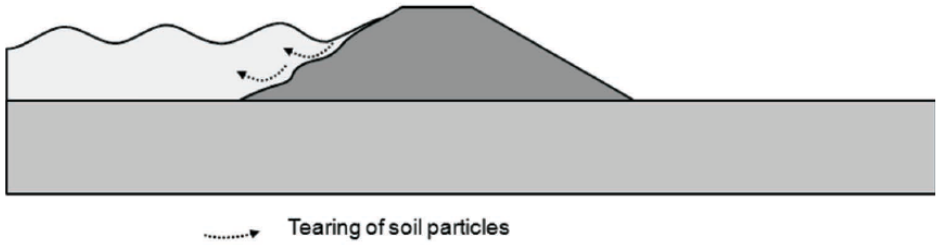

Figure 2.4 External erosion taken from the ILH (2013).

External erosion land side

External erosion land side refers to erosion at the surface of a levee due to hydraulic loading on the land side slope of the levee (Tourment, et al., 2019). The loading usually refers to discontinuous overtopping, see Figure 2.5a or the continuous overflow, see Figure 2.5b of water over the crest of the levee. Other external forces that can cause external erosion on the land side are for example: wind, precipitation, etc.

This mechanism is initiated when the load exceeds the resistance of the surface material (soil particles, grass, etc.) of the levee.

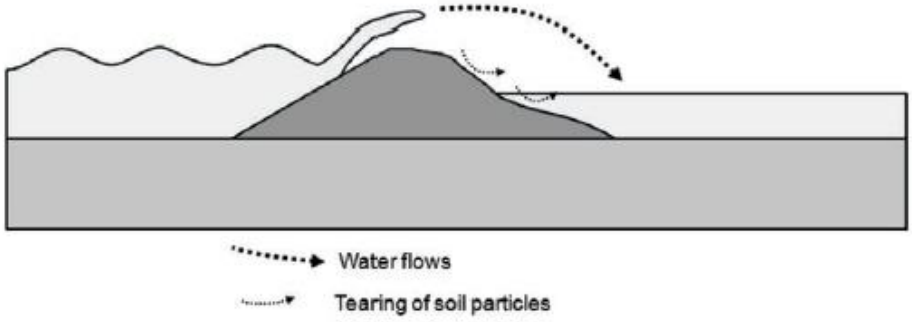

a)

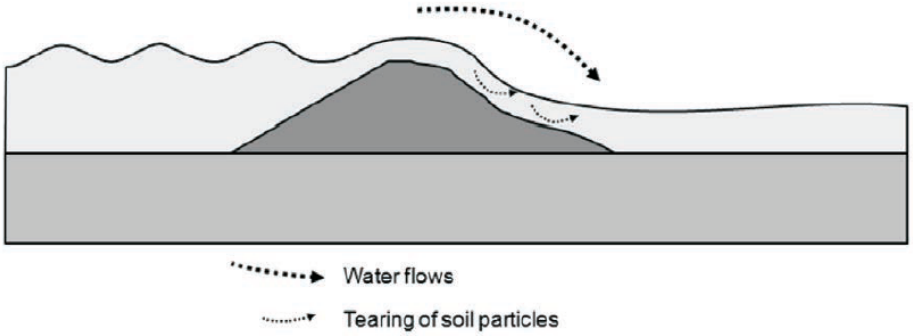

b)

Figure 2.5 External erosion land side taken from the ILH (2013). a) refers to overtopping and b) to overflow.

Internal erosion

Internal erosion occurs when soil particles within an embankment dam or its foundation, are carried downstream by seepage flow. Internal erosion can initiate by concentrated leak erosion, backward erosion, suffusion and soil contact erosion. This is according to the terminology of the ICOLD bulletin 164 (ICOLD, 2015).

1. Backward erosion

According to (ICOLD, 2015)*, backward erosion* involves the detachment of soils particles when the seepage exits to a free unfiltered surface, such as the ground surface downstream of a soil foundation or the downstream face of a homogeneous embankment or a coarse rock fill zone immediately downstream from the fine grained core. The detached particles are carried away by the seepage flow and the process gradually works its way towards the upstream side of the embankment or its foundation until a continuous pipe is formed.

There are two forms of backward erosion, “backward erosion piping” and “global backward erosion”:

1a. Backward erosion piping

In *backward erosion piping* in sandy soils the erosion pipe is essentially horizontal (Figure 2.6) and the roof of the pipe is formed by a cohesive soil layer.

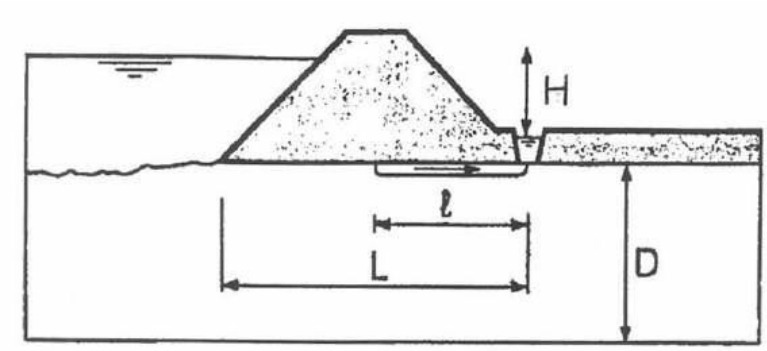

Figure 2.6 Pipe formation due to backward erosion piping taken from *(Koenders & Sellmeijer, 1992)*.

1b. Global backward erosion

Global backward erosion occurs in graded silty sand and gravel cores when short backward erosion pipes form but collapse successively resulting in widespread erosion.

2. Suffusion/suffosion

According to (ICOLD, 2015), *suffusion/suffosion* is a form of internal erosion of internally unstable soils which involves selective erosion of finer particles from the matrix of coarser particles, in such a manner that the finer particles are removed through the voids between the larger particles by seepage flow, leaving behind a soil skeleton formed by the coarser particles (Figure 2.7). The volume of finer particles is such that they fit within the voids formed by the coarser particles, that is the voids are under-filled.

The difference between suffusion and suffosion is explained in (Fannin, et al., 2015) as:

- *Suffusion* is characterized by a mass loss without a change in volume and with or without any change in general hydraulic conductivity but with a change in local hydraulic conductivity;
- *Suffosion* is characterized by a mass loss accompanied with a change in volume and a change in hydraulic conductivity.

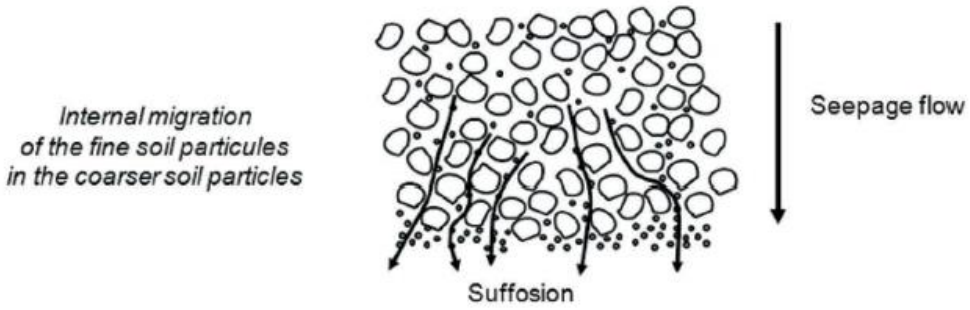

Figure 2.7 Suffosion/suffosion taken from the ILH (2013).

3. Contact erosion

According to (ICOLD, 2015), *contact erosion* (also known as parallel contact erosion)is a type of internal erosion which involves selective erosion of fine particles from the contact with a coarser layer, caused by the flow passing through the coarser layer. For instance, along the contact between silt and gravel sized particles. It relates only to conditions where the flow in the coarser layer is parallel to the interface between the coarse and fine layer (see Figure 2.8).

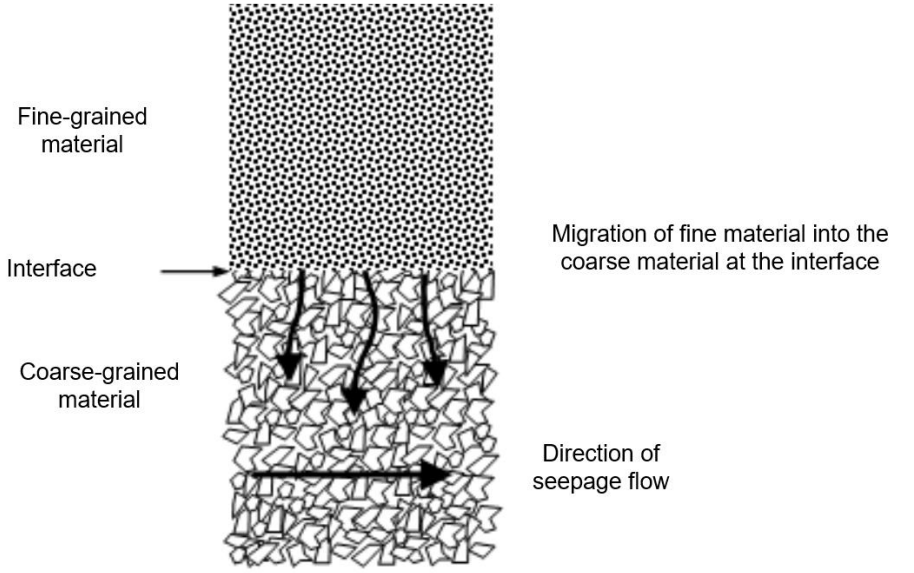

Figure 2.8 Contact erosion taken from (ICOLD, 2015).

4. Concentrated leak erosion

According to (ICOLD, 2015), *concentrated leak erosion* occurs where there is an opening, through which concentrated leakage occurs, the walls of the opening may be eroded by the leaking water (see Figure 2.9). Such concentrated leaks may occur through a crack caused by settlement or hydraulic fracture in a cohesive clay core for example, or through desiccation and tension cracks at high levels in the fill, or through cracks resulting from settlement of fill. In some circumstances, these openings may be sustained by the presence of structural elements such as spillways and pipes, or by the presence of cohesive materials able to 'hold a roof', as it is described, below which an opening is sustained, the periphery of which is eroded. It may occur in a continuous zone containing coarse and/or poorly compacted materials which form an interconnecting voids system. The concentration of flow causes erosion of the walls of the crack or interconnected voids.

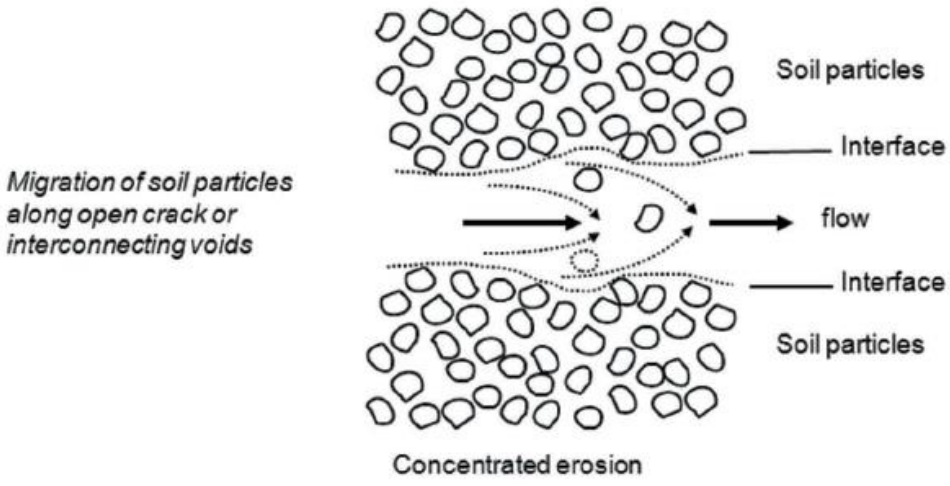

Figure 2.9 Concentrated erosion taken from the ILH (2013).

Uplift

Uplift occurs at the land side of a levee when constructed on alluvial flood plains with silty or clayey blankets, overlying sandy soil strata (Tournier, et al., 2015). The permeable sandy layer,

due to a hydraulic gradient, can cause pressure on the above less permeable layer. If the pressure head is equal or higher than the critical pressure head, uplift of the blanket layer occurs (see Figure 2.10).

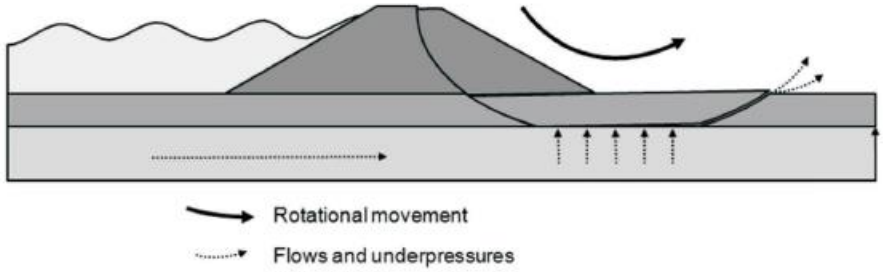

Figure 2.10 Rotational movement and uplift from the ILH (2013).

Cracking land side blanket layer
Cracking land side blanket layer occurs after uplift, see above (Tournier, et al., 2015) (Tourment, et al., 2019). A strong enough hydraulic gradient causes a crack in the blanket layer and a zero effective stress condition occurs at the top of the cohesionless soils at the land side of the levee.

Heave
Heave occurs in cohesionless soils which are confined by an overlying lower permeability stratum when seepage pore pressures are such that the effective stress becomes zero (pore pressure equals total stress) (Figure 2.11) (ICOLD, 2015). Heave may often be followed by backward erosion of the cohesionless soil if the seepage gradients remain high at the surface.

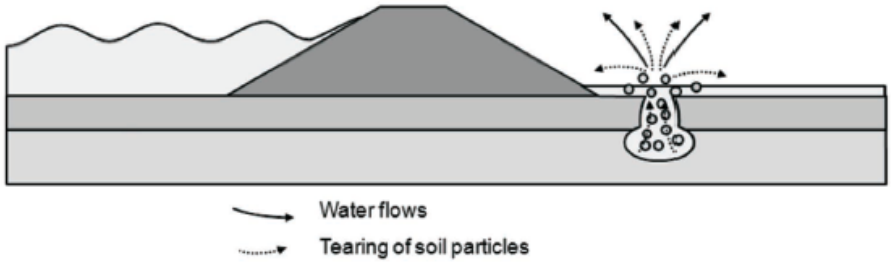

Figure 2.11 Heave taken from the ILH (2013).

Slope sliding
Slope sliding occurs when the driving loads applied on the levee (weight of the materials and/or hydraulic forces) exceed the shear strengths of the constituent materials of the embankment body and/or foundation (Tourment, et al., 2019). The unstable part of the levee then slides along the stable part. There are three types of sliding:

- Superficial sliding, see Figure 2.12;
- Rotational sliding, see Figure 2.10;
- Translational sliding, see Figure 2.13.

Sliding can occur both on the inner slope and on the outer slope, the latter typically occurs after a high-water event when the water level falls but pore water pressures in the levee remain high.

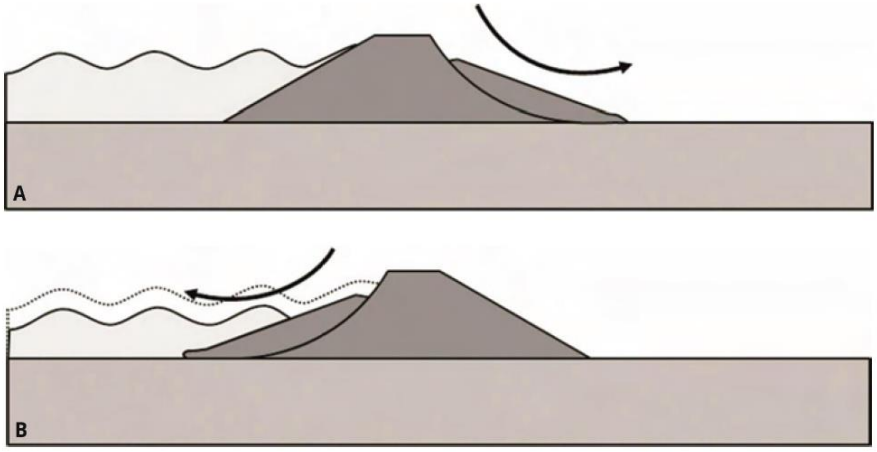

Figure 2.12 Superficial sliding taken from the ILH (2013). A) inner slope B) outer slope after rapid fall of river water level.

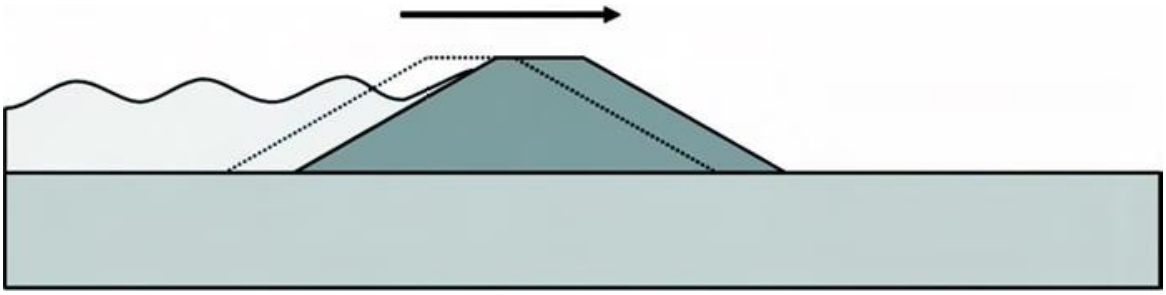

Figure 2.13 Translational sliding taken from the ILH (2013).

Flow slide

Two types of *flow slide* failure mechanisms are generally considered in literature: *static liquefaction* followed by a shear slide, and *retrogressive breaching*, generating a sustained turbidity current downslope of the location of initiation. Note that the term breaching in 'retrogressive breaching' refers to this specific process, not to breaching of the levee. Theoretically, both types of flow slide failure will result in a similar slope profile, although the evolution over time is very different. Static liquefaction is related to loosely packed sand layers in the subsurface that lose their strength instantaneously due to excess pore water pressure, whereas retrogressive breaching is related to more densely packed fine sand layers at the soil-water interface and may slowly retrogress over several hours. Both result in a flowing sand-water mixture or turbidity current that eventually redeposits on a gentle slope, see Figure 2.14 (Van den Ham, De Groot, & Mastbergen, 2014) and (Mastbergen, et al., 2016).

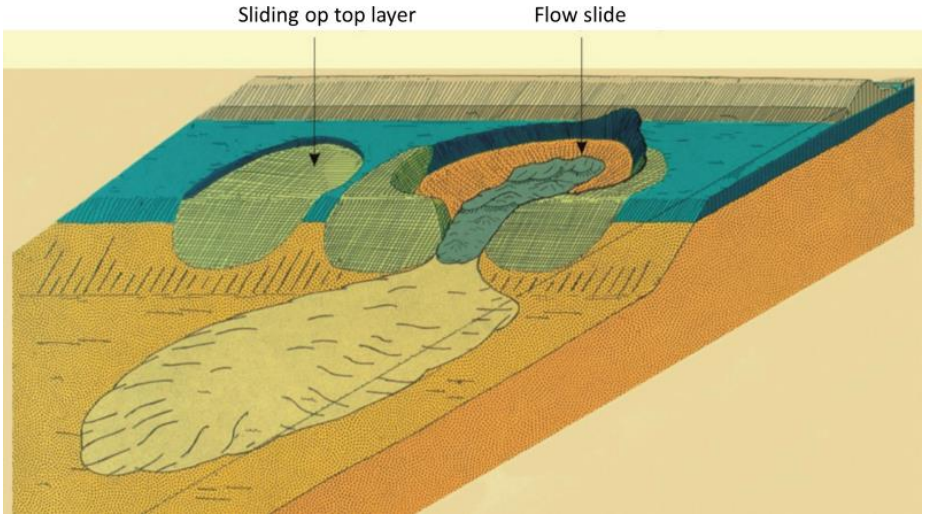

Figure 2.14 Artiste impression of sliding of top layer and flow slide taken from (Ministerie van Verkeer en Waterstaat, 2007).

2.2 Overall failure tree framework

Flooding due to hydraulic loading is often the result of the interaction of multiple phenomena, which may be part of different theoretical failure paths. In embankment analysis for assessment and design, typically, individual failure paths are assessed. Back analysis of failure events on the other hand, often indicate that flooding was the consequence of a combination of phenomena, and that site-specific characteristics play a large role in the occurrence of different events.

The intention of this section is to provide:
1. a framework to visualise how different failure paths can affect each other to lead to flooding.
2. an overview of parameters or factors that have a significant effect on the occurrence of the mechanisms in the failure path.

A conceptual framework is proposed in Figure 2.15 showing how hydraulic loading can lead to flooding. This figure is intended to facilitate the analysis of a failure by identifying discrete physical phenomena.

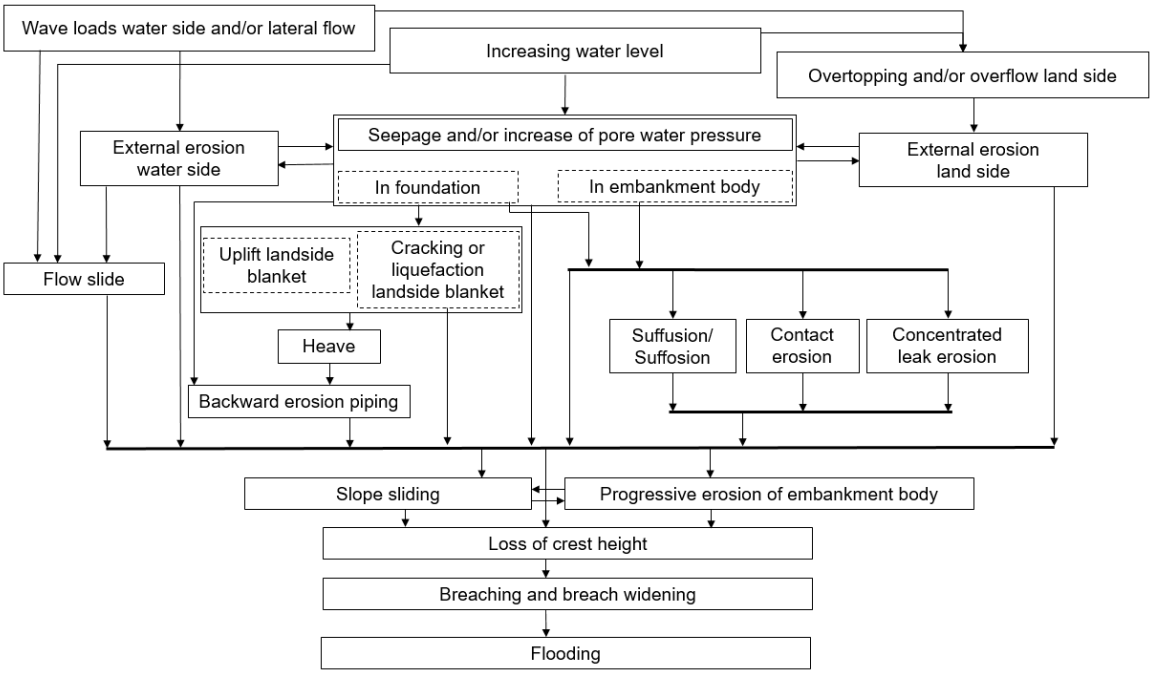

Figure 2.15 The purpose of this figure is to give an overview of the common physical phenomena that can eventually lead to flooding as a result of a hydraulic loading. They are combined into a failure tree to illustrate how factors can combine to initiate a breach. For a given situation, multiple phenomena may occur (parallel paths), and there may be interactions and feedback loops.

The thick black lines serve to reduce the number of arrows: a phenomenon with an arrow onto the black line may lead to the occurrence of some of the phenomena indicated below the black line. For example, an increase in pore pressure in the embankment may trigger slope instability. The two directional arrows between seepage and increase in pore water pressure and internal/external erosion indicate that these phenomena affect each other.

It should be noted that Figure 2.15 covers the response of an embankment to increased hydraulic loading. Other aspects not included in this chart may also affect the strength or resilience of the embankment. For example, localized settlement may create a situation where early overflow occurs and features such as desiccation cracking and animal burrowing may affect the strength and hydraulic resistance of the embankment. Such site-specific properties (geometry, subsurface, parameters), which affect the probability of occurrence of discrete events, are important to consider in the analysis as they determine which failure paths are most likely to occur.

An overview of site-specific properties which affect the occurrence of different mechanisms is provided in Table 2.1. This is based on engineering experience and the experience from the cases presented in parts B and C. This table cannot be expected to cover all factors which may occur, considering the variety of levee types and geological environments globally. This table can be used as a basis to expand upon with additional experience.

Table 2.1 Summary of important aspects or observations that affect the probability of occurrence of events in the failure tree, based on the inventories in Sections 3 and 4.

Mechanism/ phenomenon	**Important aspects or observations in case histories that affecting the occurrence of the event**
Wave loads water side/ and or lateral flow	• Large variation in water level between rainy and dry seasons; • Rapid lateral flow; • Wind and storm events; • Presence of a floodplain, and presence of vegetation on the floodplain damping wave loads; • Levee slope; • Local bathometry.
Overtopping and/or overflow inner side	• Settlement (localised) due to internal erosion may aggravate overtopping (e.g. due to drainage, tectonic settlement, shrinkage, oxidation, creep, consolidation); • Wind and wave direction; • Local bathometry; • Presence of road on the crest.
External erosion on water side.	• Presence of revetment, type of revetment; • Quality of revetment(e.g. low scouring resistance capacity of gravel soil bank slope; quality of grass for grassy outer slope). • Levee slope; • Presence of water side berm; • The steepness of the outer slope; • Presence of transition zones (for example from a hard revetment to a grass revetment, or trees on a grass revetment, etc.); • Bends in the levee; • Erodibility embankment body, e.g. quality of fill material; • Presence of wind and/or precipitation; • Presence of woody vegetation; • Animal activity on the slope. • External erosion can take place due to ice and debris drifting
External erosion on land side	• Quality of the dike revetment, (e.g. quality of grass for a grassy inner slope, or missing stones); • The steepness of the inner slope; • Presence of transition zones (for example from a hard revetment to a grass revetment, or trees on a grass revetment, etc.); • Erodibility embankment body, e.g. quality of fill material; • Levee slope; • Presence of wind and/or precipitation; • Presence of woody vegetation; • Animal activity on the slope.
Seepage and increase of pore water pressures in base of the levee	• Seepage in granular layers in the base of the levee, volumetric flow rates depend on permeability and thickness of the granular layers; • Degree of infiltration of water from the outer water body into the base, is there a direct connection between the outer water body and the granular layers in the base; • Presence of floodplain with a less permeable blanket in front of levee, which reduces pore water pressure increase in the base of the levee; • Increase of water pressure in base along cracks at sheet pile (cracks affected by shrinkage and pore water pressure); • Presence of cracks, roots, animal burrows or drains affect both the degree to which water flows into the granular layers raising pore water pressures, or the degree to which water can dissipate from the granular layers on the protected side; • Heterogeneity of subsoil, e.g. transitions between two different materials, presence of locally more permeable layer in the subsurface below the levee (e.g. an infilled channel); • Permeability of the blanket on the landward side of the levee, a more permeable blanket allows more dissipation of pore water pressures in the granular layers on the land side.

Mechanism/ phenomenon	Important aspects or observations in case histories that affecting the occurrence of the event
Seepage and increase of pore water pressures in embankment body	• Seepage through the flood side slope of the levee, permeability of the slope cover; • Animal burrows and rodent holes; • Seepage in the base of levee; • Permeability of the levee body; • Presence of drains in the levee; • Heterogeneity of levee material, transitions between two different materials.
Flow slide	• Thick, loosely packed, sandy layers to fluidization and failure within minutes or a thick and densely packed sand layer can have a slow process of sliding.
Uplift movement	• The thickness and unit weight of the blanket layer constitute the weight that needs to be lifted; • The pore water pressure below the blanket (refer to seepage and pore water pressure in the base of the levee); • Factors that lead to concentrated seepage and locally high pore water pressures below the blanket, such as an old field drain beneath the levee, locally more permeable zones in the aquifer (infilled channel), abrupt transitions from granular material to blanket layer, etc.
Cracking or fluidization land side blanket layer	• Thickness and strength (material, clay or peat, type of clay) of the blanket layer; • Presence of existing cracks or local defects; • Presence of local weaker spots, e.g. locally thinner blanket. • The pore water pressure below the blanket (refer to seepage and pore water pressure in the base of the levee).
Heave	• Pore pressures below the blanket for fluidization; • Flow rate for transport of grains.
Internal erosion: backward erosion piping	• Land side blanket uplift and cracking are required for internal erosion to initiate if there is no pre-existing defect or interruption of the blanket; • A granular material in the base of the levee and a cohesive blanket forming a roof over the pipe are required; • Permeability and thickness of the granular layers affect flow to the pipe; • Grain size, and grain size distribution of the granular layer below the blanket (in the pipe) affects erodibility of grains in the pipe; • Seepage from the river to the pipe (refer also to the factors at seepage and pore water pressure in the base of the levee); • If there is a blanket layer and a sand boil, the head drop over the sand boil can provide additional resistance.
Internal erosion: concentrated leak erosion	• Deterioration can be caused by subsequent high-water events; • Animal burrows and rodent holes can form leaks; • Ancient pavement layers may form seepage and erosion pathways; • Cracks along former transitions in embankment body may form seepage and erosion pathways; • Presence of roots of dead trees may form seepage and erosion pathways; • Erosion may occur along a crossing structure such as a cable or pipeline; • Old structures inside the levee (rocks, walls, etc.) may form seepage and erosion pathways.
Internal erosion: contact erosion	• Deterioration can be caused by subsequent high-water events; • Deterioration of revetment allowing seepage through embankment body (refer also to increase in pore water pressure and seepage in embankment body); • Contact between coarser and finer layers of soil in the embankment body or foundation.
Internal erosion: suffusion/suffosion	• Deterioration due to subsequent high-water events; • Deterioration of revetment allowing seepage through embankment body; • Grain size distribution, presence of finer and coarser grains (gap-graded soil).

Mechanism/ phenomenon	Important aspects or observations in case histories that affecting the occurrence of the event
Slope sliding	• Cracks may be observed prior to sliding; • Multiple slides may occur prior to failure, dimensions of slide may be variable; • Slope sliding may occur on inner or on outer slope; • Instability of the outer slope can occur after a high-water event, allowing more time for repairs prior to a subsequent high-water event; • Scour on the external side causing slope instability by undercutting a slope; • The presence of berms affects slope sliding; • The strength material on the slope (and in the base of the levee) affect the size and shape of the slide; • Pore pressures in a granular aquifer covered by a blanket layer can lead to uplift in combination with slope failure; • In case with retaining wall, the stability of the wall foundation; • Extremely dry conditions leading to weight loss and shrinkage of peat embankment; • Discontinuities present from past land use can form slide surfaces; • Steepness of the slope.
Progressive erosion of embankment body	• Distinction between a clay embankment body and a granular embankment body, the latter erodes easier; • Quality fill material.
Loss of crest height	• Magnitude of the freeboard, subsidence for instance due to for instance dewatering for water abstraction, or isostatic changes, might reduce the magnitude of the freeboard.

2.3 Application of framework to inventory of case histories

The application of the framework in Figure 2.15 is demonstrated in Section B. For each case the probable failure path was highlighted in the framework. Local important factors, which affect the occurrence of the different mechanisms in the failure path were identified based on Table 2.1.

The case histories showed that often multiple mechanisms interact and contribute to cause a failure. The framework of the failure tree aids in the analysis by suggesting the possible interactions among mechanisms. In many cases it was not possible to assess the relative importance of different mechanisms. Also, the sequence in which events occurred is often difficult to establish in hindsight, and after a failure little evidence remains for forensic investigation.

The time between an initiating event and a breach can be highly variable. Some cases are described where the time from observation of a defect to failure is in the order of minutes, but often this can be in the order of days during one long high-water event, or even years if this is the time between successive high-water events. This illustrates the relevance of considering the failure path fully, rather than only the limit state for an individual mechanism. Whereas exceedance of the limit state of an individual mechanism is undesirable, if this does not lead to an immediate flood, measures may be taken to mitigate the consequences. If damage can be detected, the probability of detection, and of taking appropriate response measures, can be included in the failure path. This is already included in some of the failure paths contributed for assessment and design in Part C.

2.4 Discussion

The terms “*failure*”, “*failure path*”, “*scenario*”, and “*failure tree*” are much used in the context of levee performance during extreme flood events. It is well known that when failures of flood defences do occur, they are often the result of a combination of factors such as loading events and failure mechanisms. However, in practice, the terms *failure*, *failure path, scenario* and *failure tree* are not always used consistently and hence confusion can arise.

The objective of this report is to facilitate the discussion on failure paths among researchers and practitioners internationally. This is done by:

- compiling an inventory of case histories and use of failure paths internationally;
- distinguishing between failure mechanisms and failure paths or trees
- presenting an overall framework to visualize possible relations among mechanisms and identifying key parameters that affect the occurrence of mechanisms.

Failure paths can fulfil several uses in levee assessment and design:

1. In the back-analysis of a failure, a failure path can be used to describe a site-specific sequence of events and mechanisms that ultimately led to a levee collapse.
2. For design purposes, failure paths can be used to identify viable combinations of events and mechanisms that might cause failure to verify that there is enough resistance to avoid a failure condition for each case considered.
3. When carrying out risk assessment for existing structures, it may be necessary to quantify the overall risk of failure and / or the overall risk of flooding. In this case, the risk of failure can be assessed for individual (and viable) failure paths and the overall risk of failure associated with a given flood event can be established by combining these failure paths into a failure tree.

When carrying out designs for or assessments of linear flood control structures it is important to appreciate that the system is only as strong as the weakest link in that system. Designers and assessors should therefore actively search for the weakest points in each system, such as transitions, areas of local geological features, areas of localized erosion, etc. They should identify the relevant potential failure paths and then design or assess the structures accordingly.

For embankment assessment and design, it is common to consider mechanisms such as external erosion, internal erosion and sliding collapse and to consider how these mechanisms might trigger a failure of the levee. Potential failure paths can be identified and quantified based on theory relevant to the individual mechanisms, but the danger is that such theoretical assessment does not fully reflect what can be a more complicated reality. Thus, a good knowledge and understanding of the way in which real levees perform (and fail) is a critical element of any design or assessment process.

To aid the understanding of how levees perform during extreme events, this report has compiled an inventory of levee failures for which the failure trees have been identified. These cases were used to identify important features of the flood defence that affect the occurrence of different mechanisms and failure paths. This list is neither exhaustive nor fully comprehensive. However, it is hoped that this compilation of historical levee failures will help designers and assessors to identify which features of a particular flood defence are likely to control its behaviour during a flood.

2.5 Recommendations

It is hoped that this report has highlighted the fact that most levee failures occur as a result of a combination of many factors and are rarely caused by a single mechanism. It can be argued that the performance of levees is often controlled by the balance of hydraulic actions and geotechnical resistances. However, an increasing tendency for engineers to specialize into areas of competence, e.g., structural engineers, hydraulic engineers, and geotechnical

engineers, means that to improve the quality of individual elements of design or assessment, the real behaviour of these vital structures can be missed or misunderstood.

It is considered important that the need to consider the “bigger picture” when assessing the performance of hydraulic structures such as dams or levees is stressed in universities and practice alike and that client bodies too are aware of this issue. Indeed, TC201 has an important role to play in harmonising international practice.

The analysis of failure paths allows for the consideration of all processes that lead to a failure, rather than only initiating mechanisms. However, currently there are still many questions regarding the rate at which processes take place, and the methods to assess the last steps in the failure paths. Breach growth is a process which is very relevant for the consequences of flooding, affecting the rate of inundation and the time for response measures. The case histories and the failure paths for assessment and design in this inventory do not explicitly address this process, and further investigation of this could be effective for emergency response measures in order to mitigate the impact of flooding.

3 Part B: Inventory of case histories

Case histories of actual levee failures provide valuable insights to how several mechanisms can combine leading to a breach. Members of the ISSMGE TC 201 and of the EWG-IE have contributed to several case histories in which failure path analysis was used in order to identify the sequence of events that caused a failure. The suggested failure paths are interpretations of the available information and subject to uncertainty. Often the available information after a flood is limited and multiple failure paths might be plausible.

In this section, the case summary provided by the contributors is used to identify possible failure paths that occurred and to place them in the overall framework. The failure paths that appear to have taken place are highlighted in yellow and interactions are marked by red arrows in the overall framework. Question marks are used for interactions that are suggested as possibilities but that are less certain. Based on the case description, either the likely important influencing local factors per case are identified, or the characteristics of the failure process are summarised.

3.1 UK breach in 2015

Contribution by Dr. P. Smith (Royal Haskoning DHV, United Kingdom)

Summary

This case concerns a breach which occurred in the UK in 2015 following a period of heavy rain during a named storm event[3]. Overtopping and erosion on the land side appear to have played a dominant role in the breach. Several factors were identified that probably contributed to the breach.

Influencing local factors

- Overtopping and/or overflow land side:
  - Settlement of levee over time prior to high-water loading (localized consolidation);
  - Possible internal erosion of fill (embankment body) or of the foundation soil, leading to local settlement.
- External erosion land side:
  - Lack of scour protection;
  - Overly steep landward slope;
  - Lack of a landward berm;
  - Poor quality fill material (low resistance to overflow erosion).
- Uplift movement:
  - Old field drain beneath the levee caused higher water flow towards the toe at the landward side.

[3] *According to www.metoffice.gov.uk visited in 2021: "The criteria used in the UK for naming storms is based on the National Severe Weather Warnings service. This is based on a combination of both the impact the weather may have, and the likelihood of those impacts occurring. A storm will be named when it has the potential to cause an amber or red warning. Other weather types will also be considered, specifically rain if its impact could lead to flooding as advised by the Environment Agency, SEPA and Natural Resources Wales flood warnings."*

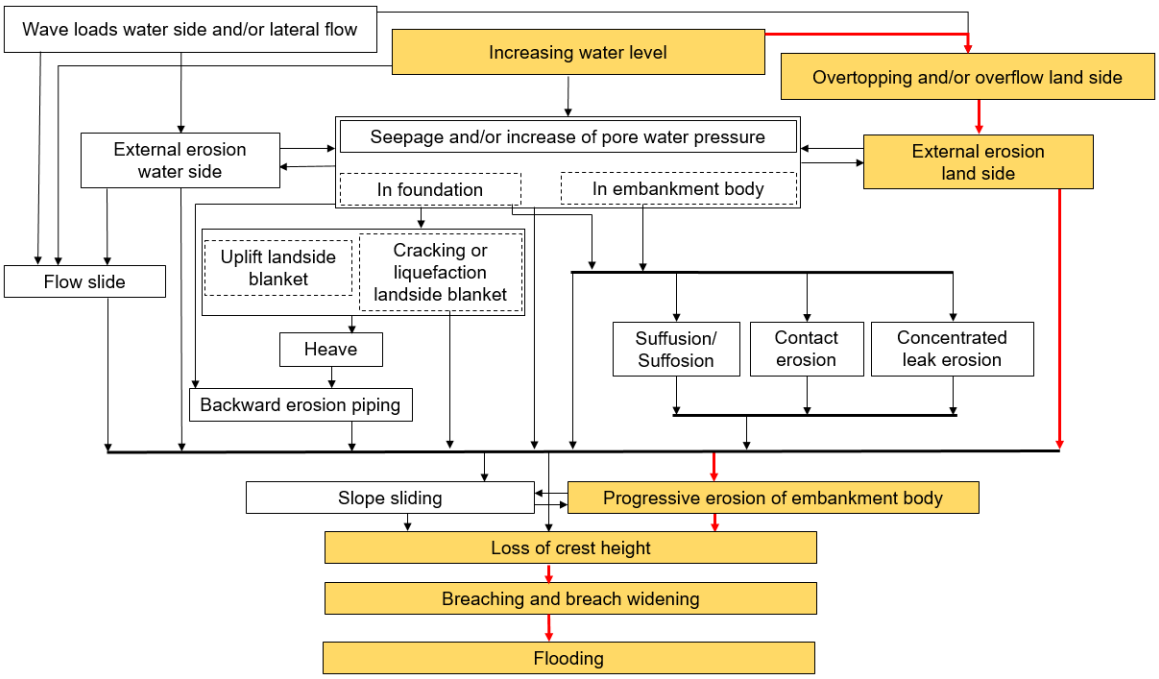

Figure 3.1 Failure tree of the UK breach, 2015.

Case description

The breach occurred in the UK in 2015 following a period of heavy rain during a named storm event.

Figure 3.2 Photograph of the situation.

The flooding resulting from the breach, affected approximately sixteen properties and a large area of agricultural land. A scour hole of up to 10 m depth was caused by the flow through the breach.

Figure 3.3 Photograph of the breach.

A forensic review of recent LiDAR images showed that the original crest level at the location of the breach was up to 100 mm lower than at surrounding areas. Furthermore, the location of the breach was underlain by both an in-filled historical meander and an old field drain. It is likely that the localized settlement of the crest in the vicinity of the breach was originally caused by consolidation of the in-fill material in the old meander. This meant that the crest level at this location was lower than at surrounding areas; overflow at this location caused rapid external erosion of the levee because of the steepness of the landward slope, about 30 degrees, the quality of the levee fill material (erodibility) and the lack of a landward berm.

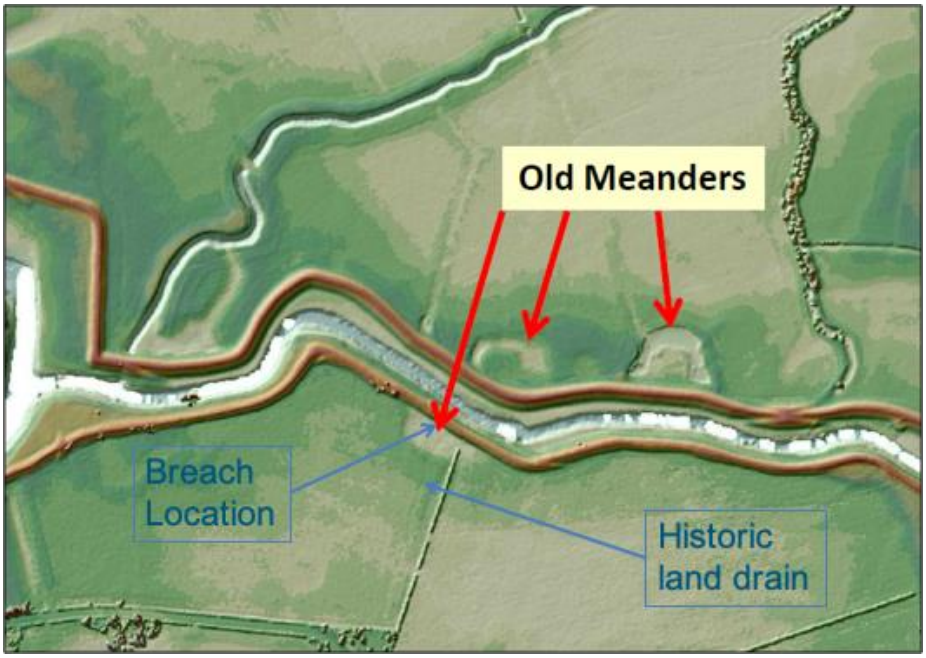

Figure 3.4 Overview of the situation.

The presence of an old field drain beneath the levee is believed to have influenced the failure. The alignment of the drain can be seen on the LiDAR image and evidence of seepage was found during the post-breach inspections.

Possible evidence of piping failure on landward side of levee at the location of the breach appears to coincide with the location of historic land drain. This seepage may have led to softening of the toe or possibly uplift beneath the landward slope of the embankment.

Figure 3.5 Close-up of the situation.

In summary, the causal factors in this case are:

1. Very high-water levels in the river caused by rain associated with a named storm.
2. Localized lower crest levels resulting from historical local settlement of infilled meander and possible internal erosion associated with land drainage. This led to localized overflow.
3. A steep landward slope created turbulent flow at the toe of the landward slope after overflow commenced.
4. The resilience of the landward slope was potentially reduced by seepage and/or uplift at the location of the historic land drain.
5. The relatively poor-quality embankment fill material (locally won and agricultural) meant that the levee had reduced resilience to overflow erosion.

Figure 3.6 indicates how the factors above can be combined into a fault tree to show how these elements can combine to create a situation where a breach occurs. In this case there are several potential influencing factors. As we cannot say for certain what the dominating factor was, or what the contributing percentages were, these are connected by an OR gate.

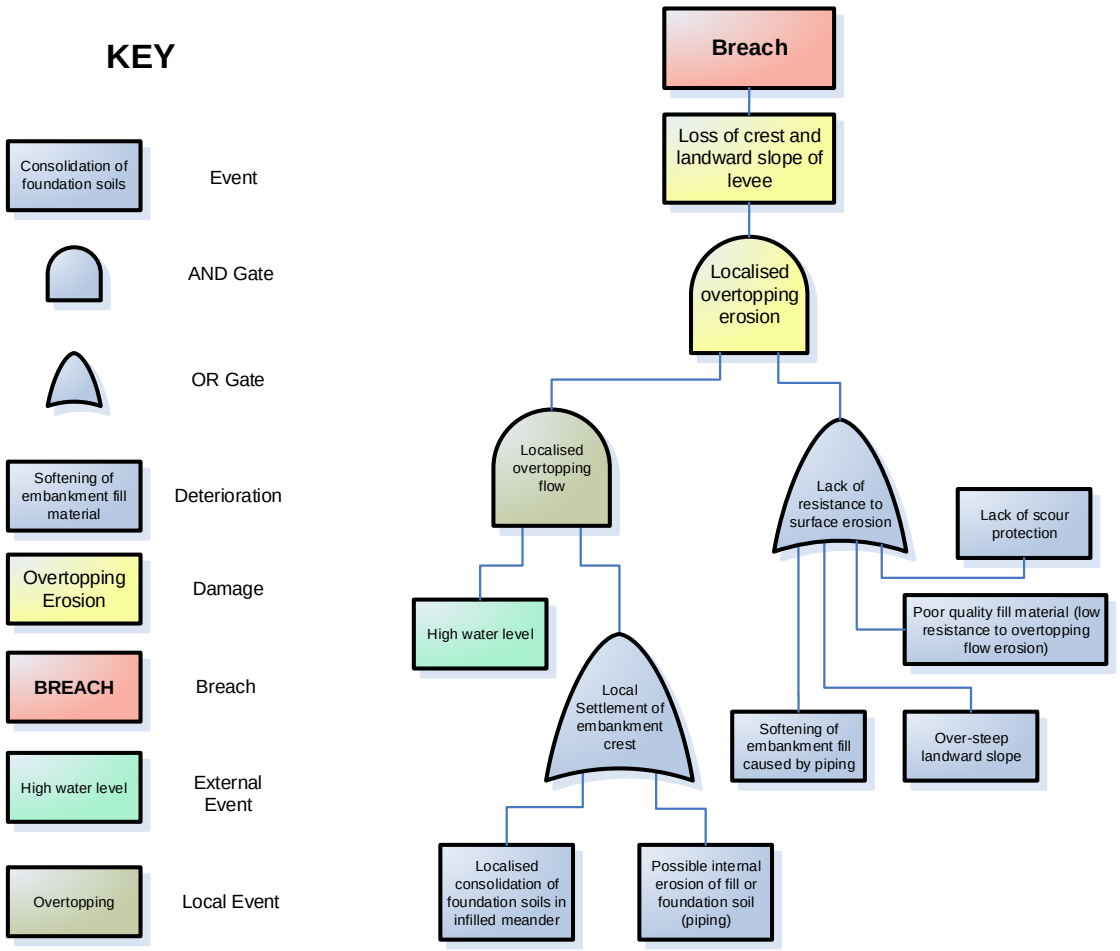

Figure 3.6 Fault tree UK breach 2015.

3.2 Several cases of breaches from the US

Contribution by M. Sharp

3.2.1 US: Pin Oak levee System breach

Summary

This case concerns a flood as a result of a river rise during a spring event and loading of the levee for three weeks. Causes of the breach are due to through seepage.

Characteristics

- Water level exceeded design level;
- Previous history of poor performance in the levee system;
- Addition of sandbag wall on levee crest to prevent overtopping;
- Increased pressure on levee leading to through seepage, evidenced by seepage on the land side slope;
- Attempts to put sandbag around the seepage initially worked but eventually became less effective;
- Placement of plastic tarp on the flood side (water side) of the slope of the levee to control seepage inflow;
- Seepage steadily increased with observations of significant fines;
- Reports and observations of rodent holes in levee at location of breach.

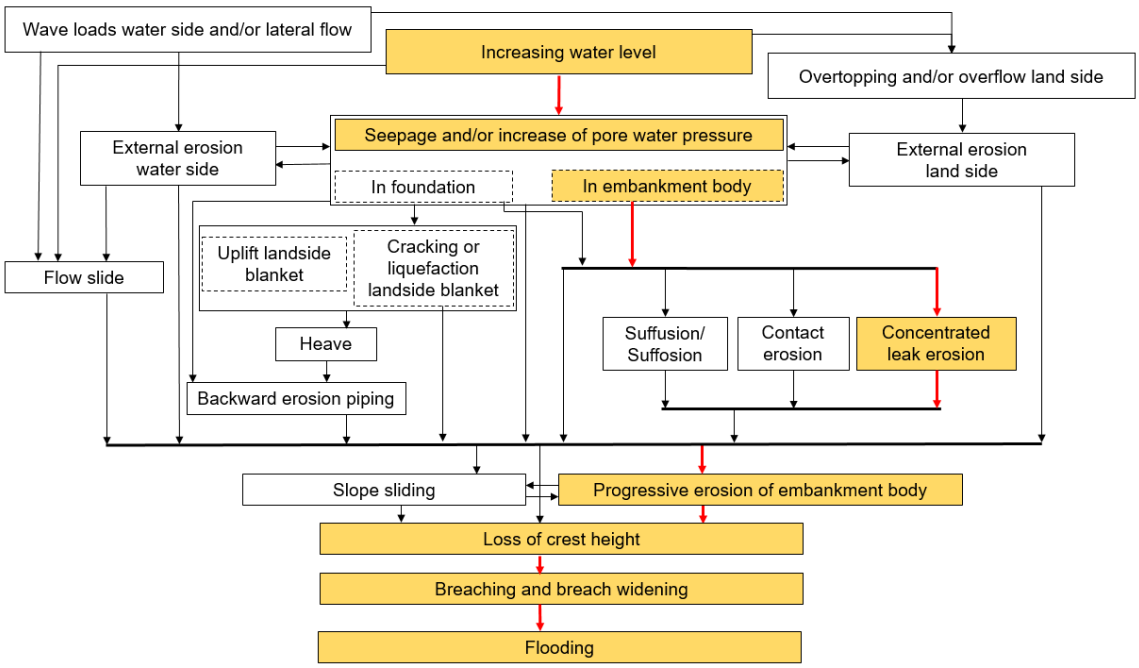

Figure 3.7 Failure tree of US Pin Oak levee system breach, Zwanenburg.

Case description

General

The Pin Oak Levee system is located near Winfield, Missouri, approximately 64 km northwest of St. Louis, Missouri. The Pin Oak Levee system protects the city of Winfield and adjacent farmland from Mississippi River backwater flooding (see Figure 3.8). The flooding of Mississippi River backs up in drainage canals located along the levee system.

Based on the height of the levee, this system provides up to a 15-year level of flood protection. Two breaches had occurred in the Pin Oak Levee system area due to overtopping during the 1993 Flood. No information about breach location was provided in the report, but it was noted that these breaches inundated the city and farmland surrounding the city.

As shown in Figure 3.8, the Pin Oak Levee system experienced significant distress and subsequent breach during the Spring 2008 Flood. The Spring 2008 Flood lasted approximately three weeks and ended in a breach of the system on 27 June. Based on information provided by the USACE St. Louis District, the flood event was considered to be a 50-year event at the Pin Oak Levee system.

In anticipation of the Spring 2008 Flood, local, state, and Corps forces placed a 0.75 m-high sandbag parapet wall on the levee crown to increase the height of protection. As the flood loading on the levee system increased, levee distress became visible and widespread, and included land side slides along the east portion of the system and heavy through seepage emerging near the toe of the levee at two separate locations. The levee system breached at one of the heavy through seepage locations where a large quantity of water was flowing through apparent defects within the levee section.

At the time of the breach, some portions of the sandbag stack/wall were not loaded while other portions were inundated up to 0.5 m. After the breach occurred, local, state, and federal forces made a heroic effort to protect the city from flooding by constructing an emergency flood protection wall around the city (see Figure 3.8).

The following sections describe details from the site visit and describe the levee breach and other levee distress (e.g., seepage and land side slides).

Figure 3.8 Aerial view of the Pin Oak Levee system.

Levee breach

The levee breach occurred in the southeast corner of the system around 0500 hr on 27 June when the water level reached the height of the embankment. Before the levee breach and early in the flood stage, severe leakage of water was evident at the toe of the levee at this location, where an irrigation canal runs parallel with the levee at the land side toe. Firsthand accounts of the events that occurred at this site were provided via personal communication. A brief summary of their communication is provided below:

Initial seepage erupted from the protected side (land side) toe at 0100 hr on 23 June 2008. The term “erupted” is used to describe the seepage, as it was flowing vigorously similar to a geyser, suddenly and without warning. A flood-fight team started with a sandbag ring around the seepage in an attempt to contain it. As the height of the sandbag ring increased to about one meter, seepage then erupted on the slope of the levee at just about the height of the sandbag ring. An effort was then made to construct a sandbag ring around the seepage that erupted on the levee slope. The sandbag rings did not seem to deter the seepage as seepage was vigorously overtopping the sandbag rings. The next attempt was made around 0600 hr 23 June 2008 to slow the seepage by placing a plastic tarp on the flood side slope of the levee. Once the plastic tarp was in place and sealed with sandbags, the seepage creating the geysers within the sandbag rings essentially ceased. After a couple of days, seepage began to increase and nearly returned to its original state. Attempts to place more plastic tarp on the flood side slope was made with the assistance of divers. However, there was little success in slowing the seepage. An observer of the seepage indicated that there were chunks of clay emerging from the seepage. Muskrat or

other small mammals were observed diving in the area where the plastic tarp was placed. Several people reported that an animal burrow was located on the flood side of the levee and that the seepage was associated with muskrat or other rodent holes/dens. On 27 June 2008, the levee breached at this site. Figure 3.9 and Figure 3.10 show images of the levee.

During the site visit, the width of the breach measured approximately 46 m. However, photos taken during the breach show a narrower initial width, indicating that the breach enlarged with continuing flow. The cross section of the embankment was exposed on both sides of the breach allowing the assessment team to inspect the levee embankment materials. Based on the cohesive nature of the soil, the levee embankment materials appear to be clay. A sample of the levee material (taken about mid-height in the levee profile) was removed for laboratory testing for geotechnical properties (e.g., Atterberg limits, sand content, organic content, and soil classification). The results of the tests were used to provide a description of the levee embankment material. The information can also be used to estimate erodibility, cracks, or concentrated leaks in embankments. From these soil properties, the erosion rate of the levee embankment material would be estimated as moderately rapid.

Figure 3.9 Seepage occurring at the toe of the levee prior to breach (taken around 0800 hr, 23 June 2008) (left), and Sand bag effort prior to breach (taken around noon on 26 June 2008) (right).

Figure 3.10 Breach occurring (taken around 0700 hr, 27 June 2008).

Along the alignment of the levee, the breach scour depth only extended down to the foundation level. However, rodent holes (ranging from 5 to 7 cm in diameter) were found around the perimeter of the levee and at the water side toe of the breached levee section. There were also indications of rodent holes about 1.3 m below the flood side mid-slope near the base of the levee (see Figure 3.11).

Figure 3.11 View of animal burrows beneath water side mid-slope of breach section (22 July 2008).

Discussion

During the Spring 2008 Flood, animal burrows and dens may have had adverse impacts on the Pin Oak Levee system. As stated previously, animal burrows and dens in the levee at the breach site are suspected to have caused the seepage and subsequent internal erosion causing a breach. Also, it is likely that animal burrows and dens caused the severe seepage that occurred along the northern alignment of the levee system. Both sites are appealing to muskrats as often water inundates the flood side (from the drainage canal). At the breach site, water periodically inundates both the flood side (from the drainage canal) and land side (interior drainage ditch) toe of the levee. With these conditions at the breach site, muskrats can burrow into the levee on both sides. The burrows/dens on each side of the levee may become connected through the levee by rupture or hydraulic fracture caused by pressure from flood loading.

3.2.2 US: L-575 levee breach

Summary

This case concerns a flood as a result of a river rise following a large rain event and loading of the levee. Causes of the breach are due to underseepage.

Characteristics

- Water level exceeded design level;
- Increased pressure on levee leading to underseepage evidenced by seepage on the land side slope;
- Numerous observations of collapses in seepage paths on the land side;
- Attempts to stop the seepage unsuccessful;
- Eventual breach of levee.

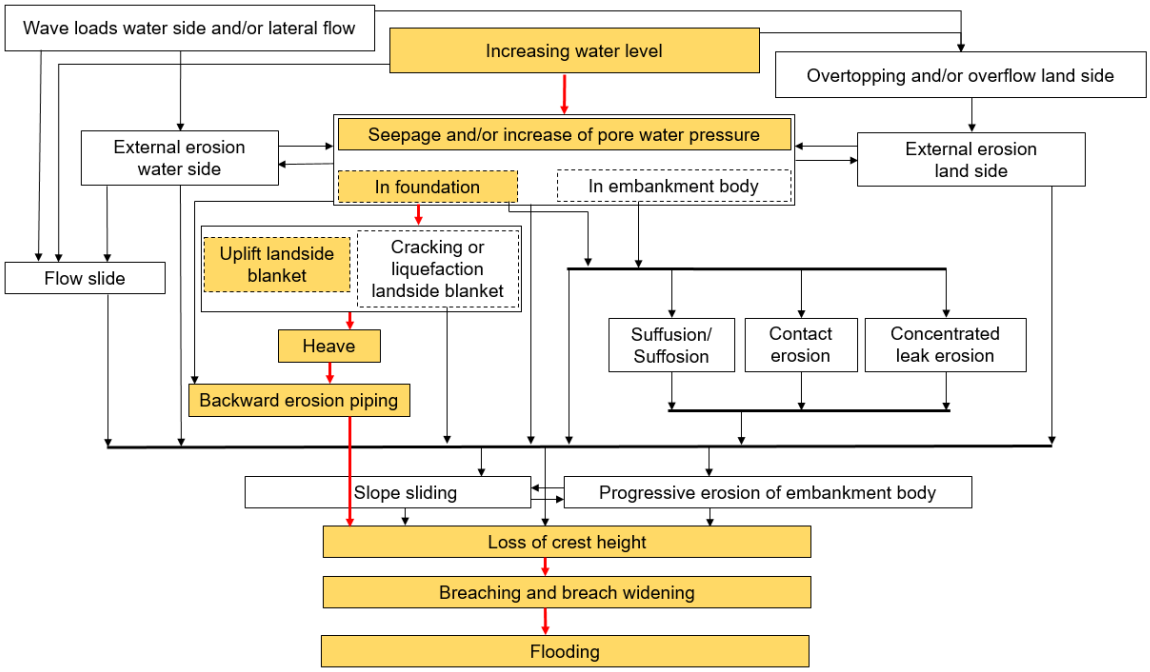

Figure 3.12 Failure tree of US L-575 levee breach, 2011.

Case description

One of the breaches that occurred during the Missouri River flooding of 2011 occurred in the L-575 levee district which protects a large area of agriculture along with the city of Hamburg in southwest Iowa. The breach occurred in an area that had demonstrated several incidents of levee underperformance. Initial distresses, as shown in Figure 3.13 and Figure 3.14, narrowly avoided a full breach as the levee collapsed on itself, sealing off the underseepage path. Emergency repairs were initiated to reinforce this section of levee. The contractor and levee personnel were on site when the next distress appeared. There was a report of a “gurgling” sound, and then the levee collapsed on itself beginning from the protected side (land side) seepage berm and continuing toward the water side. As seen in Figure 3.14, an alluvial fan appeared at the protected side toe of the seepage berm. One additional incident (for 3 total) like this occurred before the final section of the levee breached. For all of these incidents, including the breach, there were a few meters of freeboard on the levee at that time.

Figure 3.13 The initial distress in the levee L-575.

Figure 3.14 Initial distress in levee L-575 showing alluvial fan.

When the fourth incident occurred, the levee was not able to collapse on itself and seal the underseepage path. When Corps personnel arrived on-site several minutes after the breach was reported, the breach was about 3 m wide. While on-site, the breach continued to widen and deepen, Figure 3.15. The protected side continued to flood, eventually equalizing with the river as shown in Figure 3.15. Due to the forecasted water levels and the threat of breach due to the distresses showing up in the main stem levee, a temporary levee was built to protect the city of Hamburg. The temporary levee successfully held back the Missouri flood waters for the duration of the flood.

Figure 3.15 The initial breach of the levee L-575 (left), and the levee breach after complete interior flooding (right).

3.2.3 US: Birdland levee breach

Summary

This case concerns a flood as a result of a river rise following a rain event and loading of the levee. Causes of the breach are due to overtopping and erosion of the river side (water side) slope.

Characteristics

- Sharp bend in the levee (90 degrees);
- History of river side erosion of slope not protected with riprap;
- Documented poor material used for levee construction (rubble);
- Heavy vegetation encroaching on levee;
- Overtopping in combination with river side erosion leading to breach.

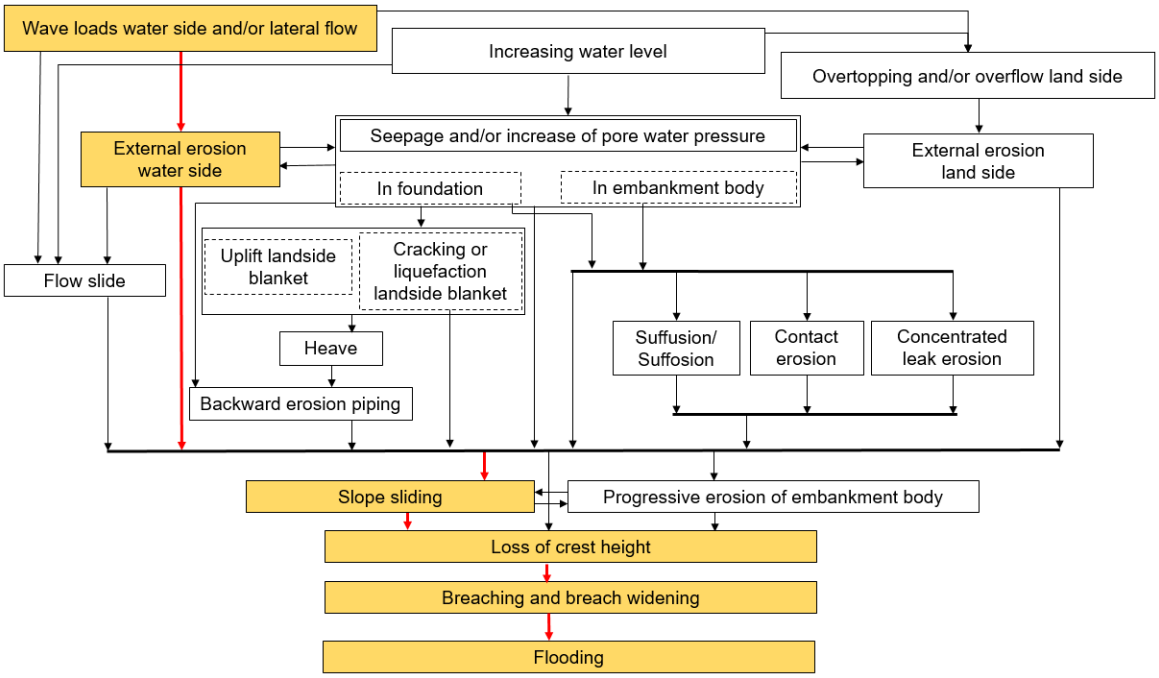

Figure 3.16 Failure tree of US Birdland levee breach, 2008.

Case description

General

The Birdland Levee system is located along the Des Moines River in Birdland Park and north of downtown Des Moines, IA. The field team visited the Birdland system during this assessment. The city of Des Moines constructed the levee in the 1950s and it protects approximately 220 homes, several dozen businesses, and North High School. The Neal Smith Trail, part of the City of Des Moines recreational trail system, also runs along the top of the Birdland Levee. On 13 June 2008, a section of the levee breached. This section was located between the river and an oxbow lake and was in a sharp river bend (see Figure 3.17). Even at a low stage of flow, the velocity of the water here would normally cut away at the riverbank and cause erosion without some reinforcement. A flood event in 1993 had caused a breach at this same location.

Concern over the vulnerability of the levee system had been ongoing and the Corps, Rock Island District, coordinated a feasibility study for failure potential of the Birdland Levee. The report noted that the levee was *constructed with miscellaneous fill materials and contained rubble and debris*. The slope was also variable due to erosion. Sand seams were present within the levee and were considered to be the cause of some of the seepage that had occurred. Concern was also raised that trees and brush were growing on or in the levee area. The report recommended the following improvements:

a. Remove all woody vegetation from the levee to a distance of 4.5 m.
b. Dig an inspection trench along the bottom of the levee to determine types of unsuitable construction materials within the levee.
c. Rebuild the levee (they suggested three different rebuilding alternatives). Included in the rebuilding alternatives was a plan to widen the top of the levee to accommodate a walking and bike trail.
d. Construct a seepage berm in areas where the ground surface is below 10 m.

The report predicted that, in the levee's current state of disrepair, there was a 50% chance of failure for a 50-year flood event. By 2008, only a few minor improvements had been funded.

Figure 3.17 Location of the Birdland Levee breach (taken 2007).

On 12 June 2008, the adjacent neighborhood was evacuated due to encroaching floodwaters. National Guard and volunteers added an additional 0.6 m of height to the levee with sandbags.

In the area behind North High School, local residents reported that the levee was “sinking” and that the water was “waist high” by 1600 hr. Figure 3.18 shows an image of the breached levee.

Figure 3.18 View looking to the southeast over the Birdland Levee breach (16 June 2008).

Discussion

Many trees and bushes are growing in and near the levee and had previously been a source of concern. Heavy vegetation makes it difficult for access, blocks adequate visual

inspection of levees from the crest, and requires more effort to inspect along the toe. Several trees remained intact in the area where the breach had occurred. There is no substantial information from field observations to indicate whether the vegetation on the levee played a role in the breach of the levee.

3.3 Portugal collapse of embankment in 2019

Contribution by J. Ribeiro Vlaanderen (Witteveen+Bos) and A. Pinto (JETsj)

Summary

This case concerns a flood as a result of a river discharge exceeding the design flood discharge. Causes of the breach are subject of further investigation.

Influencing local factors:

- Overtopping and/or overflow land side:
  - Water level exceeded design level.

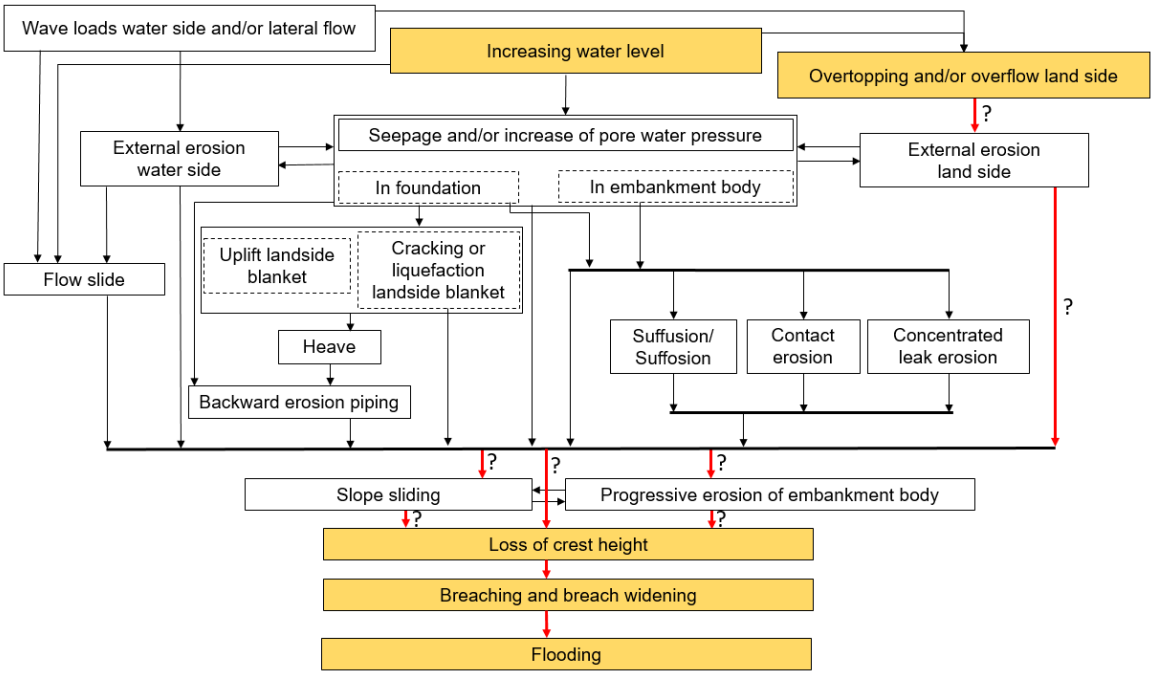

Figure 3.19 Failure tree of Portugal levee breach, 2019.

Case description

In 2019, between 19 and 22 December, the Mondego River in Central Portugal overflowed. The embankments alongside the river were designed for a service water level of 18 m high, and an extreme water level of 19 m high, corresponding to a flow of 2000 m^3/s. In December 2019, the river flow exceeded these values; it is estimated that the embankments resisted up to a flow of 2300 m^3/s, collapsing when this flow was exceeded. Consequently, the river embankments collapsed in Santo Varão, Montemor-o-Velho.

The causes of the failure are still being studied. Available information indicates that there was overtopping before the collapse.

The collapse led to the flooding of the fields in the Central Valley of the Lower Mondego and the cutting of communication routes. Infrastructure was severely damaged, not only the embankment but also the road and the conducting channel at the right bank, for the water supply of agriculture and industries.

Figure 3.20 View of Santo Varão shortly after collapse of the embankment [4].

Figure 3.21 View of Santo Varão after collapse of the embankment [5].

[4] *https://www.publico.pt/2020/06/21/fotogaleria/30-anos-fotografia-publico-401539#&gid=1&pid=36*

[5] *https://www.noticiasdecoimbra.pt/dique-recuperado-no-rio-mondego-a-tempo-de-abastecer-campos-agricolas-neste-verao/*

Figure 3.22 Top view of collapsed embankment in Santo Varão [6].

A plan is currently under development to reinforce the Mondego embankments. This plan will consist of integrated solutions, to be implemented in the coming years.

[6] *https://www.publico.pt/2019/12/27/sociedade/noticia/barragem-fundamental-gerir-mondego-cancelada-2016-1898664#&gid=1&pid=3*

3.4 Several cases of breaches from Japan

Contributions by Professor K. Maeda, Nagoya Institute of Technology, M. Ishihara Senior reseacher, Public Works Research Institute, and H. Mori Associate Professor, Yamaguchi University.

3.4.1 Slope slide Nagara river 1975

Summary

This case concerns a slope sliding event in which emergency response measures were attempted but insufficient to prevent a breach.

Characteristics

- For slope sliding:
  - Formation of cracks prior to slope sliding;
  - Two successive slides prior to failure;
  - Attempted emergency response measures were not successful.

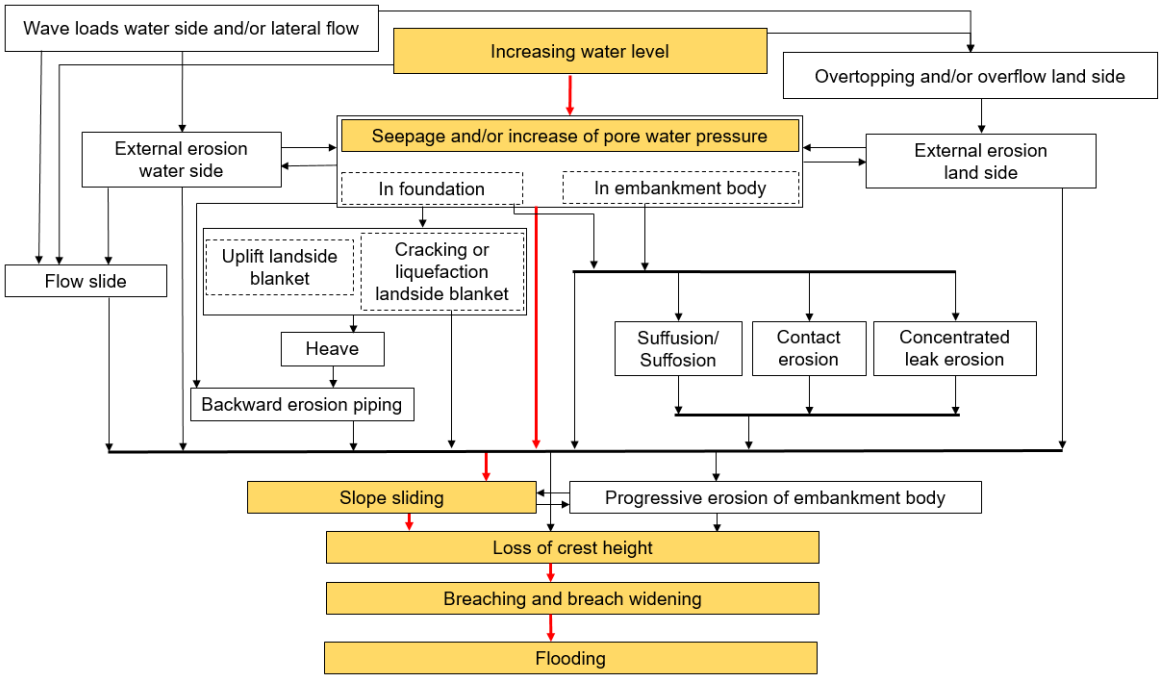

Figure 3.23 Failure tree of Nagara levee breach, 1975.

Case description

An example of the failure tree for a slope slide on the Nagara river in 1976 is shown in Figure 3.24. The failure path includes the times of different events.

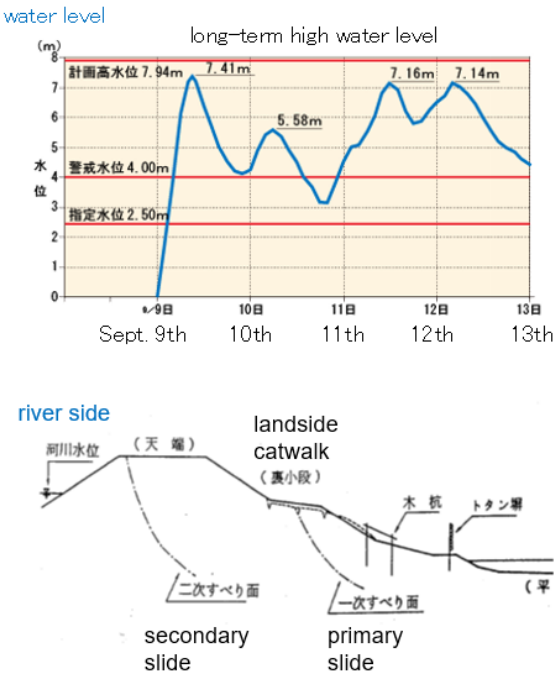

Failure time tree and the process were written down; from cracking to secondary large slide.

- ✓ Sept. 12th , 06:30 --- crack in landside catwalk
- ✓ Sept. 12th , 07:40 --- a crack line in the center of landside catwalk, paralleled to levee
- ✓ Sept. 12th , 08:10 --- two crack lines of landside catwalk: the lengths of 40cm, 60cm and the width of 5-10cm
- ✓ Sept. 12th , 09:10 --- herbicidal works
- ✓ Sept. 12th , 09:30 --- levee protection works with pile driving. Growth of cracks with level difference of 50cm on landside catwalk
- ✓ Sept. 12th , 10:20 --- Primary slide on landside catwalk, and then secondary slide from levee crown in a couple of minutes.
- ✓ Secondary slide and inflow of river water…..breach

After Ministry of Land, Infrastructure and Transport

Figure 3.24 Example of slope slide from the presentation 'Picture-Card Show Project' in JGS-JSCE by K. Maeda, M. Ishihara and H. Mori, using materials from the Ministry of Land, Infrastructure, Transport and Tourism in Japan.

Figure 3.25 illustrates the protection works that were installed as well as the situation following the breach.

levee protection

Just after breach

Gifu Prefectural Government

Figure 3.25 Example of slope slide from the presentation 'Picture-Card Show Project' in JGS-JCES', contribution by K. Maeda, M. Ishihara and H. Mori, using materials from the Ministry of Land, Infrastructure, Transport and Tourism in Japan.

3.4.2 Piping erosion Yabe river 2012

Summary

This case concerns a breach due to backward erosion piping for a levee that contained a layer of gravel in the base of the levee.

Influencing local factors

- Internal erosion - Backward erosion piping:
  - No land side blanket so no uplift required for internal erosion;
  - Sand gravel layer in base of levee.

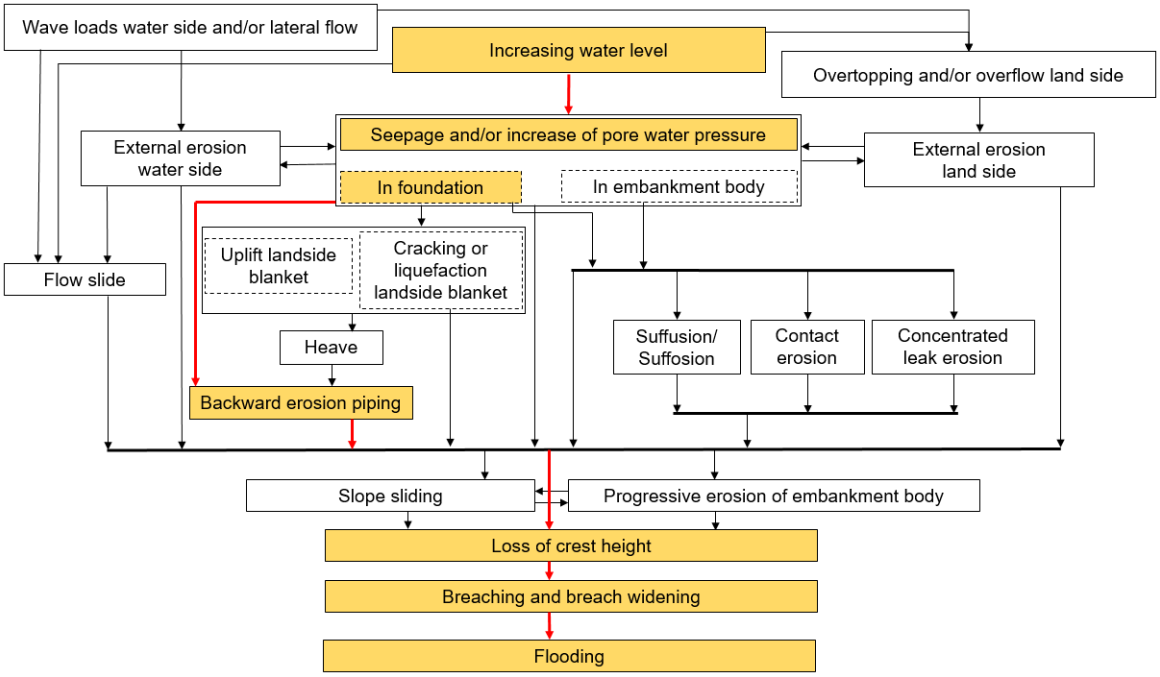

Figure 3.26 Failure tree Yabe river levee breach, 2012.

Case description

An example of levee failure due to piping erosion is illustrated below for a case on the Yabe river in 2012. In this example the high-water event caused erosion in a sand gravel layer at the base of the levee, which resulted in an eroded 'pipe' below the levee base. This resulted in collapse of the levee body and washing out of the levee, see Figure 3.27.

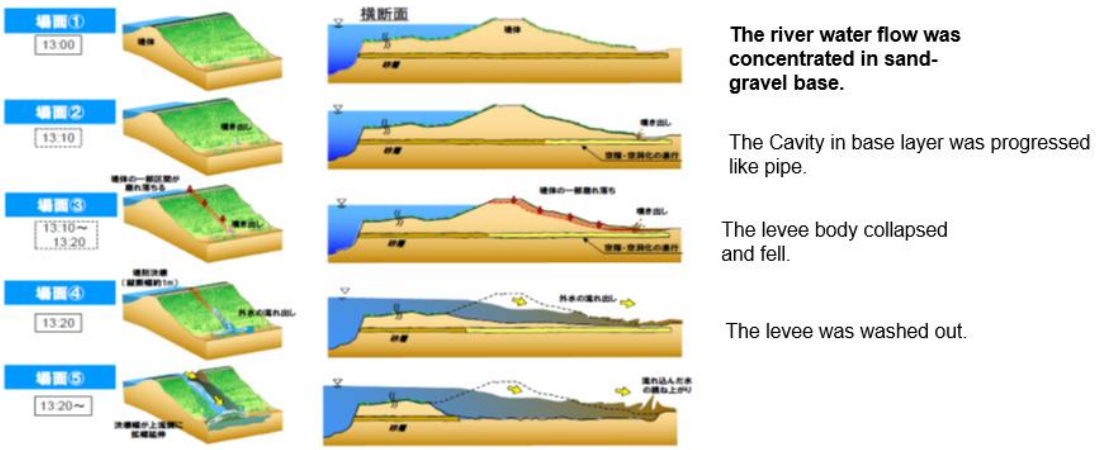

Figure 3.27 Example of piping erosion from the presentation 'Picture-Card Show Project' in JGS-JCES', contribution by K. Maeda, M. Ishihara and H. Mori, using materials from the Ministry of Land, Infrastructure, Transport and Tourism in Japan.

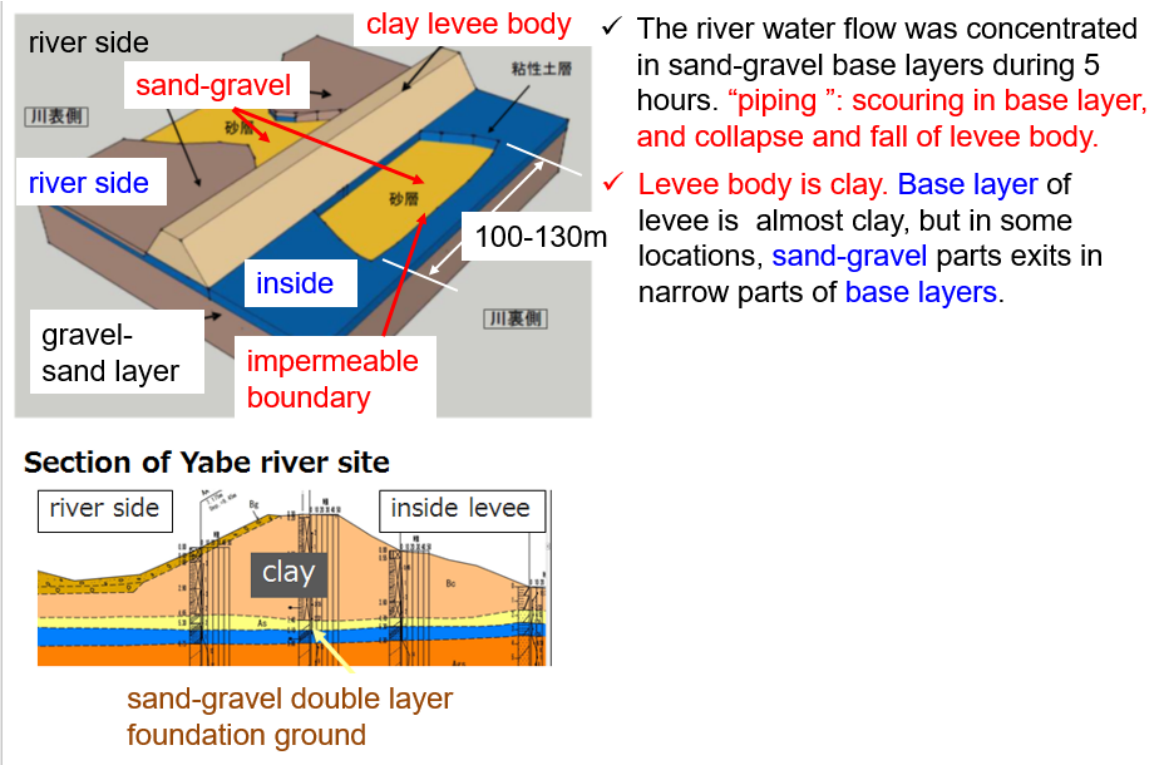

Figure 3.28 Example of piping erosion from the presentation 'Picture-Card Show Project' in JGS-JCES', contribution by K. Maeda, M. Ishihara and H. Mori, using materials from the Ministry of Land, Infrastructure, Transport and Tourism in Japan.

3.4.3 Several cases of overtopping erosion Typhoon Hagibis

Summary

This case concerns a breach due to overtopping that led to flooding at several locations during Typhoon Hagibis.

Characteristics

- For overtopping:
  - Different types of failure were distinguished, starting from the top of the inner slope, from the bottom and from the center.

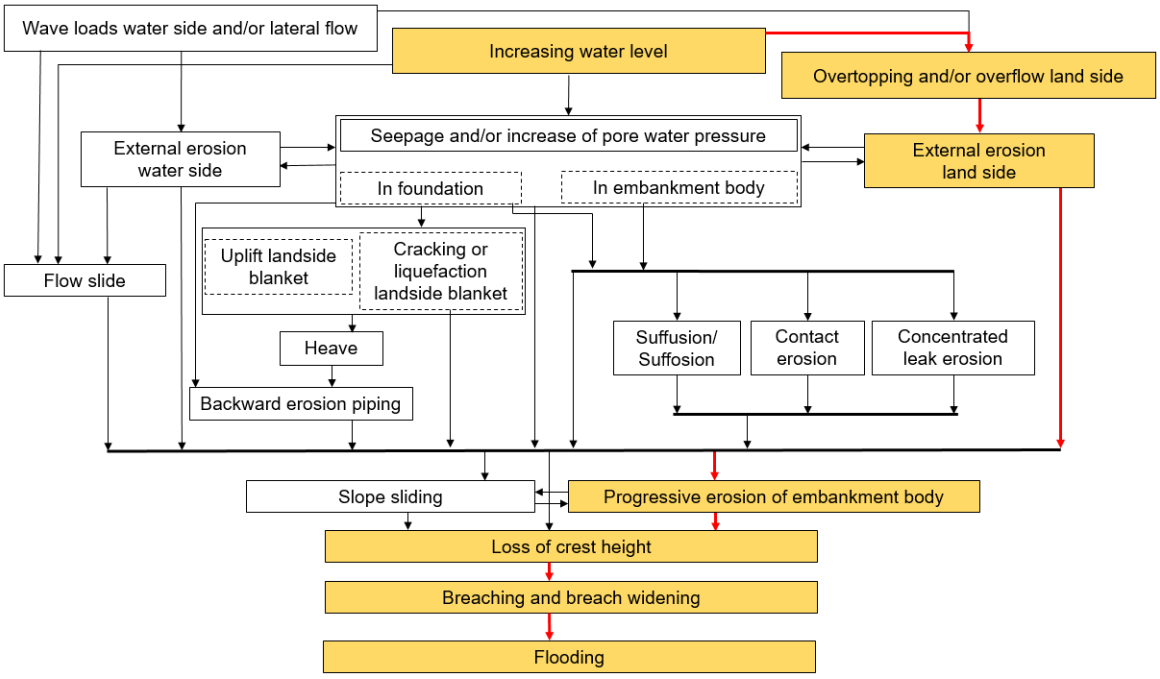

Figure 3.29 Failure tree Typhoon Hagibis, 2019.

Case description

Overtopping erosion was a main cause of breaching during Typhoon Hagibis, Typoon No. 19 in 2019.

Figure 3.30 Location of overtopping from the presentation 'Picture-Card Show Project' in JGS-JCES', contribution by K. Maeda, M. Ishihara and H. Mori, using materials from the Ministry of Land, Infrastructure, Transport and Tourism in Japan.

Different types of failure due to overtopping can be distinguished as shown below.

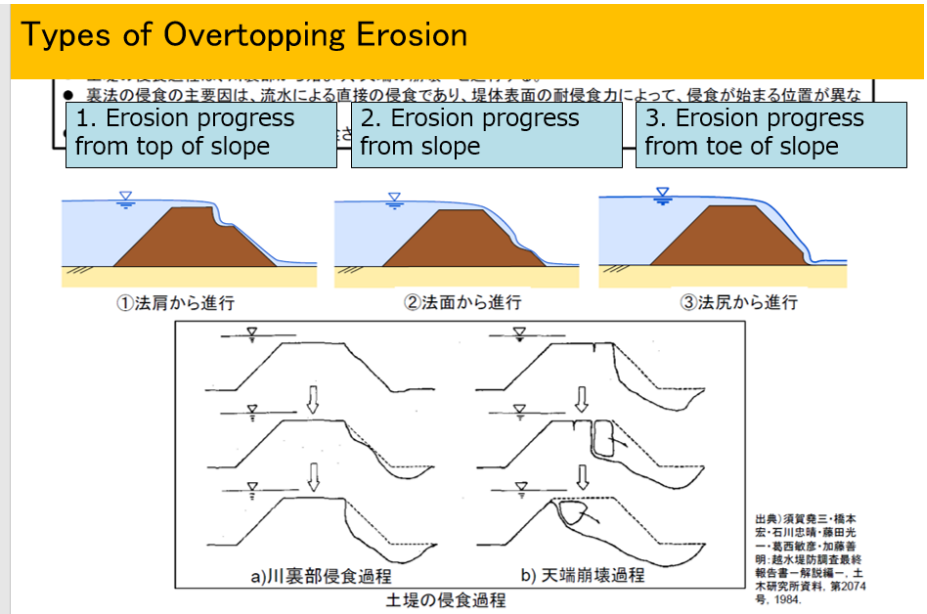

Figure 3.31 Type of overtopping from the presentation 'Picture-Card Show Project' in JGS-JCES', contribution by K. Maeda, M. Ishihara and H. Mori, using materials from the Ministry of Land, Infrastructure, Transport and Tourism in Japan.

The figures below show some sites where overtopping erosion occurred on the Kuma river in 2020.

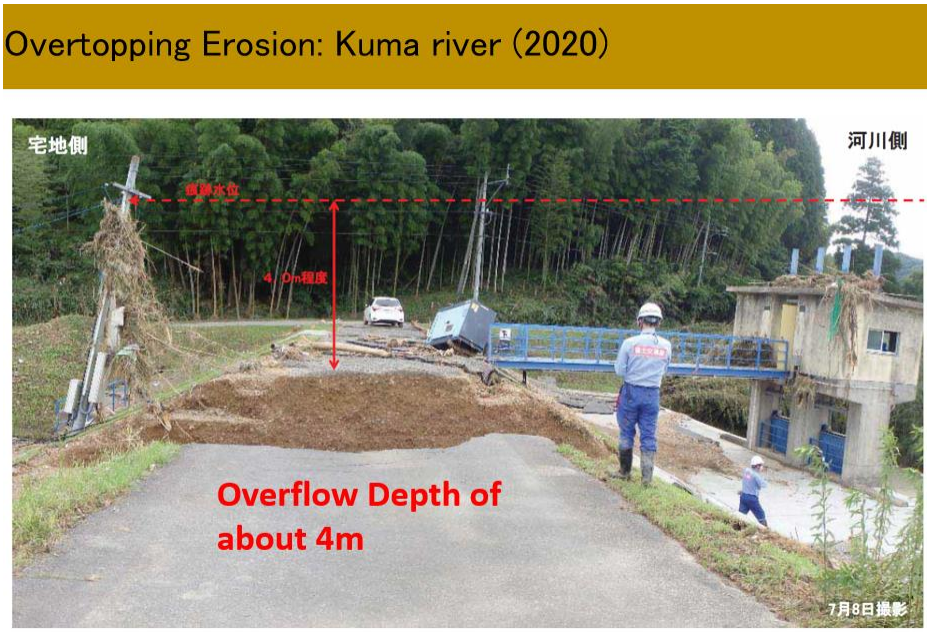

Figure 3.32 Picture of overtopping from the presentation 'Picture-Card Show Project' in JGS-JCES', contribution by K. Maeda, M. Ishihara and H. Mori, using materials from the Ministry of Land, Infrastructure, Transport and Tourism in Japan.

Figure 3.33 Example of overtopping from the presentation 'Picture-Card Show Project' in JGS-JCES', contribution by K. Maeda, M. Ishihara and H. Mori, using materials from the Ministry of Land, Infrastructure, Transport and Tourism in Japan.

3.5 Several cases of backward erosion piping from Hungary

Contribution by E. Imre (EKIK, Hydro-Bio-Mechanical Systems Research Center, and Bánki Donát Faculty, Óbuda University, Hungary), E. Koch (Széchenyi István University, Győr, Hungary), L. Nagy and Zs. Illés (BME, Hungary).

Summary

Several cases of backward erosion piping are described. From these cases a distinction is made between sand boils and 'fast' piping, the possibly liquefaction induced breach. The latter happens in a matter of minutes whereas in the former emergency response measures can be effective.

Influencing local factors

- Internal erosion - Backward erosion piping:
  - Thickness and packing density of the sand in the foundation of the levee;
  - Permeability of the river bed foundation;
  - Existence of old meanders in the subsurface (infilled with sand);
  - The presence of a cohesive cover layer to form a roof over the pipe;
  - Remedial measures, sandbags ringing the sand boil can be effective as emergency response measure.

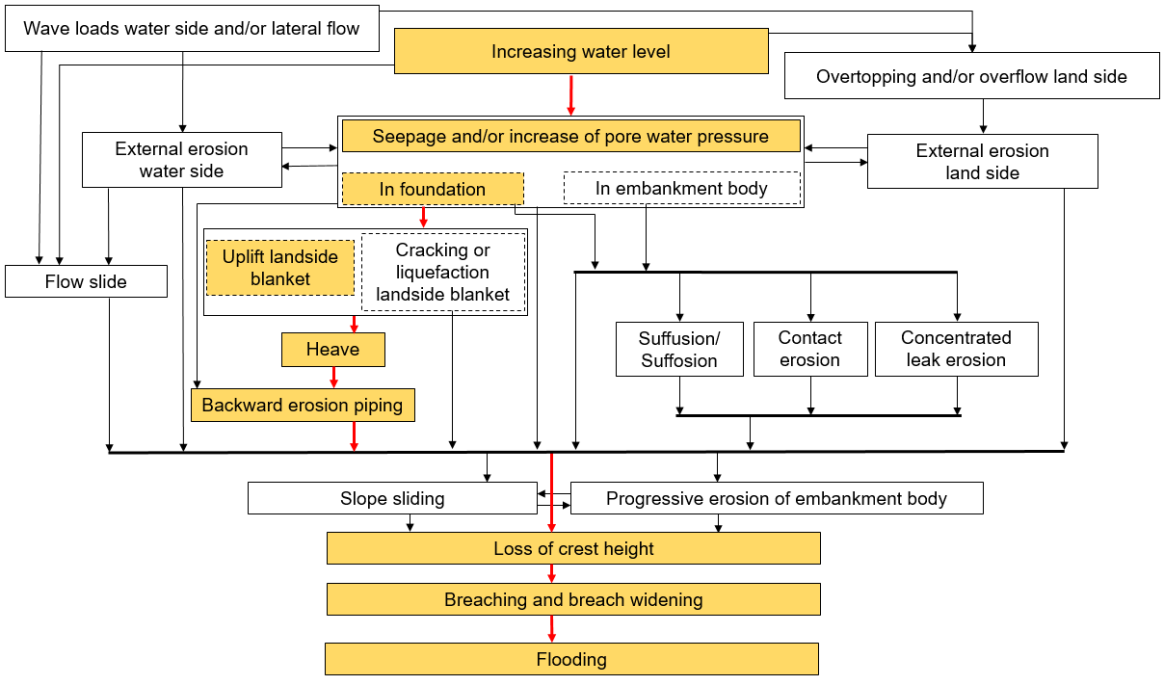

Figure 3.34 Assumed failure tree of several backward erosion breaches in Hungary.

Introduction

Experience to date ((Benedek, 1932), (Galli, 1955), (Szilvássy & Vágó, 1967), (Fehér, 1973), (Szepessy, Bogárdi, & Vastagh, 1973), (Szepessy & Fehér, 1981), (Szepessy, 1983), (Imre & Rétháti, 1991), (Imre E. , 1995), (Horváth, 2001), (Imre & Telekes, 2002), (Imre E. , et al., 2012), (Nagy, 2014), (Imre, et al., 2015), (Garai, 2016) and (Imre, et al., 2019)) shows that during major floods hundreds of sand boils may develop but only a small percentage may need

significant response measures and only a small fraction of these have caused breach disaster. These processes are still not very precisely understood.

Backward erosion and liquefaction piping may develop in a fine grained soil, with no cohesion, which is poorly graded and can be extremely loose. It is called „liquefiable sand" or „liquid sand" in Hungary. The current name of it is silty fine sand according to soil classification, earlier it was called *sand flour (Mo)*. It can be noted that this sand is simultaneously internally unstable based on the grading entropy criterion and liquefiable according to well-known criteria (Nagy, 2014) and (Imre, et al., 2019).

In thin layers of poorly graded sand, the increasing flood water level may lead to sand boils, which can be mitigated by counter-pressure. The event-tree can be seen in Figure 3.35. Remedial measures, i.e. sandbags ringing the sand boil, can be effective as emergency response measure if a protocol is followed to keep counter pressure. At the end of the flood the sand material of the ringing sand bags is used to fill the pipe followed by some additional measures.

In case of thick layers of loose, poorly graded sand, the flood may lead to 'fast' piping, failure within minutes/seconds. This means that after the observation of a sand mud geyser, a vortex funnel in the river simultaneously appears and moves towards the dike. The reason of breach is assumingly liquefaction according to (Szepessy, 1983) based on case studies 4, 5 and 6, which happened in 1954, 1965 and 1980 respectively. The pipe in the water side is formed along the least resistance, under minimum energy principle before the breach.

In this work it is found that case study 3, which happened in 1926, has a similar failure scenario and failure path, see Figure 3.35 as in case studies 4 and 5 except that in the 1926 case study there is an early stage of the flood with usual sand boils, which probably may occur if no clayey soil cover is present. The failure scenario was as follow.

- In the first days of the flood, small, usual sand boils occurred. This may occur if no clayey cover soil layer is present;
- Then the breach happened within minutes/seconds after the observation of first mud geyser, at the place of the first sand boil, and simultaneously a moving vortex funnel towards the dike in the river.

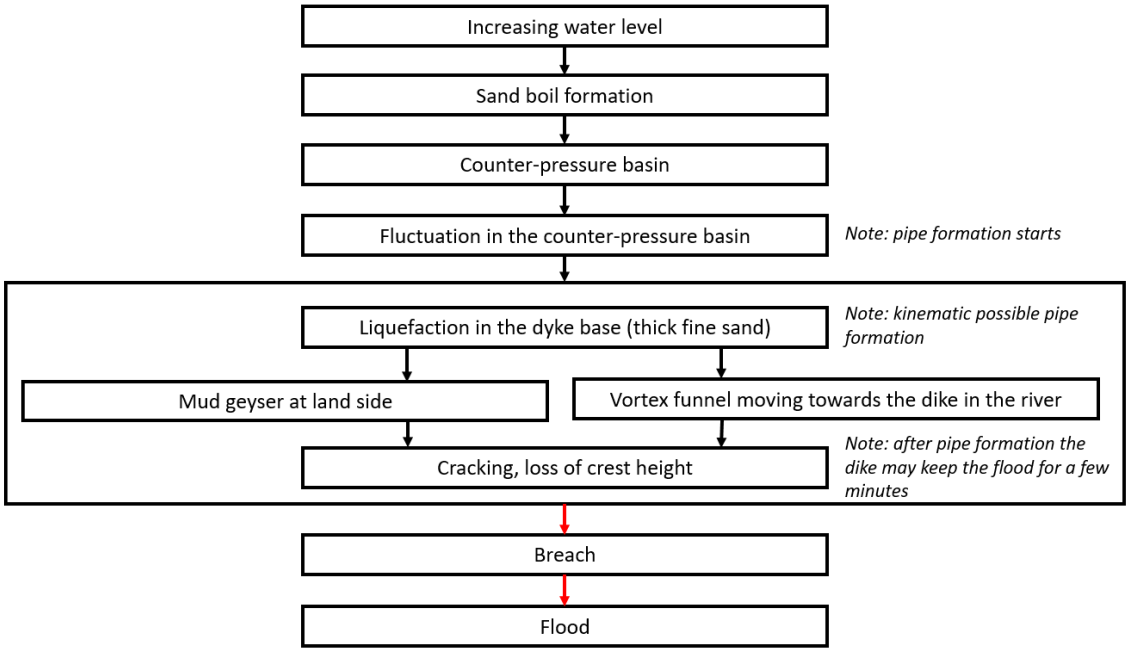

(a)

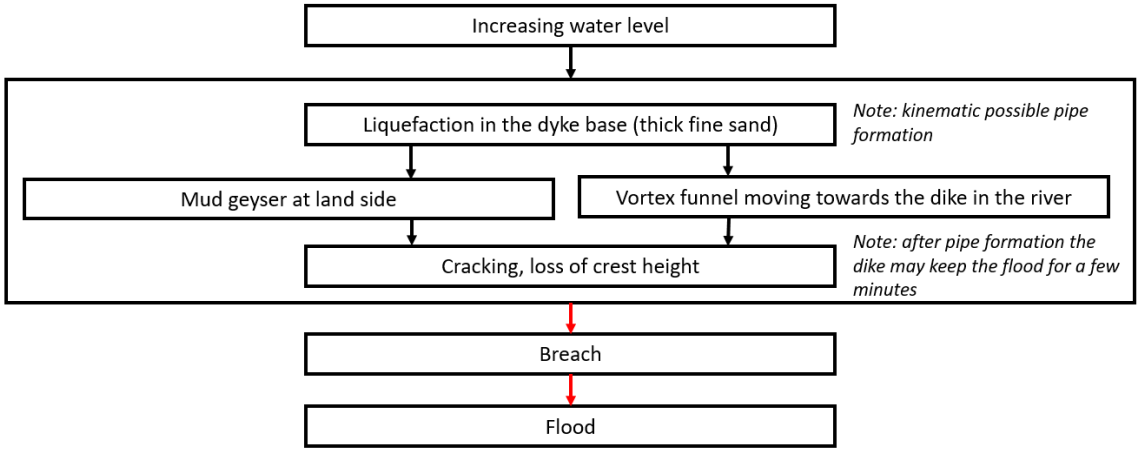

(b)

Figure 3.35 Fast piping, please note the thin (poorly graded) fine sand layers, event trees. (a) starting with normal sand boil, (b) starting with geyser. Fast piping after sand boil formation, which can be missing in case of clayey cover layer. It is a question if static liquefaction, dynamic liquefaction may occur or both.

Sand boil treatment

Protection (sand boil capture) is made mainly using sandbags to form counter-pressure pools. The measure at the sand boils is made by applying a proper counter-pressure pool water level with continuous observation. At high-water level, back pressure should be created on the land side, as it can be used to stop the particles moving out to be washed out. The more general defence protocol is based on reducing the hydraulic gradient by counter pressure, by increasing the leakage path length and draining the leaking water (see Figure 3.36).

At the beginning of the sand boil capture, the water head can be estimated. If the outflow water forms a dome with a height of 4-5 cm with respect to the ground surface, the expected height of the first counter pressure pool is about 1 m with respect to the ground surface, with 15000 to 20000 sandbags. Some general rules are as follows.

- A guard must stay at the sand-boil to watch it all the time.
- The outflow water volume, temperature and composition are measured, more than one counter pressure basin is built if needed for the new „children" sand-boils.
- No crashed stone is used in Hungary, although it could help.
- The change in the outflow indicates the pipe; it is varying periodically.
- Protection; A high-water level should be created on the land side, as it can be used to stop the particles from moving out to be washed out. This is typically done by using sand-bags to create a kind of pool.
- After the flood, the sand of the sandbags is used to fill the sand boil and cover the soil surface. Then additional measures may follow.

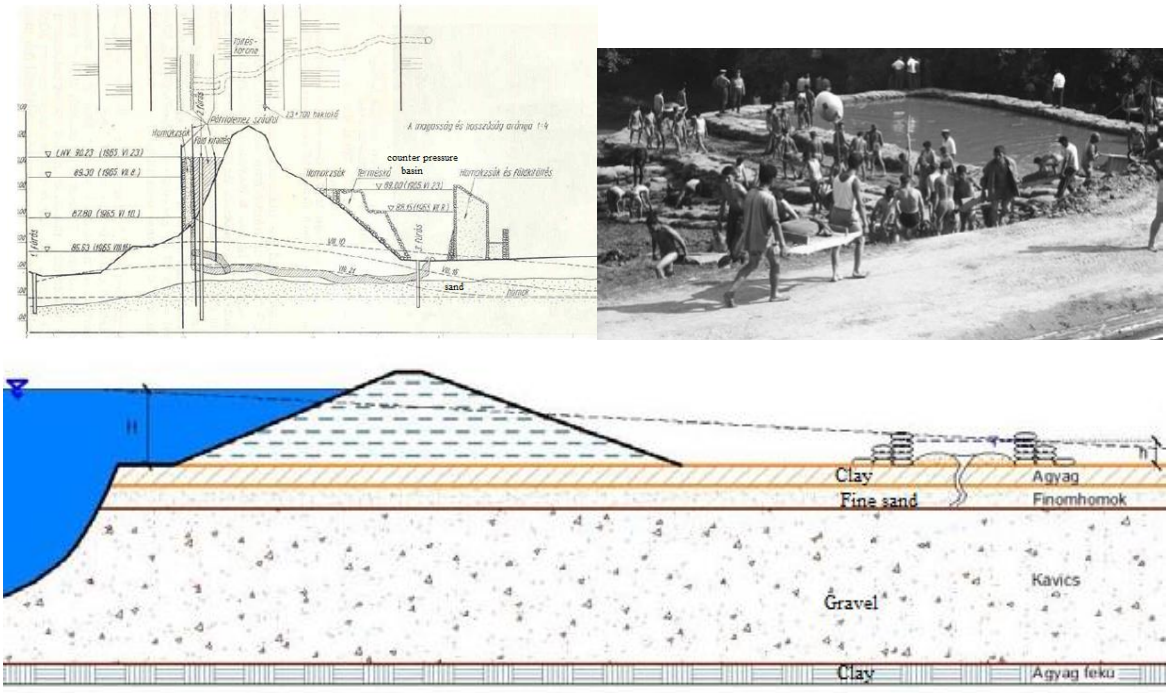

Figure 3.36 Danube, Margitta Island sand boil counter-pressure (top right) and diaphragm walls at the waterside (top left), the cause was the vicinity of an old meander (Garai, 2016). Water level of the counter-pressure basin (bottom).

Case descriptions

General

Hungary has the longest river dike system in Europe along the two big rivers (Danube and Tisza) and their connecting parts (see Figure 3.37). The main characteristics are as follows.

The Danube valley has a 0.5-6.0 m thick silty fine soil cover, which is prone to piping and liquefaction. The river bed is lying in granular soils. The dike material is sand on the northern part and silt on the southern part. The most frequent flood damage is piping.

Dikes of Duna river have the following leading dimensions. The height is about 6 to 8 m, the crest width is 4 m, the water side slope is 3:1, the landside slope is 2:1. The dikes have been built of silt (I_P=12-20%), sand or sandy gravel. Typical stratification under dikes comprises a sandy, silty cover overlying a highly permeable sandy gravel bad.

The subsoil of the Tisza-Kőrös valley varies from the granular (northern part) to the highly plastic (southern part). The dike material is granular soil on the northern part and of plastic soil on the southern part. The surface is generally covered by plastic soil.

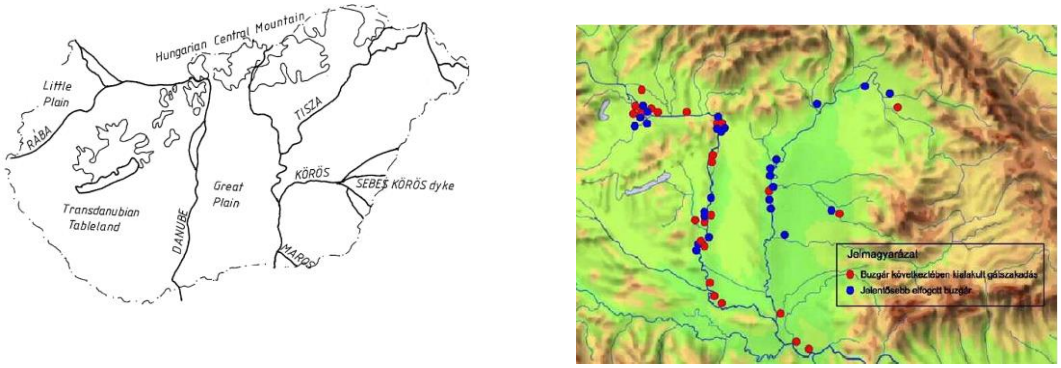

Figure 3.37 The big rivers and piping failures (red) and defended sand boils (blue) in Charpatian basin based on (Imre & Telekes, 2002) and (Nagy, 2014).

3.5.1 Sand boil case study 1: Dunafalva, Dunakiliti

Summary: No breach, typical slow piping layering and grading curves. Based on (Galli, 1955), (Szilvássy & Vágó, 1967), (Fehér, 1973), (Szepessy, Bogárdi, & Vastagh, 1973), (Imre & Rétháti, 1991) (Imre E. , 1995), (Imre & Telekes, 2002), (Imre E. , et al., 2012) and (Imre, et al., 2015).

Sand boils were observed at several locations along the Duna river in Szigetköz and Mohács areas in the flood period of 1965. Piping took place in the thin, poorly graded silty fine sand layers situated above the sandy gravel bed. Strange softening of the surface soil layer within some meter distance from the downstream toe was also observed.

Soil layers below the levee were explored at two piping sites: at Dunakiliti and Dunafalva (see Figure 3.38). The Danube valley has a thick silty cover: 0.5 m thick silt layer and a 0.5 m thick Mo layer were found above the sandy gravel layer at Dunakiliti (Mo is a soil category between silt

and sand in an earlier soil classification systems). Mo, silt, Mo and sand layers were found with thickness of 0.6, 0.9, 1.3, 0.2 m respectively, above the sandy gravel bad at Dunafalva. The grading curves are shown below.

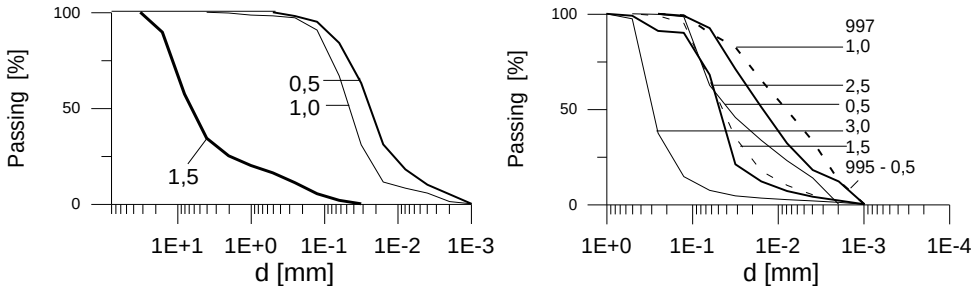

Figure 3.38 Grading curves for the (a) Dunakiliti soils and (b) the Dunafalva soils.

3.5.2 Sand boil case study 2: Tiszasas

Summary: No breach, extremely long flood period and sand boil defence. 1.8-2.0 meters water pressure was in the innermost backwater pool above the original terrain level. Based on (Nagy, 2014) and (Horváth, 2001).

During the flood in 2020, four sand boils had occurred along the largest flood control section 10.5 from which the section of 14+710 was the largest one. The sand boil of Tiszasas occurred on the 18th of April 2000, on the left side of Tisza (Nagy, 2014). On 16th of April it seemed to be a sand boil with 3-5 cm diameter which transferred little granules but clear water as well. In the next two days there was no protection added in this area.

The sand boil with 25-30 cm diameter arose 4 m from the land side levee toe. The height of the groundwater mound was almost the same. The discharge brought large amount of soil, in context of flood protection “material”, with little soil clots. The protection began immediately, soldiers of the nearby area were detailed to the site.

According to the workers the outbreak of the sand boil was not indicated. The moment the sand boil occurred, an eddy formed on the water side almost 30 m from the levee at the border of the forest zone.

43 people, who were on the site, started to create a 5-row counter-pressure basin. The surface of the water was strongly bubbling and it transferred granules. According to the protection group, the capturing of the sand boil lasted till 12:30 and was 1.7 m high.

A secondary sand boil arose with a quite strong blow-up under the counter-pressure basin around 3:00 pm. Therefore, the water level in the counter pressure basin, which was already built up, lowered almost by 0.5m in a few minutes. The power of the blow-up was very concerning. Construction of the counter-pressure basin of the first cassette was carried out by soldiers and civils, its walls were 3 sandbags wide and 8 high. The basin of the first cassette fitted the previous semi-circumference shaping. Then, there was a need for building a new counter pressure basin (2nd cassette) in order to prevent another failure (see Figure 3.39).

Figure 3.39 Counterpressure basin for related cassettes (left) and location of sand cassettes (right).

There was a strong water blow-up in the first cassette at 3:00 pm (Nagy, 2014) and three rows were added to provide the counter pressure, meanwhile the water level started to lower in the first counter-pressure basin. Due to the lifting the blow-up stopped. However, the water started to foam heavily, and thick, brown foam occurred at the surface of the water from the first counter-pressure basin.

The 3rd cassette, fitting the 2nd cassette as well to the counter pressure basin, was built up in order to prevent another failure. Namely opaline coloured water blowed up from the base of the basin. The height of the 1st cassette was increased to the level of the counter-pressure basin with the same leakage level in order to make an immediate locking up possible in case of a failure in the counter pressure basin. The overtopping in the counter level stopped for a while and afterwards it started again.

The overtopping stopped in the cassette between 8:00 and 8:30 am, the water level lowered 10 cm when the eroded soil, made by the secondary sand boil, occurred. At the same time, the water in the counter pressure basin became blurred. The lifting of the basin level's height (by four rows) was carried out. In the 1st cassette the water level was arising slowly, but it did not top over. The height of the counter reservoir's water column was lifted at the same time with the cassettes' leakage level (with 1-2 rows) taking constant attention of the stability.

Two days later the water side of the levee collapsed because of a trailer tractor in the early morning. The soil was lifted by handwork from the collapsed area, which was 1.2 x 1.5 m wide and 1.4 m deep. The wall of the hole was widened like a bell-shape by a defined failure surface. The walls were hard but after hitting them they had a rumbling sound effect. The refilling was made with the help of sandbags.

Based on the measurement of the eroded material it could be stated that three cubic meter soil left the levee. This soil is missing from somewhere. The collapse by the tractor in the morning made clear that regarding the stability of the levee it is very dangerous if the soil is eroded in a larger quantity. Therefore, a mass balance is needed with the help of an approximate method. Most part of the eroded material could come from the collapse. In fact, it was satisficing to know the origin of the eroded soil.

In the afternoon a trimming cassette (shape like a horseshoe) fitting the levee was constructed. The four-sandbag wide trimming cassette embraces all cassettes 2 m away from each other.

Divers arrived at the site and they found the supposed opening hole of the sand boil quickly, which was approximately 3 m far from the waterside crest edge. After filling the opening hole with more than 30 sandbags they started foiling the waterside.

Thanks to the lowering water level of Tisza, the sand boil as well as the water of the cassettes subsided further during the night, in so much that a crater occurred in the sand boil. There was a little functioning sand boil in the crater, but the leaking water disappeared between the sandbags. The water level in the crater of the sand boil was 2.7 m lower than the water level Tisza river.

Soil investigation showed that basically the embankment was constructed by fine grained soil, but a layer of transitional soil was also discovered. The layers of the embankment and the upper part of the subsoil were relatively mixed. There was a clay layer from 5.9 m beneath the crest, which had absolutely nothing to do with the occurrence of the sand boil. The site investigation also showed that the problem is not the sand boil in the subsoil, but it appears that the pipe formed in the dike body.

Based on the washout soil, which was more than two cubic meters, a sieve analysis was carried out. The uniformity coefficient of the silty sand was C_U = 2,74, d_{80} = 0.11 mm. The opening of the sand boil could only take place at the beginning of September. The cut through the levee showed the stratification and the path of the sand boil, which was first deep at the bottom and then it went up the waterside. Figure 3.40 shows the investigation and suggested that the sand boil occurred in a thick silty sand layer, which was covered with arched clay.

Figure 3.40 Opening of the sand boil.

The sand boil of Tiszasas proved that the big as well as the medium-sized sand boils always need to be constantly observed and measured. These measurements must be analysed. A decision can only be made based on the observations. The measurement possibilities are limited regarding the fact that the stability of the levee cannot be endangered. Therefore, possible measurements are: observation of the surface like the blurriness of the water of the counter pressure basin, the temperature and amount of the leaking water, the amount of eroded soil from the counter pressure basin as well as its development in time. The behaviour of the levee must be valued based on these factors. Probably the great sand boil of Tiszasas is the only one in the world which has a Memorial (see Figure 3.41).

Figure 3.41 Tiszasas sand boil on 1st of May (*left*) and *memorial of Tiszasas sand boil* (*right*).

3.5.3 Piping breach case study 3

Summary: Ended in fast failure approximately five days after the first sand-boil, deep and large diameter pipe development in 1926. Based on (Benedek, 1932) and (Nagy, 2014).

A few days before the dam breach, a sand boil was spotted 10-12 m from the land side toe of the embankment. According to their well-established method, a barrel was put on the spring, and the barrel was reinforced by protective material. At the same time a boat about 10 m long and 2 m wide was put on standby. A water funnel or vortex about 30 m on the upstream side appeared, which was constantly approaching to the embankment. When it approached the levee at 15-20 m, the boat allegedly began to tilt into the vortex, his nose up and made the path dived under water and reached the other side of the dike Figure 3.42.

The scenario in detail:

- 5 days before breach: sand-boil at 12 m distance from the land side toe. A counter pressure basin was used;
- 2 days before breach: the water level in the counter pressure basin started to oscillate indicating pipe formation, therefore, defending material (boat to sink if needed, piles, sand bags, piles etc) was carried over there.
- Breach day: The breach happened as follows within some minutes. A mud geyser appeared at the spot of the first sand boil. Seeing this, the chief engineer immediately ran up to the embankment crest and glanced at a funnel about 30 m from there, which was constantly approaching the embankment (see Figure 3.42). He allegedly set the boat perpendicular to the embankment and carried earth sacks in the tail of the boat to sink (see Figure 3.42). During this time, there were again two to three volcanic muddy water eruptions at the land side and these were already stronger than the first.
  When the vortex water funnel - constantly approaching the embankment - was in 15-20 m away from the crest, the boat according to observers began to tilt, his nose staring at the sky and made a path marked with numbers while diving under the water. Reports from the time indicate that the boat appeared on the other side of the levee. Subsequently the crest began to crack. At the same time, the embankment settled to a length of 8 to 10 m, the water began to flow into the saved area, and the dike breach soon widened to 80 to 100 m. The depth of the washout at the rupture site was 24 m below the level of the flood.

a)

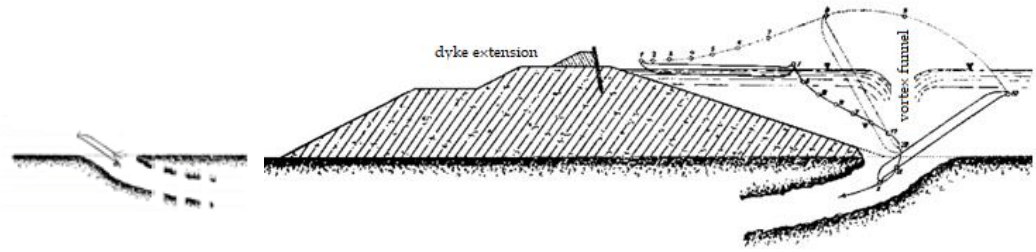

b)

Figure 3.42 Illustration of the boat diving to the pipe, (a) condition some minutes before breach, (b) the path of the boat, which ended on the land side at around the first sand-boil spot.

3.5.4 Piping breach case study 4: Hosszúfok

Summary: Fast piping, 5 minutes after the first geyser. Based on (Szepessy & Fehér, 1981), (Szepessy, 1983) and (Nagy, 2014).

At the river Kettős Körös, Hosszúfok, in 1980, the dike guards who were responsible with observing damages during this flood did not notice any signs of damage until early Morning on July 28, 1980.

At 6:35 a.m., the guards were about 100 m away when a very strong water geyser spurt was observed. The water, they reported, was "black and thick muddy." The dike burst took about 5 minutes. Width of the tear grew rapidly, reaching a final width of 78 m. This was the first dike failure where detailed soil mechanical exploration was made afterwards. What happened was possibly a dynamic liquefaction of the extremely loose and thick sand lens, at the thickest dimension of the layer. The possible dynamic effect was the tearing off the clay cover layer at the first geyser spot and the sudden displacement of the dike body due to the increased horizontal load.

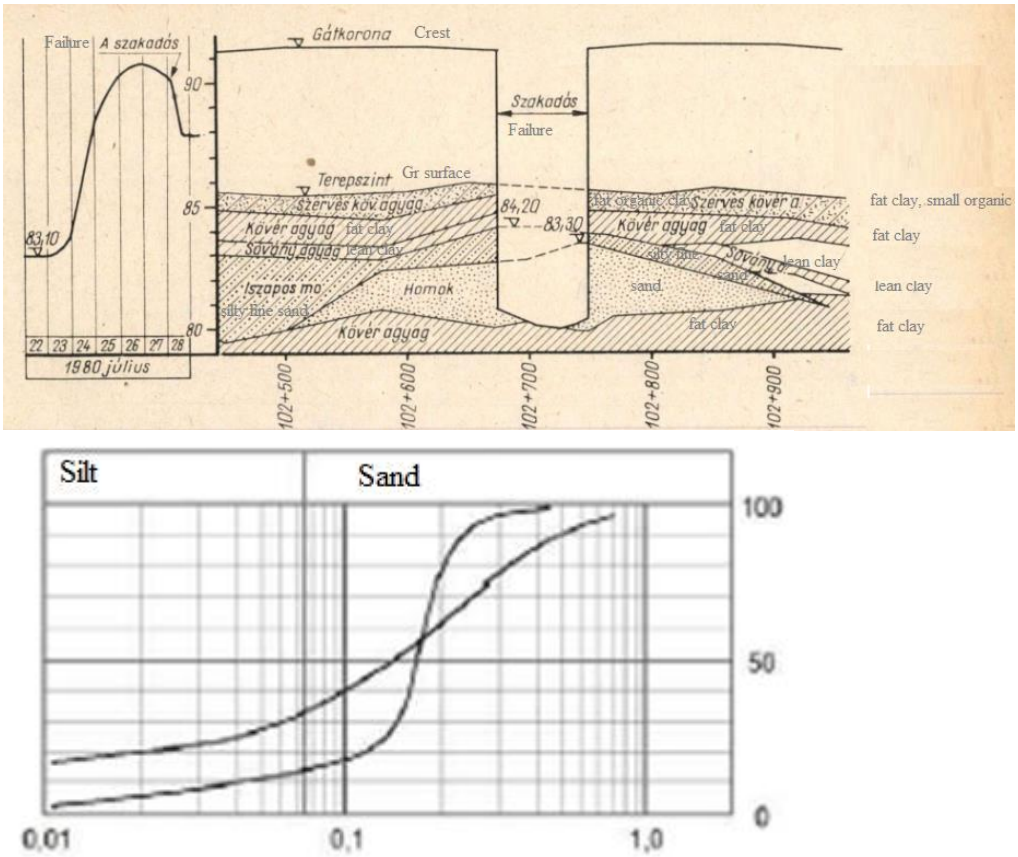

Figure 3.43 Kettős Körös, Hosszúfok in 1980, fast piping failure, failure location at top from (Szepessy, J.(1983)), with time history of flood. Bottom: grading curves, indicating the very loose sand inclusion with 3<Cu and e~0.8.

3.5.5 Piping breach case study 5: Ásványráró, Csicsó

Summary: Fast piping, breach few minutes after the first geyser type sand-boil. Based on (Szepessy, 1983) and (Nagy, 2014).

The first observed event is a 0.5 m diameter geyser suddenly appeared at 5 m from the land side toe, throwing off the cover layer. Within 2 seconds, the pipe reached the riverside since a vortex funnel developed at the river approaching the dike and then the dike collapsed. In this case, the poorly graded silty sand layer was extremely loose and thick (15 July,1954 at Ásványráró). A similar case occurred in 1965 in Csicsó, but there is no precise description. Some information indicated that in these environments several smaller sand-boils appeared beforehand, which were not mitigated by counter-pressure basins properly due to the lack of workers. This comment is not changing the fact that the fast piping occurred starting from a water geyser that suddenly appeared, not from a usual smaller sand-boil and the failure was extremely fast.

Sand boil research

There is a general experience that hydraulic failure in an upward flow can occur at much lower hydraulic gradients than the well-established theoretical critical hydraulic gradient value. In the following some explanation and experimental result supporting this explanation are presented.

(Garai, 2016) states that the equilibrium requirements on a micro level controls the start of the sand boiling. Garai agrees that the whole grading curve also influences the process. If the grains are spherical the relevant equation was derived from employing Stokes law.

Conditions influencing the formation of the sand boil were examined in 1957 as part of its research program by VITUKI. The aim of Hugo Lampl's experiment (Lampl, 1959) is to provide useful results by learning about the different phases of sand boil formation.

The key role of the fine grains at the start of the sand boiling is supported by the laboratory tests of (Lampl, 1959), who reports on the experiments carried out to determine how the presence in different percentages of the silt fraction between 0.01 and 0.1 mm affects the sand boil formation and the percentage of silt content for which piping will not occur. Lampl found that sands with a silt content of larger than about 7% are generally no longer dangerous for the formation of piping. The following noteworthy phenomena were observed:

- The finer-grained materials before the starting of the sand boil may swell to about 1-3% of the layer thickness.
- The moment the sand boil is broken, the hydrostatic pressure is sudden decreases, but the amount of flowing water increases.
- With a fall in river level the sand boil can be deactivated, and when the river level increases, the sand boil starts again.
- If after a certain time the experimental layer is pressurized again, the sand boil bursts again in the same place. In the next flood event, the re-braking of the sand boil is prepared in a fixed position.
- The particles are segregating according to their sizes in the hole. According to (Lampl, 1959), the size of the grains in the formation of the sand boil may show segregation. The larger gravel grains in the sand boil chimney are below and grains are arranged upwards in ascending order of magnitude.
- As a by-product, the results of the tests showed that the permeability of the otherwise good water permeable washed sand (4 10^{-4} m/s) decreased strongly with an increase in fine grain fraction. According to the experiments, the presence of 5% fine grains reduced the value of the permeability, k, to 1.6 10^{-4} m/s. The fine grains content of 7.5% to 10% reduced k below 8.4 10^{-5} m/s.

Evaluation of piping case studies

a. Sand boil
   The sand-boil formation is related to poorly graded, fine sand. The pipe formation may be related to backwards and tunnel erosion, which may be aided by the increment of shear stresses and static liquefaction. The pipe formation can be very fast, aided by the fluidization of a whole layer due to liquefaction, depending on geometry and soil density.

b. Slow piping with tunnel or backwards erosion
   In Danube delta, slow piping may occur in the case of a thin layer of poorly graded fine sand (see site geometry in Figure 3.44). The sand boil is started by individual grain movements on a micro level due to upwards seepage forces.

c. Fast piping with liquefaction
   Fast piping may occur in the case of thick layer of extremely loose and poorly graded fine sand, generally in the vicinity of some old river bend crossings (see Figure 3.44 and Figure 3.45). The breach may happen within seconds/minutes of observation of the

first muddy geyser on the land side and simultaneously appearing vortex funnel in the river. The vortex is moving towards the dike, the process is controlled by liquefaction of the soil in the whole fine sand layer.

The liquefaction may be caused by the following effects: high pore water pressure in the dike base, the tear off the clayey cover layer or slope instability (i.e., sudden shear strain increment of the dike base, due to the increased load, cracking of the dike, gradual saturation of the dike material).

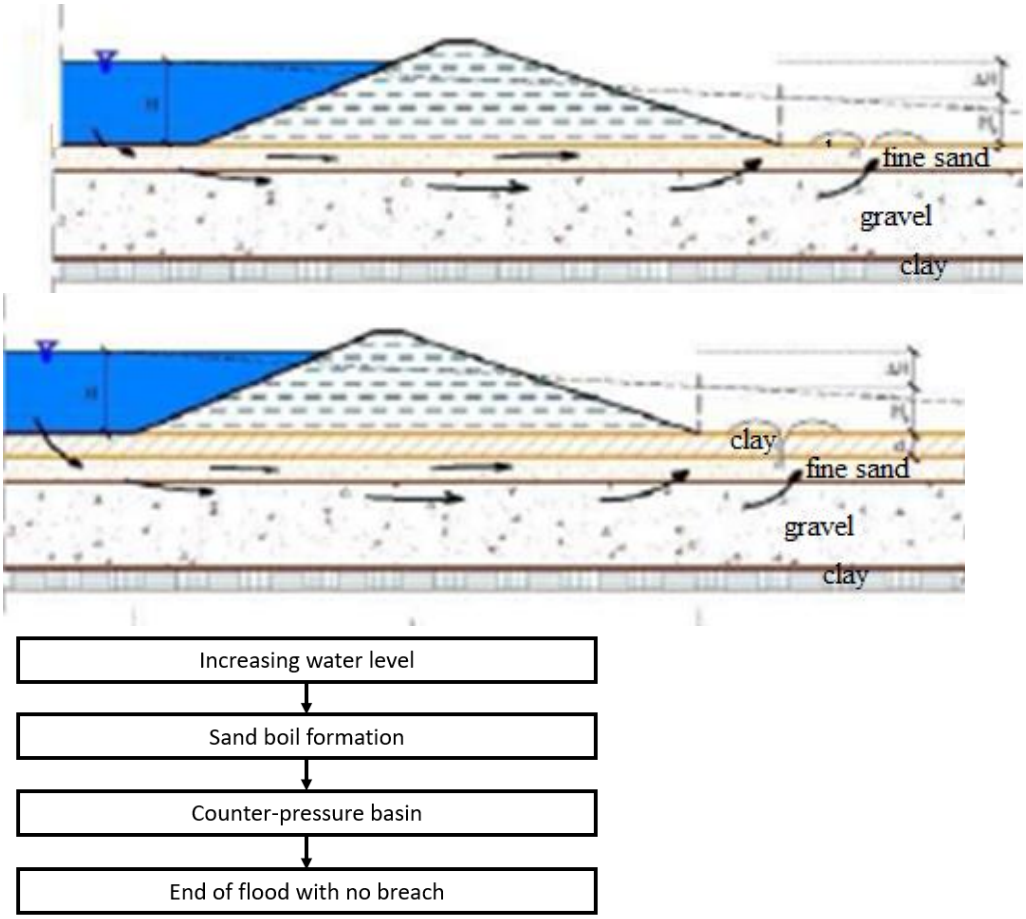

Figure 3.44 Event tree of slow piping in 2 and 3 -layer systems, please note the thin (poorly graded) fine sand layers.

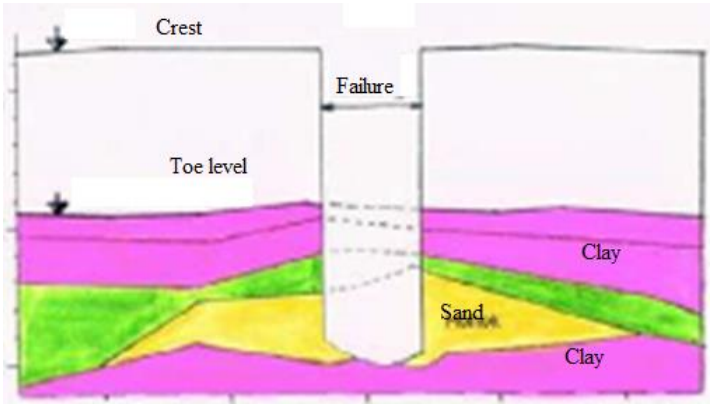

*Figure 3.45 Fast piping in case **of thick and loose cover layer**, deposited in an old meander with arching; this process may start with a sand boil in case of a clayey cover (adapted from Szepessy, J, 1983).*

Conclusion
Neither the two different processes of piping failure („slow“ or „fast“) nor the sand boil formation are completely understood. The role of a definite poorly graded fine sand layer, its density and its layer thickeness are some of the main factors. Likely some micro-level modelling may explain the starting and formation of a sand-boil and some optimum modelling may explain the fast piping. The slow piping is deeply related to the increase in shear stress level and the decrease in shear resistance in the dike base and around the toe.

3.6 Breach on the Agly river levees in 1999, sand boils in more recent floods

Contribution by R. Tourment (INRAE, France)

Summary

This case concerns levees along the Agly river. A breach in 1999 caused by overflow is described, as well as evidence of internal erosion in the form of sinkholes and sand boils for locations where there was no breach (Zwanenburg, et al., 2018).

Influencing local factors

- Overtopping and/or overflow land side:
  - For some locations, erosion due to overflow on the landward side was stopped by the road revetment on the crest;
  - Settlement due to internal erosion (pipe crossing the levee) aggravated the erosion due to overtopping. This was local, as overtopping did not lead to failure at other locations.
- Internal erosion in the embankment body (contact erosion or concentrated leak erosion):
  - Pipe beneath the levee cause seepage along the pipe;
  - Old structures inside the levee (rocks, walls, etc.) caused seepage through the levee.
- Uplift and cracking land side blanket:
  - A layer of rather impermeable materials in the foundation of the levee that extends in the protected area (land side) and covers the non-cohesive alluvium (sand, gravel, etc.) of the foundation. This results in sand boils.

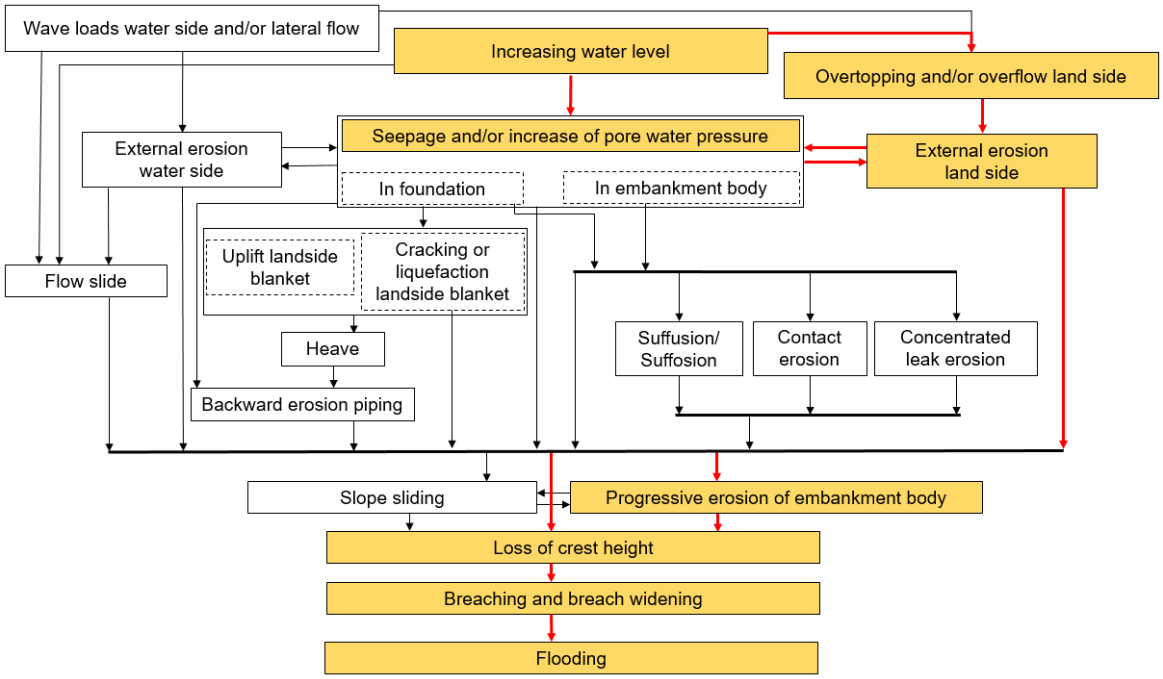

Figure 3.46 Failure tree 1 of several possible failure paths along the Agly river, 1999.

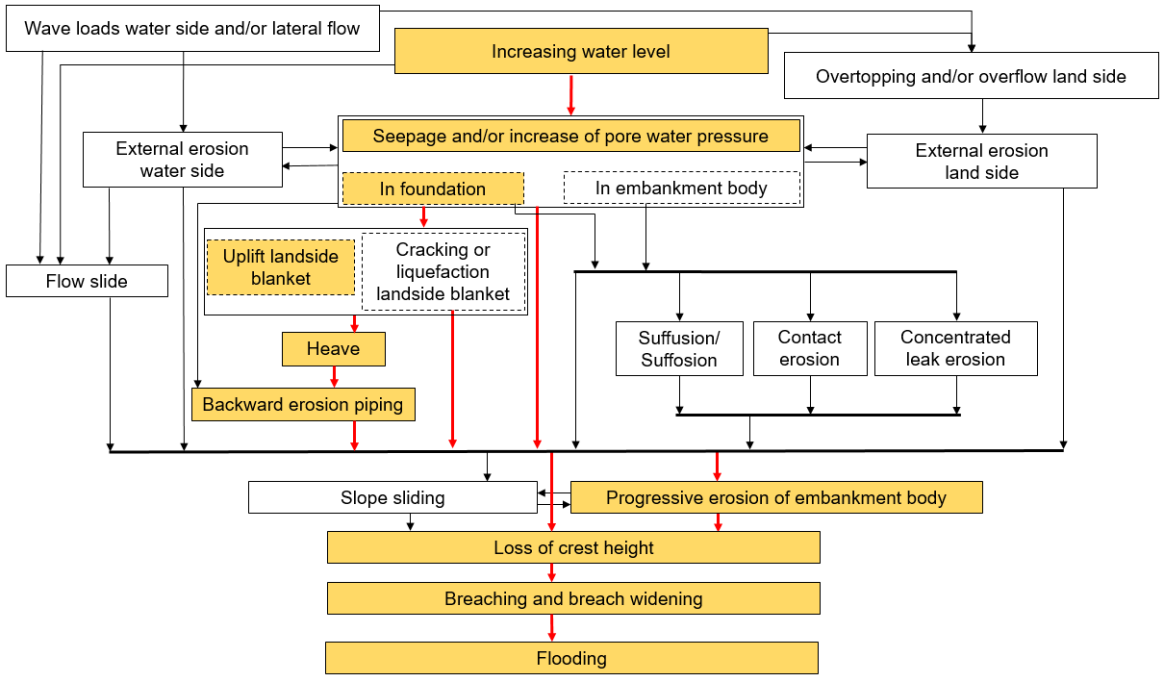

Figure 3.47 Failure tree 2 of several possible failure paths along the Agly river, 1999.

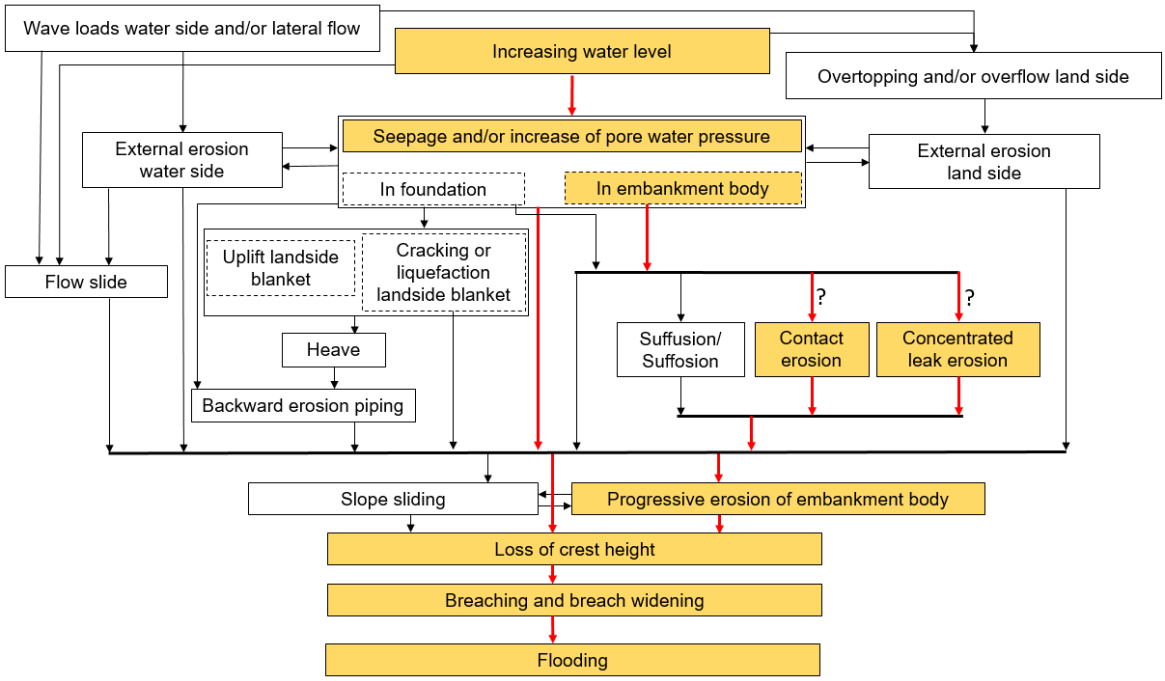

Figure 3.48 Failure tree 3 of several possible failure paths along the Agly river, 1999.

Case description

The downstream section of the Agly river in the Pyrénées Orientales (66) region in France is surrounded by levees close to its minor bed. This part of the river is 13.2 km long. It is situated in the maritime plain downstream of a mountain area that is prone to intense rainfall: 200 mm in a single day is a common event, and the recorded maximum was 840 mm in 1940. In 1970, the riverbed was re-profiled and the levees were built to its current configuration. The protection level is 1250 m^3/s, which is a 1/30 annual probability. The presence of abundant vegetation here has a major effect on the discharge and water level rating curve. Safety spillways were included in the initial plan but not built: the levee system is not resilient to overflow. A dam was built upstream in 1992-1994 to control flooding.

In recent years, these levees have been impacted by major floods which, in some cases, resulted in damage and breaches: specifically, in September 1992, November 1999, November 2005, January 2006, March 2013, November 2014 and January 2020. The damage during each of these events is described in detail in (Zwanenburg, et al., 2018), (Tourment, et al., 2018) and Tourment, Mallet, Patouillard, & Salmi (2022).

During the 1999 flood, the upstream dam managed to contain the entire flood in its catchment area: about 40% of the total catchment and overflow from the river bed happened upstream of the leveed section. Even given this reduction in discharge, the flood in the lower (leveed) part of the river was still the highest since the levees were built. The annual probability of the event was estimated at 1/100, with 2000 m^3/s at Rivesaltes.

The levees were submerged on several kilometres: ten places were identified with an overflow head of 20 to 30 cm for about two or three hours. There was severe damage as a result of overflow, but also caused by internal erosion, external erosion and instability. The event obviously exceeded the design level of the levees.

Detailed reporting of the damage can be found in a report from Cemagref (internal report, 2000). There was a breach near a sewage treatment plant that was attributed to the general overflow (see Figure 3.49). But it is possible that the presence of a pipe beneath the levee caused the breach here rather than in any other element of the system. In many places, the landward side of the levees was completely eroded due to overflow and erosion was only stopped by the road revetment on the crest.

Figure 3.49 Breach in 1999 at St-Laurent-de-la-Salanque.

There was internal erosion in some places as well, as shown by some sinkholes and subsidence on the crest or traces of sand boils in the land alongside the levees. These internal erosion problems were mainly in the foundations, but they were also observed in the levees themselves: some seepage through the levee was also observed in areas where there were either intersecting pipes or old structures (rocks, wall) inside the levee.

Works after the event included repairing the breach, repairing the eroded land slope (with drains and compacted fill) and repairing the damaged toe protection. Some non-exhaustive work also took place to prevent leakage (masonry on the river side) and sand boils (drainage and seepage system) in different places for each of the problems.

The 1999 breach has been caused by overflow at the location of the waste water treatment plant where internal erosion along a pipe crossing the levee also took place. This pipe probably aggravated the situation, because many other parts of the levee also were damaged by overflow but did not breach. Figure 3.50 shows this in the form of a diagram. It is even possible

that the two main mechanisms (external erosion and internal erosion) had some interaction and mutually furthered themselves, as both external erosion and internal erosion have a negative effect (saturation) on the remaining part of the levee and so aggravate the vulnerability of the material to the other mechanism.

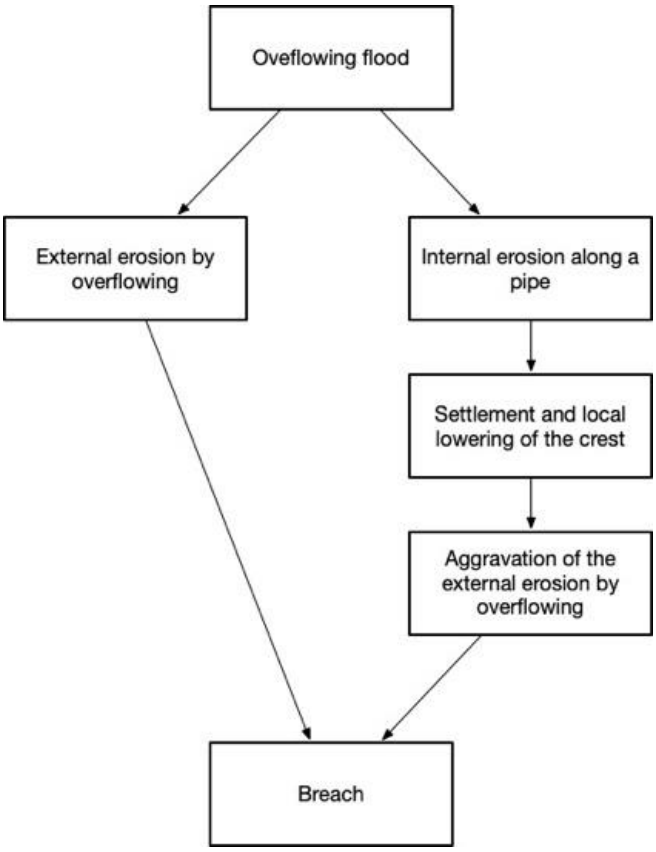

Figure 3.50 Failure path for the 1999 Agly breach (Rémy Tourment).

Given the multiple intense floods that affected the levees and the severe deterioration and damage that can be observed after each of these floods, the Agly levees can be seen as a "real size laboratory" in terms of analysing failure mechanisms and scenarios. A lot of thought is now given to the role of seepage in the foundation, the subsequent sand boils and the various subsequent deterioration mechanisms that can be observed after each intense flood, like instability, sinkholes (see Figure 3.51), aggravation of external erosion by overflow, etc. These sand boils appear in areas where there is a layer of rather impermeable materials in the foundation of the levee that extends in the protected area and covers the non-cohesive alluvium (sand, gravel, etc.) of the foundation, see Figure 3.52. Strangely, after floods, under the resulting sand "volcano" where there was a sand boil and no further development, the top layer of the foundation is again whole and cohesive, which makes the actual mechanism(s) for the failure of the top foundation layer somewhat uncertain. We can nonetheless analyse the resulting scenarios initiated by the failure of this top layer, as seen in Figure 3.53.

Figure 3.51 Sinkhole on the levee crest (Photograph by Patrice Mériaux).

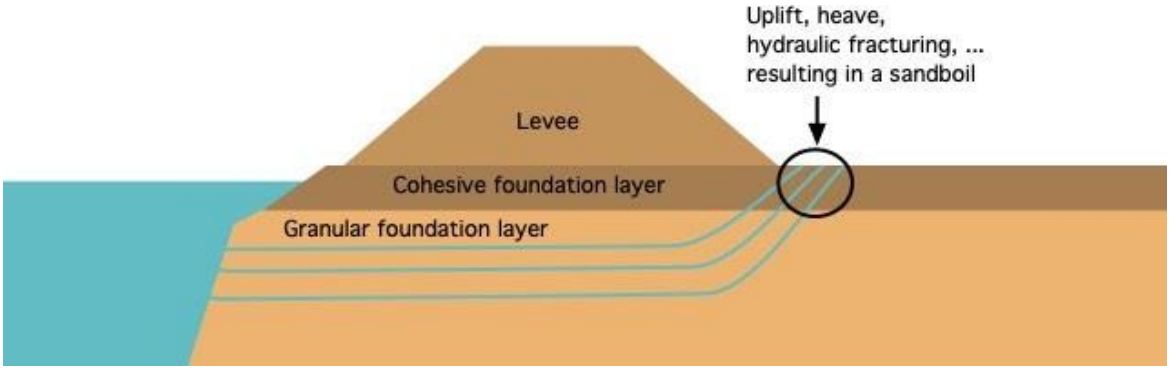

Figure 3.52 Foundation configuration where sand boils may appear (Rémy Tourment).

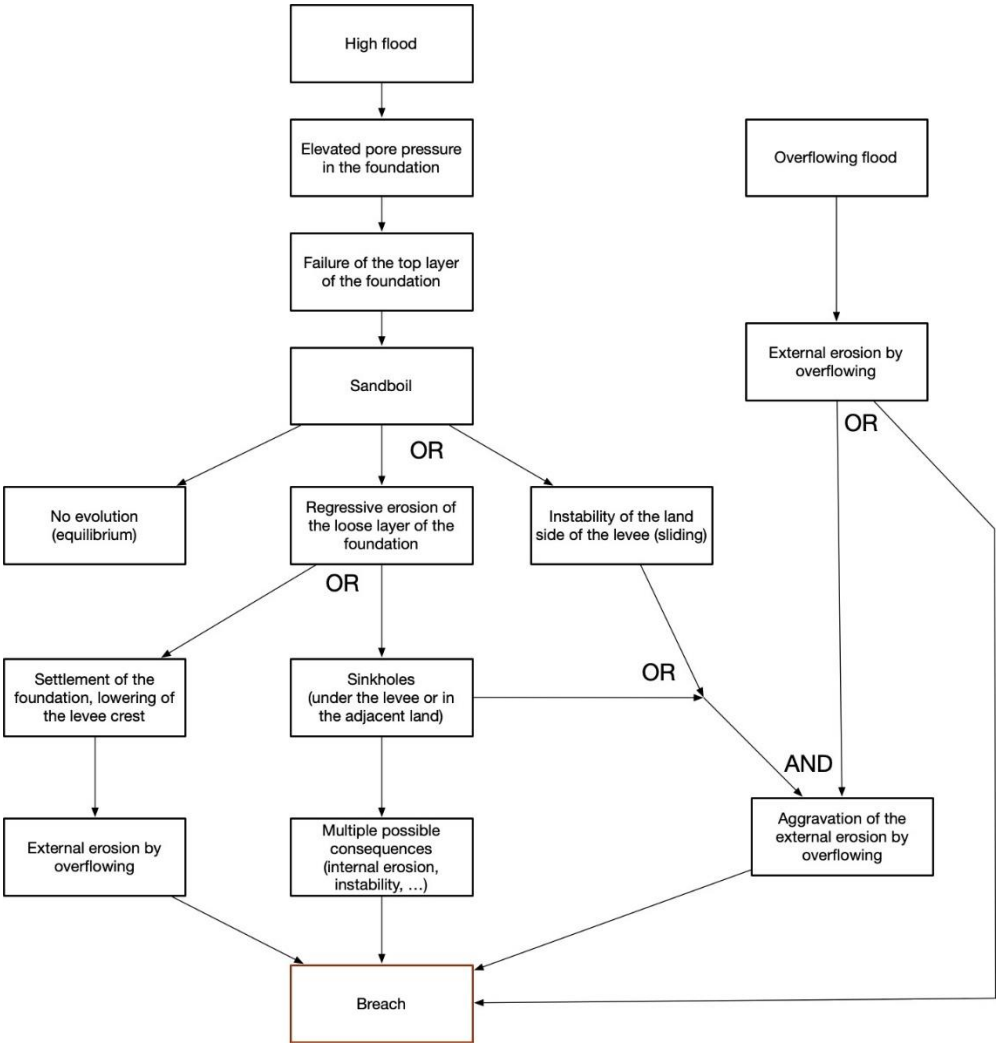

Figure 3.53 Failure tree involving a sand boil (Rémy Tourment).

Figure 3.53 was developed based on the analysis of the various observed damages in relation to the sand boils, using expert analysis. However, for actual cases not all damages lead to the final step of a breach as the condition for continuation to the next step is not always met.

3.7 The Netherlands Wilnis failure of a peat levee during a dry period

Contribution by Dr. ir. M. Van (Deltares, Netherlands)

Summary

This case concerns the sliding failure of a peat embankment during a dry period. At the time, the water level in the canal was not exceptionally high. The dry weather had led to deterioration of the stability against sliding.

Influencing local factors

- Increase of water pressures in base:
  - In tensile cracks along sheet pile (cracks affected by shrinkage and pore water pressure);
  - Presence of locally more permeable silt layer in foundation peat layers conducting water along cracks to foundation.
- Slope sliding
  - Extremely dry conditions leading to weight loss and shrinkage of peat embankment;
  - Higher pore water pressure in foundation due to shrinkage at sheet pile and enhanced by presence of local silt layer;
  - Discontinuities present from past land use.

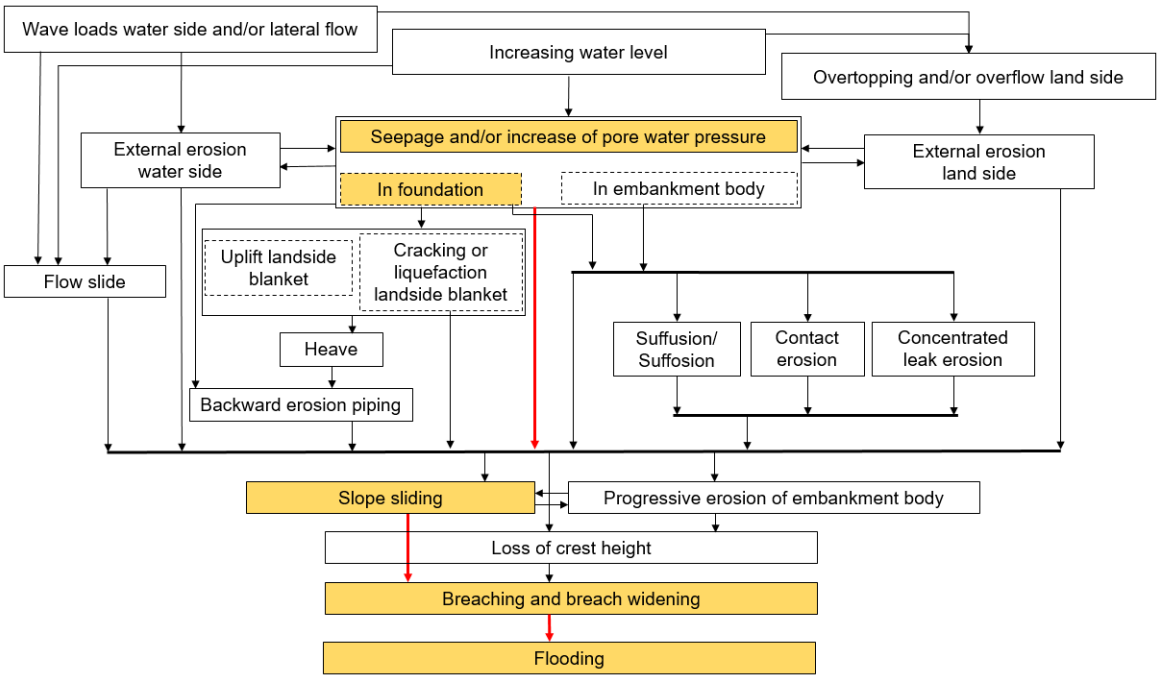

Figure 3.54 Failure tree of Wilnis levee breach, 2003.

Case description

At the end of the very dry summer of 2003 in the Netherlands a containment levee of a polder canal failed. The levee consisted of peat, which in the saturated zone has a gravimetric water content of over 800%, making the water defence mainly composed of water. The failure made clear that there were flaws in the safety of the land below the sea, see Figure 3.55. Moreover, the type of failure was not foreseen, although near failures in the past had indicated that the stability of peat levees can be endangered in dry summers.

The damage resulting from the water mass spilling was limited to a shallow sheet flood temporarily inundating the levee hinterland, and carrying mud and sand, which was deposited in a housing area. Further damage resulted from bank collapse along the emptied canal and dramatic groundwater lowering, resulting in surface settlement and damage to foundations. Timely damming of the canal, that was connected to a lake, limited the extent of the damage.

The failed levee section is a remnant of a former regional peat accumulation initially at or above mean sea level but lowered to well below sea level by continued drainage for agricultural land use, oxidation, and peat mining. The levee, therefore, consisted of predominantly the original peat.

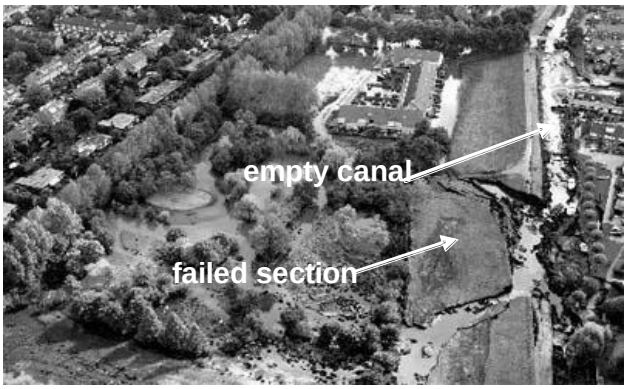

Figure 3.55 Failed canal levee at Wilnis, August 2004.

This contribution presents findings of an analysis pinpointing mechanisms in the chain of events resulting in the failure. Detailed information is in the Dutch reports (GeoDelft, 2003a) and (GeoDelft, 2003b) and summarized information can be found in (Bezuijen, Kruse, & Van, 2005), (van Esch & Van, 2007) and (Van M. A., Zwanenburg, van Esch, Sharp, & Mosher, 2008).

The archetypal build-up of the subsurface at the site of the failed levee section is given in Table 3.1. A horizontal anisotropy in the structure of the peat is existent by horizontal fracture planes, so-called splits. The splits are common in the coastal plain peats in the Netherlands, and are thought to result from, probably repeated, uplift of free methane containing peat in response to a water table rise during riverine or marine floods. The production of free methane is significant in the organic subsurface. Free methane gas induced uplift of peat has been witnessed to occur also nowadays. In grassland on peat almost 0.5 m thickness of peat soil per 100 year is oxidized. For the peat levees, with a somewhat thicker aerated zone, the mass and thickness of peat disappearing in the atmosphere will be higher than this figure. A peat levee carved 200 years ago, will therefore have been lowered by about 1 m, in an irreversible process that continues at the present day which not only affects the height of the levee, but also conditions concerning stability.

Table 3.1 Schematic build-up of the original subsurface at the failed levee section.

Depth starting from ground surface	Material
0.5 - 1 m	Peat weathered
4 m	Peat, mainly reed peat
1 - 2 m	Peat with clay intercalations
1 - 2 m	Peat, various peat types
9 m below original ground surface	Sand, Pleistocene accumulation

The illustration in Figure 3.56 provides an overview of the piezometric levels, build up and geometry of the levee, canal and terrain at Wilnis before failure. The levee has a grassland cover. A sheet pile wall with board lengths up to 4.5 m, had been placed along the canal about a decade ago for bank protection. Maintenance dredging of the canal to a water depth of about 2 m was carried out 1 year before the failure. A wide ditch drained the toe of the levee and was lined with shrubs and some tall poplar trees. The clay layers in the subsurface increase in thickness towards the west along the levee and decrease in thickness eastwards from the failed section.

Detailed historic maps of the area show that the levee at the location was in use as shipyard terrain when the mined-out area (now the polder) was still a lake; notably small harbour inlets did occur at the site. The levee crosses a riverine shoestring sand, locally about 1.5 m below the surface at the toe of the levee.

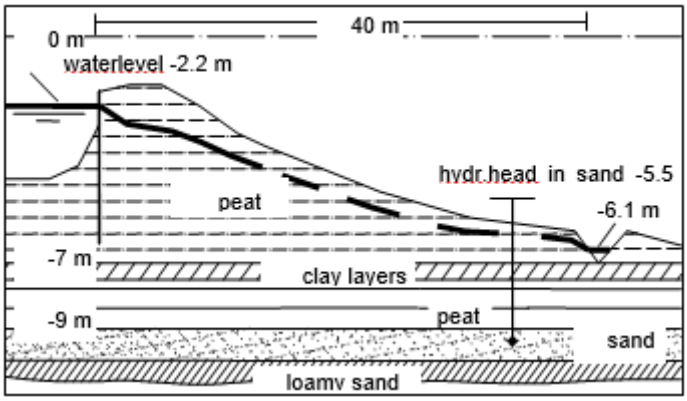

Figure 3.56 Cross section with relevant geometry specifics for the Wilnis location.

Chain of events of the failure

At the location water was heard or seen running from cracks in the levee's landward side 0.5 - 1 hour preceding the main failure event. The main failure event was a lateral translation of several meters of a section of the levee, taking less than 15 minutes. The canal emptied through the wide opened lateral cracks resulting in a sheet flood. The flow in the failure's main bounding cracks eroded peat and a significant amount of sand from the Pleistocene below the peat and clay.

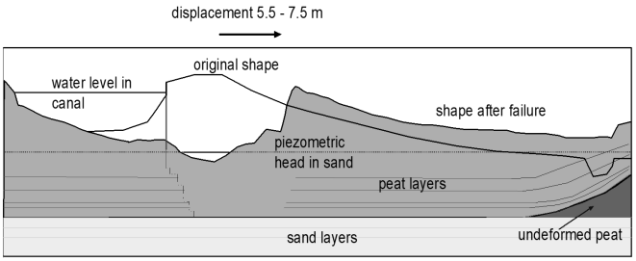

Figure 3.57 Embankment geometry before and after the failure at Wilnis. The various layer boundaries in the subsurface are indicated after failure, as well as the original water level in the canal and the piezometric head in the sand.

The failure consisted of coherent horizontal translation of about 6 m over a 60 m stretch. Vertical displacement was less than a few decimetres. A planar horizontal basal sliding plane was reconstructed from borehole and excavation data and located to have been at the base of the peat, i.e. at the top of the sand. The failed slices were bound laterally by major linear fractures oriented outward at angles smaller than 45^0, indicating the wedge to have been pushed by a force from the canal. Displacement of the slice was accommodated in part by filling a ditch and, mainly, in a subsequent upthrust over the existing terrain surface. A tall poplar tree at the toe of the slide had remained in place with its roots firmly anchored in the underlying sand, cutting the about 4 m thick sliding peat and clay mass.

The summer preceding the failure had been exceptionally dry in the Netherlands, such as occurring only approximately 1/25 $year^{-1}$ on average. The failure within a period of two weeks at the end of the dry summer, together with the condition that the levee consisted of peat, suggested that effects of decreasing moisture content, i.e. weight loss and shrinkage, had to be considered in the analysis. The geometry of the failure, a 60 m long flat slab with only lateral displacement and with lateral bounding fractures oriented as an active wedge angle to the canal, made it clear that the water level in the canal provided the driving force for the displacement. The hydraulic heads in and below the levee were calculated for the locations as they would have been prior to the failure, based upon the known heads in the canal, the polder behind the levee, and the underlying sand in the far field. Data from tests on large samples of peat and various approximations for in situ permeability of the underlying sand, including that of a less permeable silty sand layer about 1 m below the top of the sand, were used for the determination of the hydraulic heads. The not well-known bulk permeability of the deep wooden sheet pile bank protection at Wilnis did have a notable influence on the calculated heads, as anticipated. In undisturbed condition, the high hydraulic heads in the canal were hardly communicated to the sand below the peat due to, amongst others, clay layers in the peat.

Soil mechanical force equilibrium calculations for horizontal slip of the levee upon pressure from the canal, including the calculated initial hydraulic head distribution, were made. The results suggested that for undisturbed conditions, the relatively high hydraulic head in the sand would cause uplift of the peat at the toe of the levee, thus reducing friction there, but insufficient to cause failure. The calculations used the soil weights as determined on representative samples of the failed peat, but even assuming a decrease in moisture content to very conservative values had only limited effect on this outcome.

From trial pits, it became clear that there were no evident changes in the relative position of the predominantly saturated zone, both at the top and at the toe of the levee. The base of the intensely weathered peat coincided approximately with the top of the observed largely saturated zone. This observation does not include effects of any volume changes due to dewatering. Grey (discoloration) features in the soil, however, made clear that the water table

in the levee was frequently raised for extended periods up to 0.5 - 0.7 m below the surface at the top of the levee, and up to 0.3 m below the surface at the toe of the levee.

The findings from this initial stability analysis and the observations made clear that the cause of the failure was more complex than mere weight loss. The location of the basal sliding plane at the top of the sand immediately below the peat prompted investigations after mechanisms that could result in higher hydraulic heads in the sand below the crest of the levee than assumed in the initial stability analysis.

The sheet pile bank protection along the canal, locally piercing clay layers in the peat, had a major influence as came out of the initial hydrological analyses. The results from hydrological calculations incorporating leaks from the piles in the peat and clay layers made clear that the leaks had effect on the head in the sand below the bulk of the levee. The leaks would have to extend deeper than the piles, however, and had to be wider than mere local millimetre cracks in order to cause the head in the sand to rise to a level causing loss of friction at the base of the peat.

An investigation of the effects of water pressure in vertical cracks in peat showed the cracks to widen substantially upon pressure, due to the very low stiffness of the peat, and despite the peat not being very impervious (see Figure 3.58). The resulting shear stresses at the tip of the water filled cracks in the peat were found sufficient to cause fracture expansion and growth. Thus, penetration of the hydraulic head of the canal a few meters deep along the sheet piles in the peat would result in fracture propagation. Shrinkage of peat due to the dry weather conditions adversely affected stresses and deformation at the sheet pile wall. Increase in evaporation causes negative pore pressure, which induces shrinkage of peat below the already intensely fractured top layer, creating tensional stresses parallel to the levee surface over the depth of the zone experiencing negative pore pressure. The tensional stresses exert a pull on the peat at the sheet pile away from the canal (see Figure 3.58), thus enhancing creation of space along the piles and adding some tensional stress at the tip of shallower cracks. It must be noted that horizontal fracture-like surfaces are widespread in the peat mass. The extent to which the sub horizontal stresses can be transferred across such rough planes was not investigated. These planes are known to be conduits for water in peat, however, enabling high-water pressures to be transferred efficiently through the peat mass. Fracturing of the peat mass by water pressure is therefore not limited to the tip of the initial leak.

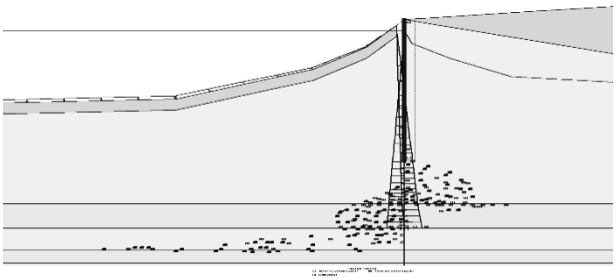

Figure 3.58 Cross section of the canal and levee with sheet pile. The dots at the base of the pile indicate occurrence of plastic behaviour in calculations using a Mohr Coulomb model.

The build-up of a high hydraulic head in the sand below the peat at Wilnis was enhanced by the occurrence of an about 0.5 m thick silty sand layer about 0.5 m in the sand below the base of the peat. The effect of the silty layer was discernible on the pore pressures detected by piezocone cone penetration tests (CPT's). In the calculations, the silty layer did allow even

limited flow from the canal through the cracks to build up a sufficiently high-water pressure below the crest of the levee.

Summary
The drought of the 2003 summer in the Netherlands gave rise to conditions that led to failure of peat levee at Wilnis. The failure did occur due to combinations of circumstances, of which a major discontinuity along the bank of the canal, concerning bulk permeability, strength and stiffness, is common to both. The failures involved planar slides with a basal sliding plane on sand in which the high hydraulic head was relatively too high. The major discontinuities along the canal are features from present and past land use. Such features are common in much of the intensively used canal levees of The Netherlands and can, therefore, be expected to exist at other locations.

The chain of events described above for the failure of such a levee can be well appreciated in hindsight but was not foreseen despite an extensive safety evaluation programme in the 1970's and 1980's for this levee. The failures discussed here did involve hitherto not diagnosed nor anticipated mechanisms in stability evaluations of the peat levees. In part this is due to the material at hand. The failures involve peat which is a peculiar soil: Only 10 - 20% of the volume of the peat discussed here, is an actual solid. Changes in ambient conditions, notably weather, surface and ground water, and vegetation have significant and partly self-explanatory effects for levees of such soil. The influence of these changes on the stability of the levee is not immediately evident as follows from the analyses described above. However, in order to come to a systematic safety evaluation of the many thousands of kilometres of levees the routine geotechnical analysis must incorporate evaluation of the effects of changes in ambient conditions. These effects involve changes in weight with evident influences on stability, and changes in volume of the soil mass with largely indirect effects. The above described chain of events of the failure suggests that mechanisms such as fracturing and unsaturated hydrology have played a significant role. The processes and parameters involved in these mechanisms are notoriously complex in real life settings and are hard to measure and uncertain.

From the analysis it is clear however, that conditions affecting the hydrology of the saturated and not saturated zone of the levee must be considered to enable systematic safety evaluation of the levees. Many of these conditions will be man-made and may be very local. In many cases only a review of the development of the levee in an historical context will be able to provide information necessary for estimation of the likelihood of adverse conditions.

3.8 China two cases of riverbank damage and repair

Contribution by Prof. J. Wang (City University of Hong Kong, Hong Kong)

Summary

These cases concern damage of riverbanks due to external erosion on the water side. No flood occurred, however the description provides insight in the relevant factors influencing external erosion on the water side.

Influencing local factors

- Wave loads water side:
  - Large variation in water level between rainy and dry seasons;
  - Rapid flow in gorge section.
- External erosion on the water side:
  - Low scouring resistance capacity due to smaller soil particles within the slope;
  - Low scouring resistance capacity of gravel soil bank slope.
- Slope sliding:
  - Cracking and outward displacement of the existing retaining wall due to serious water side scouring and insufficient wall foundation stability.

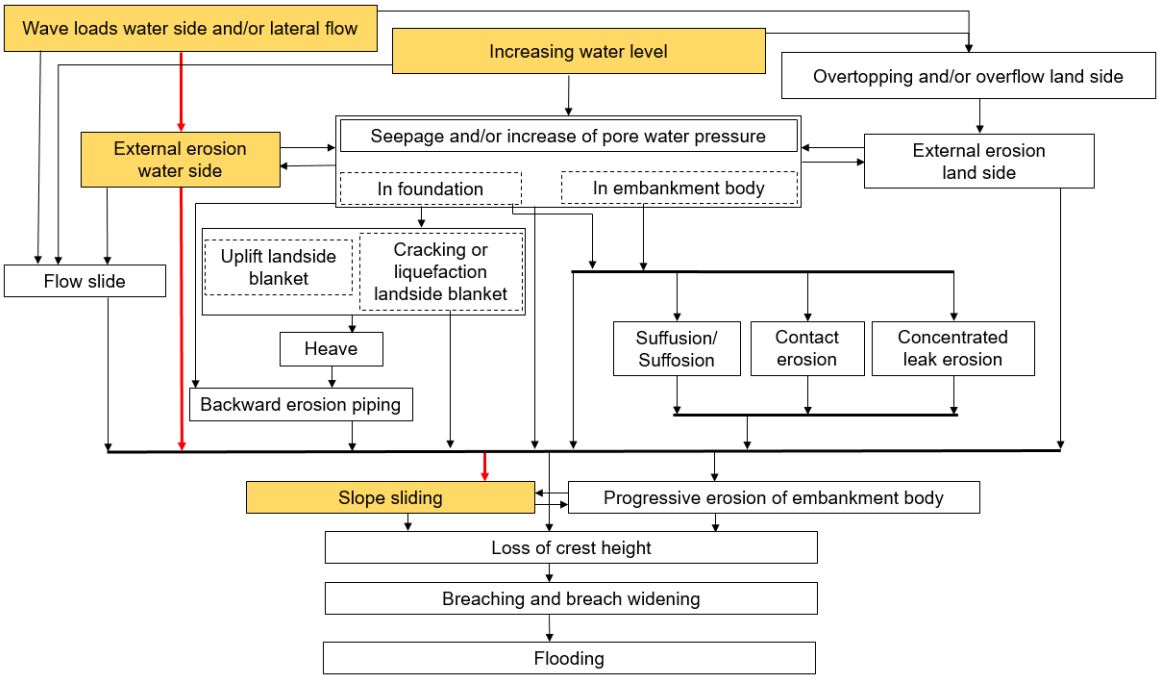

Figure 3.59 Failure tree of riverbank damage and repair in China.

Case descriptions

3.8.1 Case 1

An existing levee is completely damaged due to the surge of river water. The riverbank in this section is about 100 m wide. The river course is straight, and water flows rapidly, which is a typical gorge section within high mountains with a large variation of the water level between rainy and dry seasons. Therefore, the key to ensuring the safety of levee walls on the embankment slope of the highway is to solve the problem of river scouring.

Figure 3.60 Riverbank morphology in the damaged section of retaining wall.

The riverbank in this section is mainly composed of gravel soil. The embankment slope has a good stability, but the scouring resistance capacity is poor due to the smaller soil particles contained within the slope. The bedrock is exposed across the river, which is a thick formation of metamorphic sandstone, and the embankment slope is high and steep with a good stability and strong anti-scouring ability.

Based on the above observation and taking into account the river morphology of this section, it is recommended to build a medium water level spur levee about 8 m long at the upstream end of the levee wall to deflect the river flow of water, so that the scouring of river water for the highway embankment slope can be greatly reduced. On this basis, because of the good stability of highway embankment slope, the conventional lateral earth pressure theory is used to deal with the problem of the anti-scouring retaining wall.

3.8.2 Case 2

A road shoulder wall of mortar rubble along the river is about 9 m high and placed in the gravel soil bank slope about 12 m high. Due to the surge of river water, the bank slope of loose gravel soil in the front of the existing retaining wall has been scoured seriously. So, the resistance in the front of the retaining wall is insufficient and leads to a 15 cm overall outward movement of the retaining wall.

The river bank in this section is about 90 m wide, the river course is straight, and the water flows rapidly, which is a typical gorge section within high mountains with a large variation of the water level between rainy and dry seasons. At present, the serious scouring of the bank slope where the retaining wall is located leads to the insufficient resistance in front of the wall, and the poor stability of the wall foundation suspended above 4 m of the riverbed.

In addition, a part of the mortar rubble retaining wall is cracked about 30 cm away from the outer edge, suggesting a certain risk level of cracking or failure of the retaining wall structure.

Figure 3.61 Outwards displacement of the bank slope and retaining wall.

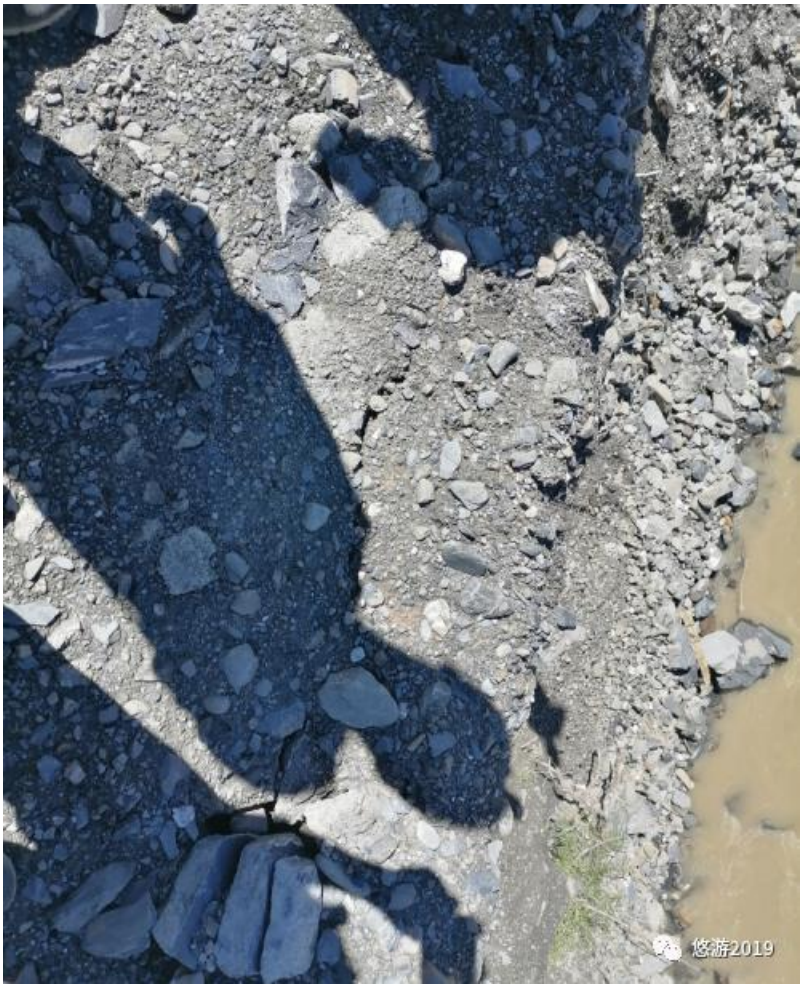

Figure 3.62 Cracking morphology of retaining wall body.

Based on the above observation, the core treatment method of the retaining wall defect is the anti-scouring protection of the bank slope, the improvement of the anti-sliding stability of the retaining wall, and the reinforcement of the wall structure.

Therefore, firstly, it is considered to build an anti-scouring secondary wall with a height of about 6 m (with a bury depth of 3 m) in front of the existing retaining wall, which can be used for the anti-scouring protection on the bank where the existing retaining wall with an upper height of 9 m is located, and prevents the bank slope from the further deformation that might lead to the collapse of the highway retaining wall.

Secondly, considering that the retaining wall has been displaced outwards and the structure of the retaining wall is poor, the 20 cm-thick reinforced concrete slabs are placed on the upper slope of the existing retaining wall, and the existing retaining wall is necessarily reinforced using two rows of 12 m-long anchor bolts. Not only can the panel-type anchor bolts be used to effectively improve the resistance of the existing retaining wall, but also the slurry backfilling technology of the reinforced concrete panel and bolt anchor are effectively used to reinforce the existing retaining wall of mortar rubble, so that the shear resistance capacity of the structure for the retaining wall is improved effectively.

The repairing methods in the above two case histories are proposed to rebuild or remedy the water retaining walls based on an effective capturing of the hydrogeology of the river, reasonably setting up the anti-scouring projects for specific sections and combining the existing materials and equipment on the site.

3.9 Several cases of (river) bank collapses due to flow slides

Contribution by Dr. G. van den Ham (Deltares, Netherlands)

Summary

These cases concern several damages due to multiple flow slides at the same location. No flood occurred, however the description provides insight into how the flow slides occurred.

Characteristics

Celotex levee failure:

- The geology of the failure reach consists of point bar deposits from an abandoned St. Bernard distributary channel. These deposits are primarily coarse-grained, silty sands and clean sands.
- Historic data indicate that channel width at the Celotex failure reach has appreciably declined while experiencing a corresponding deepening of the channel thalweg in point bar sands (sands deposited at the inner band of a river).
- The Celotex levee failure was the result of a flow slide in substratum sands triggered in the scour trench at about Greenville Bend revetment range U-19 (R100.25). This bank reach has been previously classified as susceptible to flow failure.
- Historic bank lines of record along the Greenville Bend revetment reach inclusive of the Celotex failure site indicate a regular history of failures and a past failure specifically at the Celotex site.
- The Celotex failure occurred during low water.

The Jamuna Bridge flow slides:

- The Guide Bund slopes were in very young sediments deposited by the Jamuna, primarily micaeous fine sands with a mean grain size of about 100–200 microns and a silt sized fraction of 2–10%. These were normally consolidated sands.
- The flow slides developed on relatively gentle slopes, between about 1V:5H and 1V:3.5H and came to rest on flatter slopes at about 1V:10H.

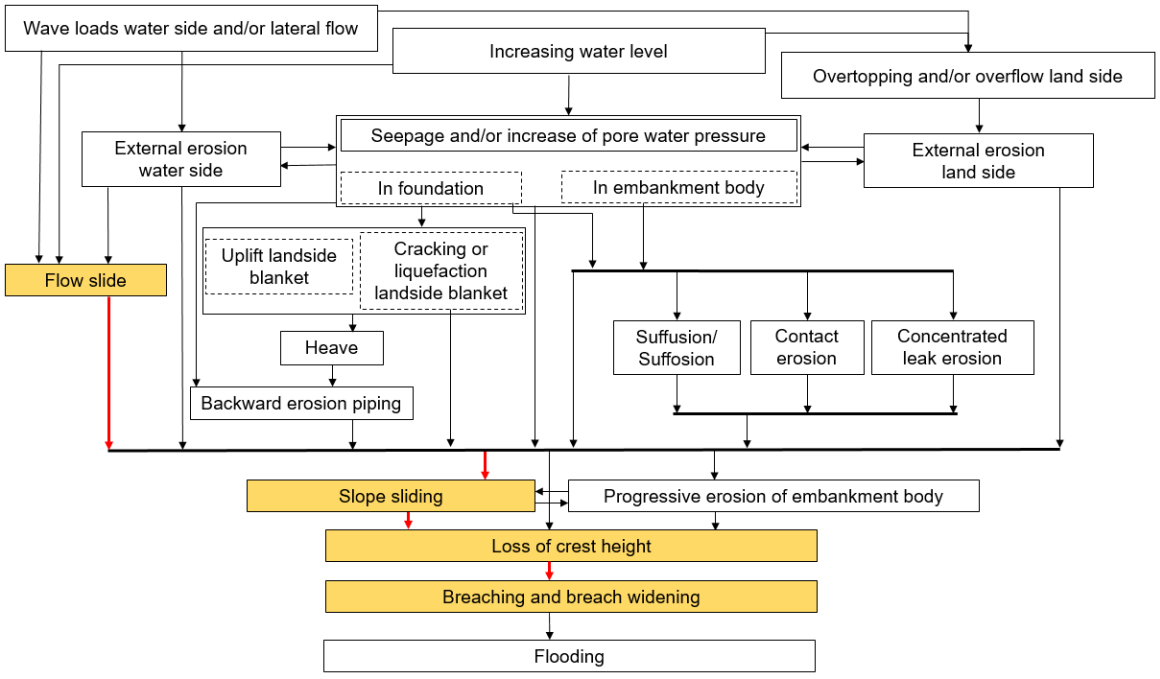

Figure 3.63 Failure tree of flow slide breach.

3.9.1 Introduction

Flow slides are a mainly subaqueous type of landslide in sandy and silty slopes along coasts, estuaries and rivers, which transform steep slopes into more gentle slopes. Flow slides can result in much longer, partly subaerial retrogression lengths in banks or foreshore, compared to other geotechnical slope failure mechanisms and can cause significant damage when occurring in the vicinity of dikes, levees and river banks or hydraulic structures. Risk indications are oversteepened slopes due to erosion at the toe or deposition at the top of a tidal channel or riverbank, lack of protection of the surface to waves or currents, presence of loosely packed and recently deposited fine sand mixed with silt or clay layers, extreme low water, heavy rainfall and human interventions like sand mining, dredging or sand deposition at sea.

Two types of flow slide failure mechanisms are generally considered in literature: static liquefaction followed by a shear slide, and retrogressive breaching, generating a sustained turbidity current downslope of the location of initiation. Theoretically, both types of flow slide failure will result in a similar slope profile, although the evolution over time is very different. Static liquefaction is related to loosely packed sand layers in the subsurface that lose their strength instantaneously due to excess pore water pressure, whereas breaching is related to more densely packed fine sand layers at the soil-water interface and may slowly retrogress over several hours. Both result in a flowing sand-water mixture or turbidity current that eventually redeposits on a gentle slope. The occurrence of flow slides can be easily recognized in the typical hourglass shaped differential pre- and post-event bathymetry in ocean floor and coastal zone surveys.

In natural flow slides it is generally not that obvious whether it concerned a static liquefaction flow slide, a breaching flow slide or a combination of both. This is because the slides occur unexpectedly, are invisible, being largely subaqueous and both mechanisms result in the same after-event morphology. Although characteristics of hundreds of flow slides have been reported, they usually concern no more than the description of layers with median grain sizes, the geometry (long) before the slide and the after-event morphology (Silvis & De Groot, 1995) and (Van Dijk, Mastbergen, Van den Ham, Leuven, & Kleinhans, 2016). This also applies to the cases described below.

Flow slides occur at many locations worldwide. They do seldom occur as a single event, rather as part of a series of flow slides over time in the same area and even on the very same spot. There are several examples from bank failures as a result of flow slides resulting in an actual flooding, however well-documented cases are not available for reasons mentioned above. Although the examples of bank failures due to flow slides given in this section did not result in flooding, they resulted in severe damage and are exemplary for events that did result in flooding.

Two multiple bank failure areas as a result of flow slides are discussed below:

- The Celotex levee failure, Mississippi River, USA, 1985
- The Jamuna Bridge flow slides, Jamuna River, Bangladesh, 1994-1998

The Celotex failure revealed to be the results of a typical breaching flow slide, just as most of the many flow slides that occurred in the Lower Mississippi Area. The Jamuna Bridge flow slides on the other hand could be well explained by static liquefaction.

3.9.2 Celotex levee failure, Mississippi river bank, USA, 1985

This case history is largely taken from the report of (Dunbar, Torrey, & Wakeley, 1999).

On 30 July 1985, a levee failure occurred on the west (right descending) bank of the Mississippi River at 100.25 river miles (161.34 km) Above Head of Passes1 (AHP) in the Jefferson Levee District. The failure location was near the community of Marrero, LA, which is part of the greater New Orleans metropolitan area. More specifically, because it occurred in front of the old Celotex Corporation industrial site, it was referred to as the Celotex failure.

Emergency repair operations were undertaken immediately after the failure. An old asbestos waste pit was discovered landward of the original levee alignment. The U.S. Army Engineer District, New Orleans (LMN) decided that an embankment setback was not the most cost-efficient restoration of the levee due to the environmental hazards which would have to be addressed. Instead, a unique repair approach was employed wherein the levee was rebuilt in its existing alignment, after the riverbank profile was restored by filling the failure scarp with shell. Repair operations were completed on 28 November 1985.

The failure involved approximately 61 m of the mainline levee embankment. At its widest point, which was approximately 61 m riverside of the centre line of the levee crown, the failure was about 183 m wide parallel to the river and extended out into the Mississippi River to approximately the -24 m National Geodetic Vertical Datum (NGVD) contour. (Torrey, Dunbar, & Peterson, 1988) estimates that the total volume of material displaced by the failure was approximately 229,000 m^3.

Boring data and geological mapping indicate that the failure area exhibits the, for the Lower Mississippi Area, particularly dangerous soil stratigraphy of thin overburden (i.e., topstratum) over a thick deposit of fine sands and silty sands (i.e., substratum).

Historic bank lines show that other bank failures occurred before at the Celotex location and at various other places downstream in comparable point bar deposits.

(Dunbar, Torrey, & Wakeley, 1999) came to the following conclusions:

- The geology of the failure reach consists of point bar deposits from an abandoned St. Bernard distributary channel. These deposits are primarily coarse-grained, silty sands and clean sands.
- Historic data indicate that channel width at the Celotex failure reach has appreciably declined while experiencing a corresponding deepening of the channel thalweg. Selected historic profiles show the cross-sectional area of the channel throughout the failure reach has generally remained constant through historic time. A constant channel cross-sectional area and a narrowing river channel requires a channel deepening. At the Celotex site, this deepening is occurring in point bar sands.
- Historic river migration patterns indicate the Greenville Bend revetment reach is an area of active channel migration and will continue to require continued revetment monitoring and maintenance to prevent natural lateral river migration.
- Thalweg profiles in the Greenville Bend reach indicate the 1985 hydrographic survey was one of the deepest river channels recorded for the nearly past 100 years.
- Scour pool data indicate the Greenville Bend pool has experienced historic downstream and lateral migration. The 1985 scour pool was at the maximum downstream extent.

- A decline in width/depth ratios has occurred between the 1894 and the 1985 hydrographic survey. This decline corresponds to a narrower and deeper channel between the survey periods.
- The Celotex levee failure was the result of a flow slide in substratum sands triggered in the scour trench at about Greenville Bend revetment range U-19 (R100.25). This bank reach has been previously classified as susceptible to flow failure.
- Historic bank lines of record along the Greenville Bend revetment reach inclusive of the Celotex failure site indicate a regular history of failures and a past failure specifically at the Celotex site.
- The Celotex failure occurred during low water. The reasons for the failure at this river stage are not fully understood. In general, scour pool behaviour during the different seasons is not completely understood with enough clarity to determine the behaviour of scour pools at changing river stages.

The Celotex case is just one of many examples of bank failures due to flow slides in the Lower Mississippi River Area where sand strata of the point bar deposits are present. According to (Torrey, Dunbar, & Peterson, 1988) flow slides pose a threat to mainline flood protection levees (dikes) often situated very near the top of the riverbank along the 230 mile (370 km) reach from Baton Rouge, Louisiana, to river mile zero. Between 1954 and 1990 more than 200 flow failures have caused revetment repair expenditures of many millions of dollars. During the great flood of 1973, major failures caused by flow slides occurred downstream of Baton Rouge at four locations. Those four failures so threatened the stability of sections of the levee that emergency construction of new sections (setbacks) further from the top of the riverbank were required. An example of severe damage to a flood defence as a result of a flow slide is shown in Figure 3.64 below.

Figure 3.64 Photo: This 210 m section of levee slid into the east side of the Mississippi River on August 23, 1983 at Darrow, in Ascension Parish, Louisiana. The slide occurred shortly after a high-water stage had receded, suggesting that toe undercutting and rapid drawdown likely contributed to the failure. Source:https://web.mst.edu/~rogersda/levees/Mississippi%20Delta%20Region.htm.

Research by the Waterways Experiment Station (WES, part of USACE) in the late 1980's and early 1990's, in particular by Torrey III, revealed that the liquefaction type failures that were originally hypothesized by the earlier studies by the Mississippi River Commission (MRC) did not fit the field evidence at these locations. Laboratory tests revealed the presence of relatively densely packed fine sands. Additionally, data from these failures indicated the process was not instantaneous, but occurred over a longer time period, indicating a retrogressive type mechanism instead of liquefaction and sudden failure. It was concluded that the flow slides resulting in bank failures in the Mississippi Area mostly concerned retrogressing breach flow slides rather than static liquefaction flow slides.

Based on these findings by Torrey III criteria were developed to predict the maximum area involved in a potential river bank failure, comprising of a retrogressive control line (RCL) and a stability control line (SCL) for determining bank stability along the river.

To respond to the bank erosion problem, the Mississippi River Commission (MRC) adopted a bank stabilization program after WW II, consisting of channel dredging and revetments. Revetment protection involves armouring of the river's banks with stone and concrete mattresses (articulated-concrete-mattress or ACM) along its submerged slope, to protect the bank against scour and confine the channel to a fixed alignment. This program of bank stabilization continues to the present. To date, nearly 50 percent of the Lower Mississippi River has revetment protection. Maintenance practices other than revetments can include grading of the bank, placement of rock in the scour pool, and setback levees.

Current Corps practice incorporates periodic hydrographic surveys of river channel slopes to determine the need for additional riverbank armouring and the requirements for additional revetment placement to stabilize slopes.

Revetment programs as described above are generally expensive, costing upwards of 1 million dollars per river mile, and involve periodic placement of new revetment when sections are eroded. Along smaller scale river systems, rock or rip-rap is placed on the banks to stabilize slopes and prevent bank erosion from occurring. Understanding the channel geometry and the attack points to the river bank are important considerations for assessing levee stability. Identifying locations of chronic bank instability and distance to the levee toe are important factors in evaluating levee stability and identifying areas where problems may occur.

3.9.3 The Jamuna Bridge flow slides, Jamuna River, Bangladesh, 1994-1998

This case history is largely taken from or based on the work of (Yoshimine, Robertson, & Wride, 1999), (Jefferies & Been, 2016) and (Van der Wal, 2020).

The Jamuna bridge is approximately 110 km northwest of Dhaka. At 4.8 km long, it is the longest bridge in South Asia and crosses the Jamuna, the fifth largest river in the world. The bridge was built over almost four years between 1994 and 1998 at a cost of $900 million. The Jamuna is a shifting braided river, consisting of numerous channels whose width and course change significantly with the seasons. Training the river to ensure it would continue to flow

under the bridge corridor was one of the most difficult technical challenges of the project and the costliest of its components. The river training works comprise two banana-shaped guide bunds, one on each side of the river, to lead the river through the bridge corridor, see Figure 3.65. More than thirty submarine flow slides occurred along the West Guide Bund.

The Guide Bund slopes were in very young sediments deposited by the Jamuna, primarily micaeous fine sands with a mean grain size of about 100–200 microns and a silt sized fraction of 2–10%. These were normally consolidated sands. The flow slides developed on relatively gentle slopes, between about 1V:5H and 1V:3.5H and came to rest on flatter slopes at about 1V:10H.

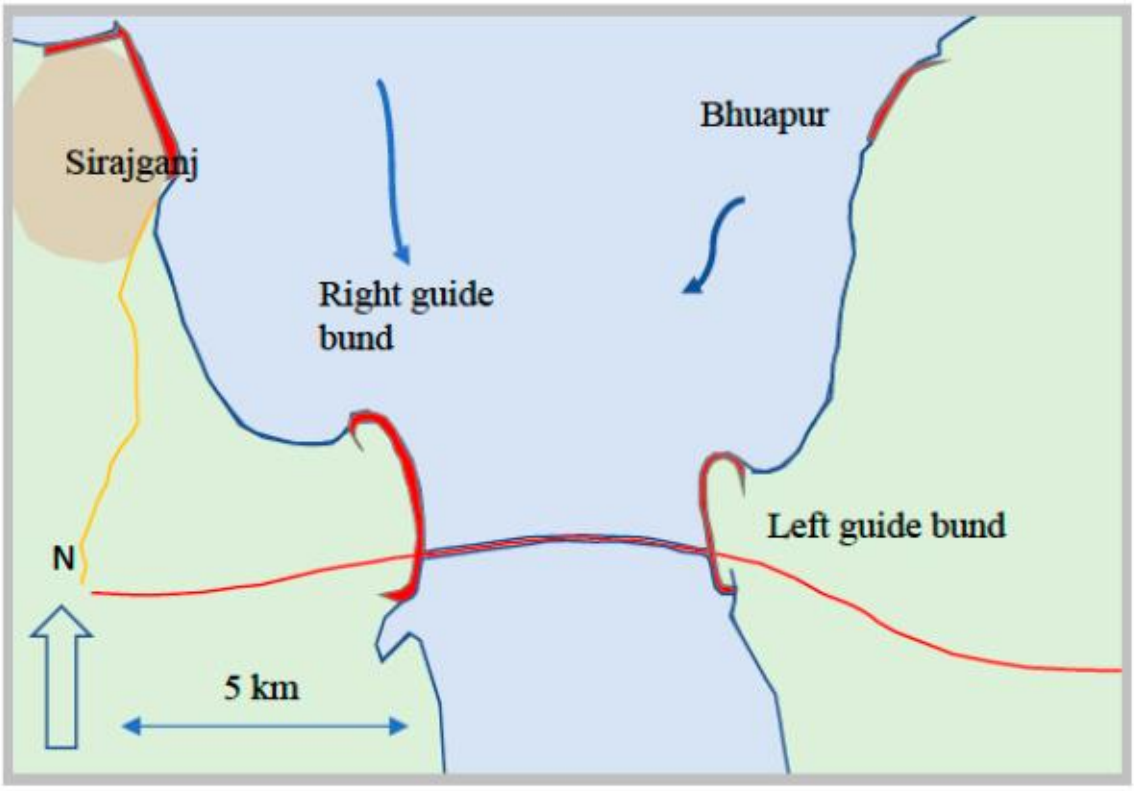

Figure 3.65 Sketch of the training works of the Jamuna Bridge. Source: Van der Wal (2020).

An example of a flow slide geometry from (Yoshimine, Robertson, & Wride, 1999) is given in Figure 3.66. Interestingly the slide extends above the river level, presumably with a regressive like mechanism as a noticeable scarp is evident at the river level after the failure.

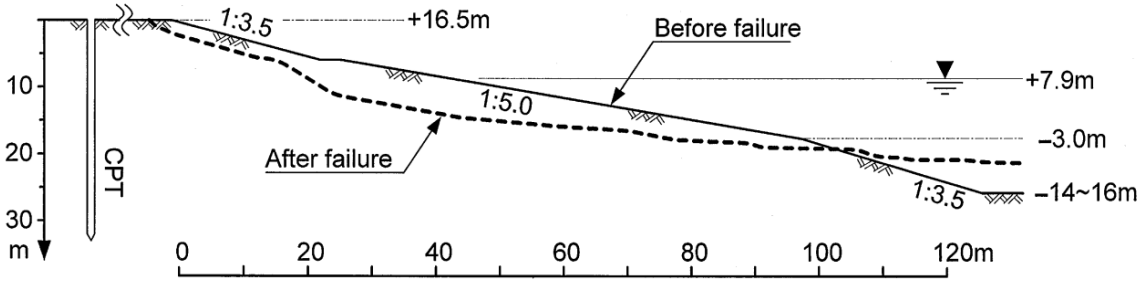

Figure 3.66 Example of flow slide geometry at Jamuna (from Yoshimine et al., 1999, with permission NRC of Canada), Source: Jefferies and Been (2014).

In the dredged area, which was about 300 m wide by 3 km length, is shown in Figure 3.67 and with the various slides being indicated by arrows (Yoshimine, Robertson, & Wride, 2001). Slides seem to be randomly distributed with the whole area being viewed as having much the same potential for flow slides.

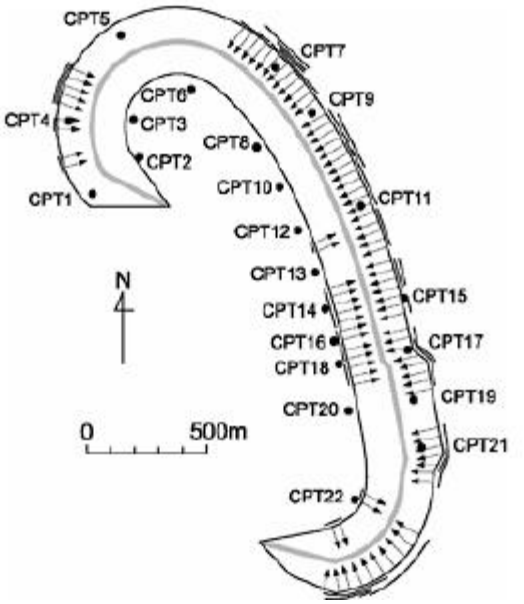

Figure 3.67 Plan view of west guide bund of Jamuna Bridge showing CPT locations (from Yoshimine et al., 2001, with permission NRC of Canada) . Source: Jefferies and Been (2014).

Detailed analysis of 22 CPTs by Jefferies and Been, applying the critical state approach, revealed that, despite of the large uncertainties, that the flow slides may well be caused by static liquefaction of the micaceous fine sands.

As in the Lower Mississippi River (case Celotex levee failure), flow slides occur on numerous locations along the Brahmaputra-Jamuna River where similar deposits are present, i.e. mostly loosely compacted alluvial deposits containing a relatively high concentration of mica flakes and related to scour phenomena. The planned form of the Brahmaputra-Jamuna River followed its natural path in Bangladesh until the construction of bank protection works started to save Sirajganj from bank erosion since the 1930s. Several so-called hardpoints such as groynes and revetments were constructed in the period 1980–2015 and the Jamuna Multipurpose Bridge was opened in 1998. The Brahmaputra Right Embankment and other projects had saved the western flood plain from inundation during monsoon floods. These river training works experienced severe damage by geotechnical failures, mostly flow slides. The design of most of these training works did not consider the risk of damage by flow slides. All descriptions of the observed damages show that scour phenomena in the channel close to a river training work and pore water outflow are important trigger mechanisms for the flow slides.

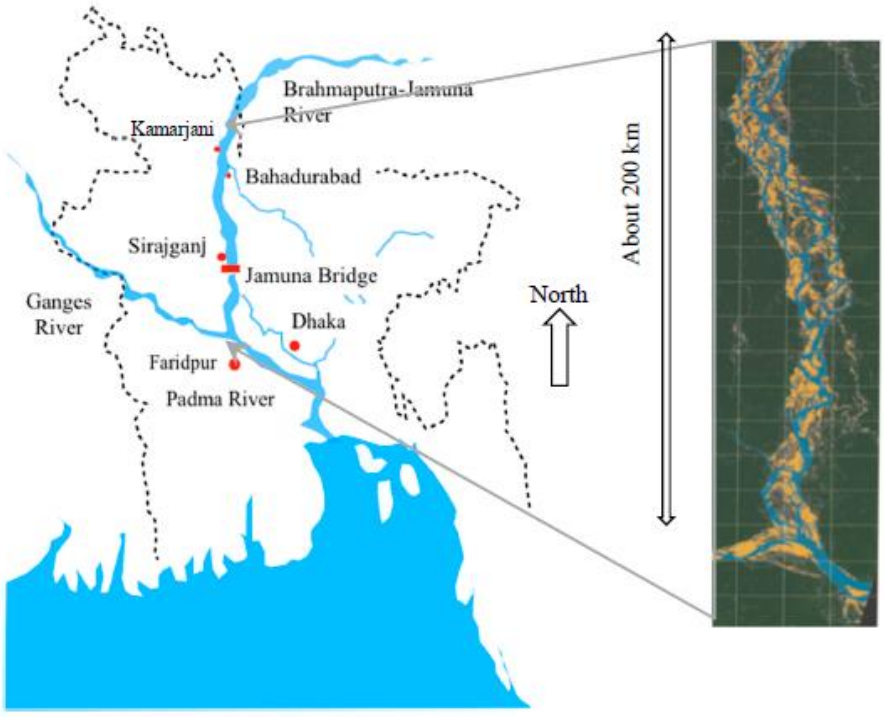

Figure 3.68 Map of the river Brahmaputra – Jamuna delta (Van der Wal, 2020).

4 Part C: Inventory of failure paths for risk assessment and design

For risk assessment and for design it is usual to consider the range of potential failure mechanisms, such as external erosion, internal erosion and sliding collapse. These mechanisms can be events in a failure path or tree leading to the eventual flood. This Part contains a compilation of examples of the use of failure paths or trees for risk assessment or for design, that are used around the world.

Failure paths derived based on theory can differ in the level of detail. These differences can reflect differences in approach, in the relevance of specific events in the failure path, or in the level of knowledge available to describe those events. All approaches are valid, and the objective of this Part is to serve as a basis for the conversation about differences and to identify knowledge gaps and, if possible, a more general framework presenting the usefulness and overall principles of the development and use of failure paths and failure trees.

A failure path can involve multiple mechanisms, however, in this section for a better overview, the examples are clustered under four sections based on the dominant initiating mechanisms: examples of failure trees involving internal erosion mechanisms, Section 4.1, slope sliding, Section 4.2, overtopping, Section 4.3 and revetment damage, Section 4.4.

4.1 Examples of failure trees/paths involving internal erosion mechanisms

4.1.1 Examples of scenarios involving internal erosion

Contribution by R. Tourment (INRAE, France)

Internal erosion can be involved in many failure scenarios, all possibly leading to a breach, according to the specific characteristics of the levee and its foundation (cross section, zones, materials properties, geometry) and the loading, flood hydrograph, where duration is an essential factor.

These scenarios can include one or more internal erosion mechanisms but can also include other types of mechanisms, for example external erosion or instability.

Generally, in an internal erosion scenario, more than one of the failure mechanisms can be involved in a failure path. This was acknowledged and described in the FloodProBE EU research project (Morris, et al., 2012), and a matrix of the possible interaction between the different internal erosion mechanisms was produced, see Figure 4.1.

Table 2.3 Matrix of the main scenarios of embankment failure by internal erosion

Type of internal erosion	Initiation	Continuation	Progression	Failure
Backward erosion	Uplift (at toe) Local defect (hole, root) Induced concentrated leakage (suffusion, contact	Beginning of pipe extension (parallel to flow)	Acceleration of pipe extension	Roof collapse Sinkholes
			→ Concentrated leak erosion	
Suffusion	Self-filtering condition not fulfilled	Without filter downstream	Yes	Settlement, Sinkholes
			→ Backward erosion	
			→ Contact erosion	
		With filter downstream	Clogging, pore pressure increase	Diffuse instability (liquefaction)
Contact erosion	Tangential flow erosion	Cavities settlements (locally)	→ Concentrated leak erosion	
			→ Backward (or forward) erosion	
Concentrated leak erosion	Pre-existing opening (settlement, structure transition, layering) Induced opening (contact erosion, settlement, backward erosion)	Beginning of pipe enlargement (normal to flow	Acceleration of pipe enlargement	Roof collapse Sinkholes

Figure 4.1 The FloodProBE matrix, from: Morris et al. (2012).

It can be noted that during the process of an actual failure involving internal erosion, these four different internal erosion mechanisms can occur in the same place at different times, and at the same time in different places as shown by Figure 4.2 and the associated failure paths. This

figure only presents a part of the total process, as after concentrated leak erosion is initiated and continues additional mechanisms can take part and lead to a breach (roof collapse or sinkhole, followed by overtopping and external erosion).

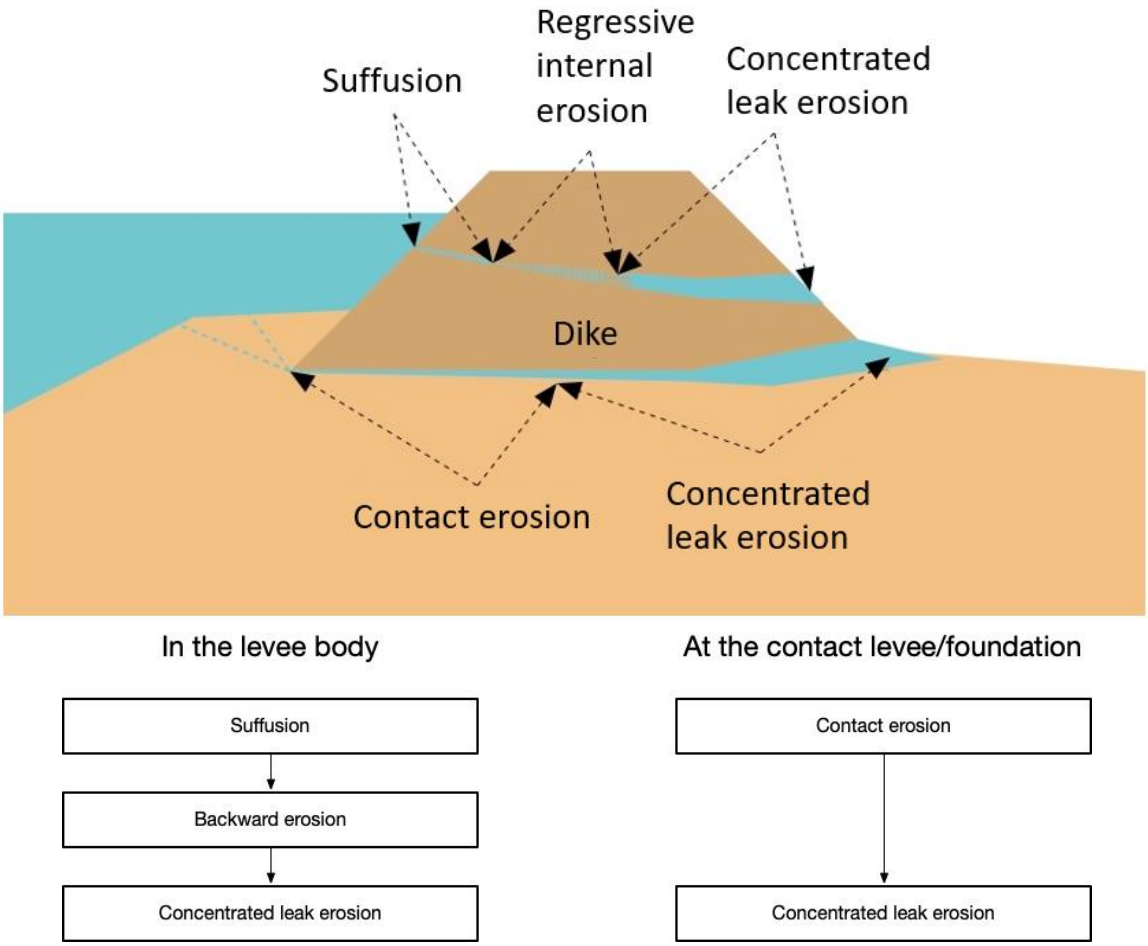

Figure 4.2 Two internal erosion failure scenarios and the associated failure paths (source R. Tourment).

We try to present hereafter in Figure 4.3 a generic failure tree of internal erosion, based on the FloodProBE matrix, although it will probably be more complete in terms of including internal erosion individual mechanisms than the other types of mechanisms, and it will not take into account the specificities of a given levee in terms of cross section and material properties. It is also like the previous example partial and not developed until the final breach.

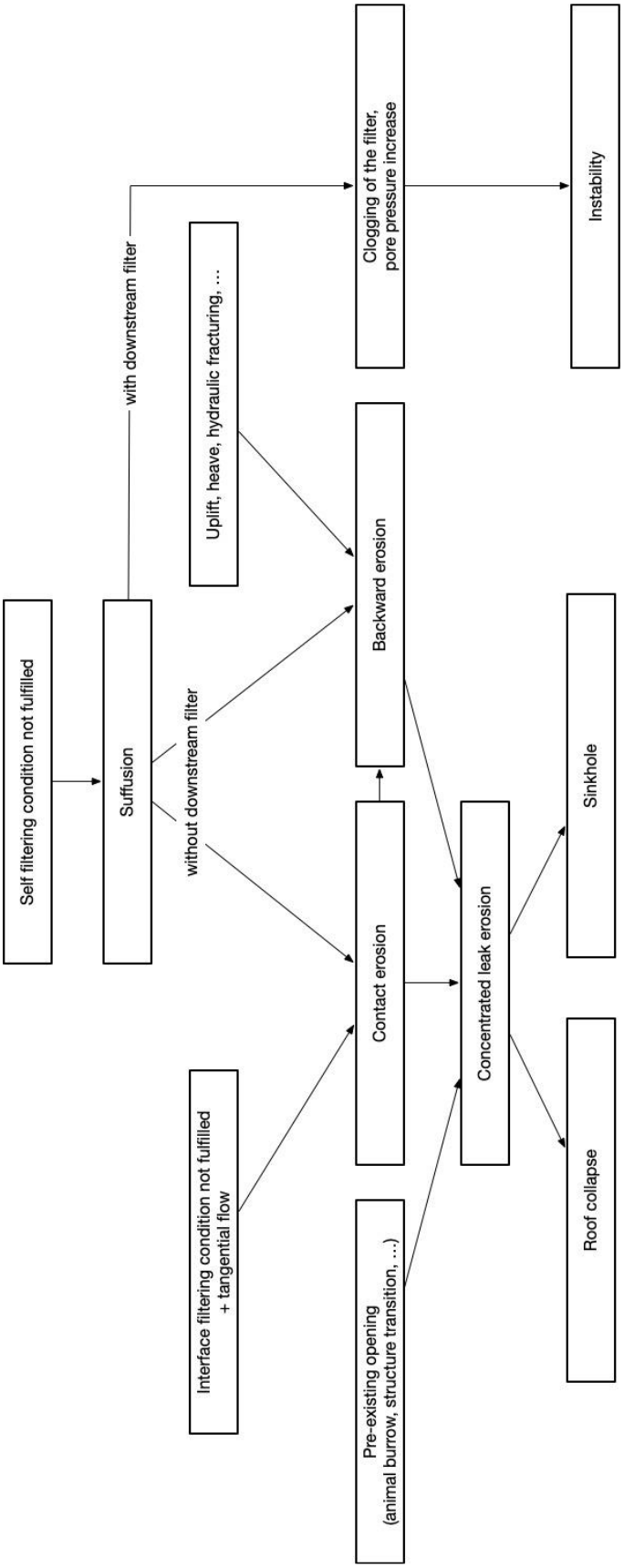

Figure 4.3 The FloodProBE matrix translated into a potential failure mode tree (Rémy Tourment).

Finally, in the following example, see Figure 4.4 of a failure path, presented during the ISSMGE TC201 workshop in Reykjavik, internal erosion is involved in a failure path of a composite levee which is made of:

- a protection revetment
- a clay layer
- a more permeable fill

It is also like the previous examples partial and not developed until the final breach.

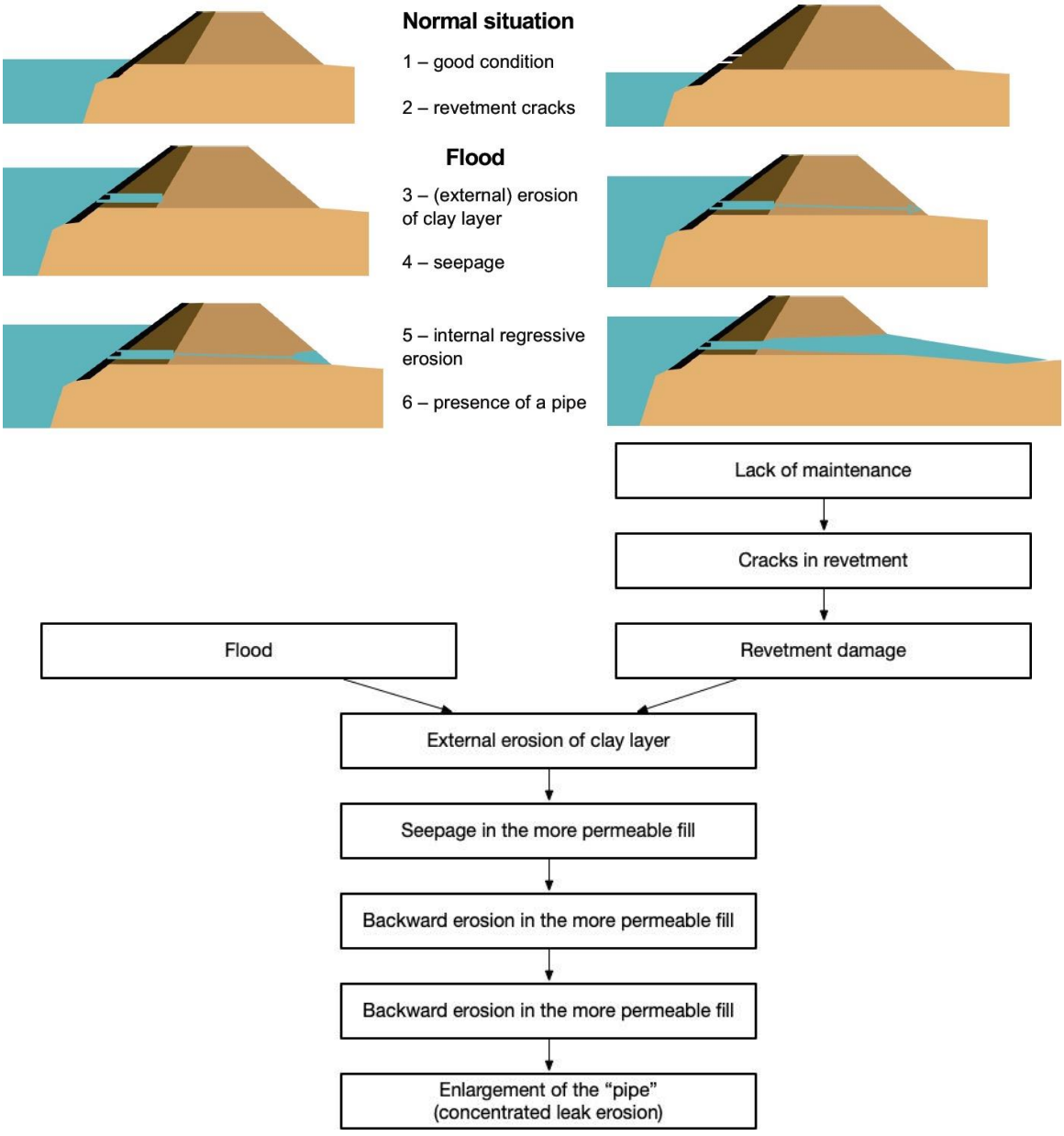

Figure 4.4 Failure path involving failure of a revetment, external erosion of a clay layer and internal erosion of a more permeable layer (R. Tourment).

4.1.2 Conceptual framework for the internal erosion process from the US

Contribution by M. Sharp

Internal Erosion Process

The process of internal erosion has been generally broken into four phases: (1) initiation of erosion; particle detachment, (2) continuation of erosion; inadequate particle retention, (3) progression of erosion; continuous particle transport and enlargement of erosion pathway, and (4) initiation of a breach.

Event Tree for Internal Erosion

A generic sequence of events has been developed for analysing internal erosion failure modes that is based on the four phases of internal erosion. In addition, a threshold water surface elevation, or several different ranges of elevations and the likelihood of unsuccessful detection and/or intervention are assessed. These sequences of events can be illustrated as an event tree as follows:

- Water level at or above threshold level
- Initiation – Erosion starts
- Continuation – Unfiltered or inadequately filtered exit exists
- Progression – Continuous stable roof and/or sidewalls
- Progression – Constriction or upstream zone fails to limit flows
- Progression – No self-healing by upstream zone
- Unsuccessful detection and intervention
- Breach (uncontrolled release of impounded water)

This event tree is applicable to scour related erosion through a zoned embankment. For other types of internal erosion processes, not all events may apply depending on the postulated failure progression and other site-specific factors. In addition, depending on how the potential failure mode is envisioned and, on the information available, it might be appropriate to decompose the initiation event into two events: 1) flaw exists; and 2) erosion initiates given the flaw exists. The event tree becomes:

- Water level loading (at or above threshold level)
- Flaw exists – Continuous crack, high permeability zone, zones subject to hydraulic fracture, etc.
- Initiation – Erosion starts
- See the above event tree for other events that apply

The two-event approach is typically used for projects designed to include flood risk management and which have not been fully loaded. This allows the identification of scenarios where the likelihood of a flaw may be a primary factor in the risk estimate. The quantification of these events can provide a better understanding of how a flaw impacts both the estimate and the uncertainty in the risk estimate. When using historical base rates to estimate initiation, the one-event approach is typically used, as historical rates of a flaw existing where erosion has not initiated are unknown. Sample event trees for concentrated leak erosion and backward erosion piping are provided in Figure 4.5 and Figure 4.6. These examples illustrate the two-event approach. If the one-event approach is used, the first two events (flaw and initiation) would be replaced by a single event representing initiation. The risk team should develop specific event trees for their identified potential failure modes.

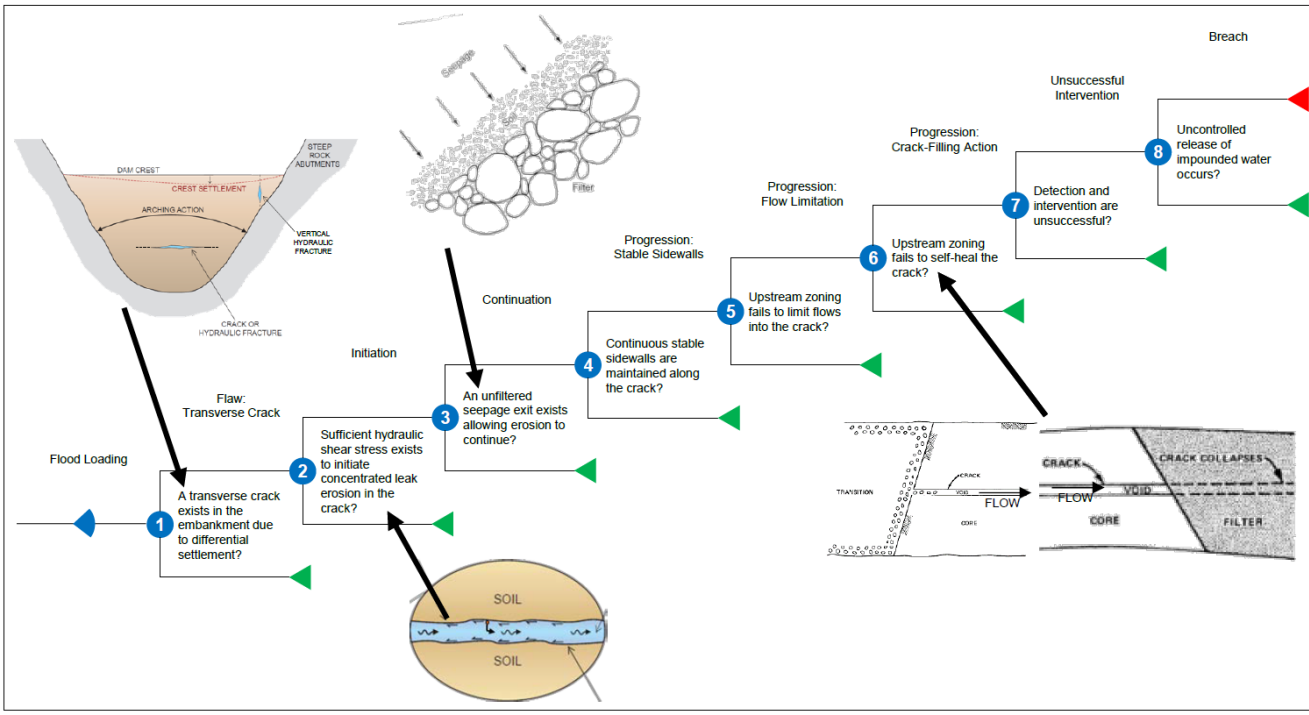

Figure 4.5 Example of event tree for concentrated leak erosion.

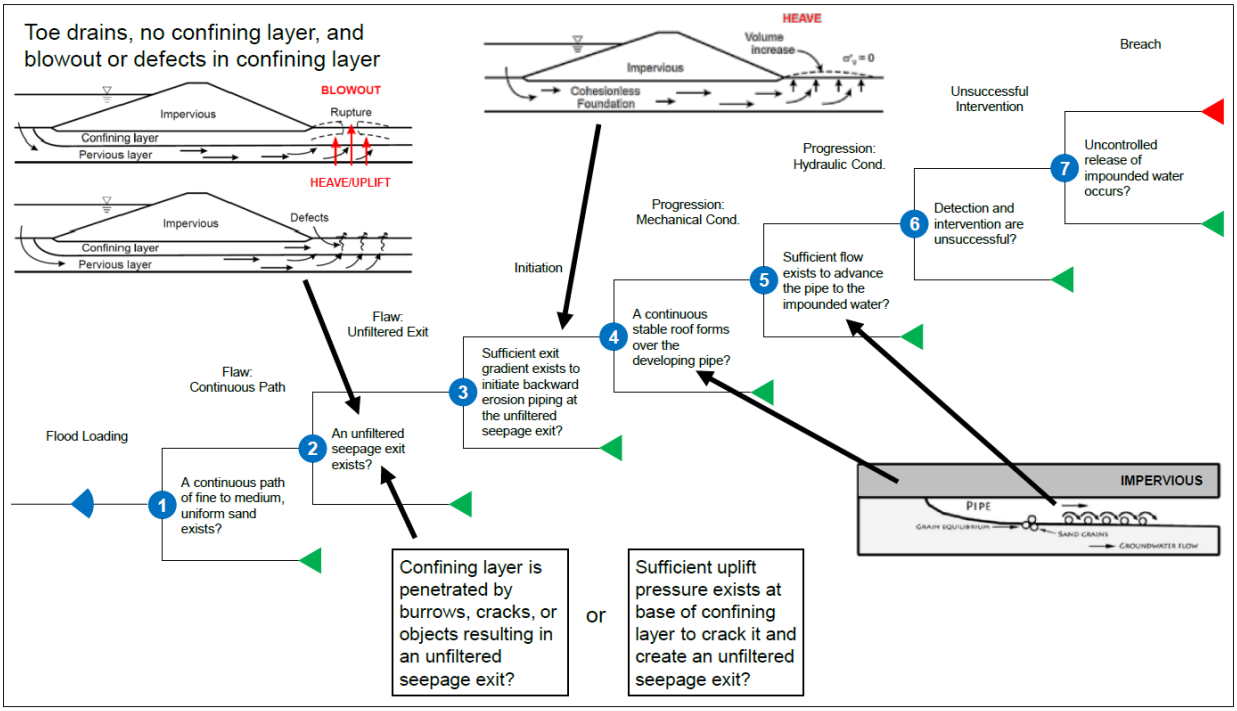

Figure 4.6 Example of event tree for backward erosion piping.

4.1.3 Example of the use of failure paths and event trees for modelling internal erosion and piping of levees and their foundations from Australia

Contribution by Emeritus Prof. R. Fell (School of Civil and Environmental engineering, Australia) and Dr. M. Foster (Dam Consulting Services Pty Ltd, Australia)

Introduction

Failure paths and event tree methods have been used in Australian Dam Engineering Practice to model internal erosion and piping in dams and their foundations since 1999 following publication of Foster (1999), Foster and Fell (1999). Since then, most of the large embankment dams in Australia have been assessed for the likelihood of failure by internal erosion and piping using quantitative risk assessment methods. Many of these dams have saddle dams, which are constructed in a similar manner to levees and dikes and are, like levees and dikes, only subject to water loading under flood conditions. The methods have also been extensively used to assess the likelihood of failure of urban flood retention structures by internal erosion and piping. The contributors have themselves been involved in more than 200 such risk assessments, including application to canal embankments and levee embankments. The methods used are directly applicable to levees and dikes.

Generic Event Tree

The generic event tree which is used is as described in (Fell, et al., 2008).

↳Reservoir (or River level) Rises
↳Initiation – Flaw exists
↳Initiation – Erosion starts
↳Continuation – Unfiltered or inadequately filtered exit exists (consider: no erosion/some erosion/excessive erosion/continuing erosion)
↳Progression – Roof forms to support a pipe
↳Progression – Upstream zone fails to fill crack
↳Progression – Upstream zone fails to limit flows
↳Detection and Intervention fails
↳Dam or levee breaches (consider all likely breach mechanisms)
↳Consequences occur

A ‘flaw” is a continuous crack or poorly compacted zone in which a concentrated leak may form. For backward erosion piping, Suffusion and Global Backward Erosion no flaw is required but a continuous zone of cohesionless soil in the embankment or foundation is required.

Initiation. There are several processes by which erosion can initiate in the embankment or foundation:

- *Concentrated leak erosion.* Erosion can commence from the walls of a crack within the soil or within the voids of a poorly compacted layer.
- *Scour at the embankment –foundation contact*. (contact erosion) Erosion of the soil may occur where it is in contact with seepage passing through the foundation either through a coarse-grained soil or open joints in rock.
- *Backward Erosion Piping.* Backward Erosion Piping involves the detachment of soils particles when the seepage exits to a free unfiltered surface. The detached particles are carried away by the seepage flow and the process gradually works its way towards

the upstream side of the embankment or its foundation until a continuous pipe is formed.

- *Suffusion*. This is a form of internal erosion which involves selective erosion of fine particles from the matrix of coarser particles (the voids are under-filled so coarse particles are not floating in the fine particles). The fine particles are removed through the constrictions between the larger particles by seepage flow, leaving behind an intact soil skeleton formed by the coarser particles.
- *Global Backward Erosion.* Global Backward Erosion occurs in widely graded silt sand gravel soils in which the voids are over-filled, so the coarser particles are "floating" in the finer soil matrix. Finer particles move within the soil matrix and may be eroded from the soil.

Continuation is the phase where the relationship of the particle size distribution between the base (embankment body or foundation) material and the filter controls whether erosion will continue. Foster and Fell (1999a, 2001) and Foster (1999) define four levels of severity of continuation; No Erosion, Some Erosion, Excessive Erosion and Continuing Erosion.

Progression is the third phase of internal erosion, where hydraulic shear stresses within the eroding soil may or may not lead to the enlargement of the pipe. Increases of pore pressure and seepage occur. The main issues are whether the pipe will collapse and whether upstream zones may control the erosion process by flow limitation or crack filling.

Detection and Intervention fails is the fourth phase of the event tree, and this considers whether the internal erosion failure mechanism will be detected and whether intervention and repair will successfully stop the failure process.

Breaching is the final phase of internal erosion. It may occur by one of the following four phenomena (listed below in order of their observed frequency of occurrence).

- Gross enlargement of the pipe (which may include the development of a sinkhole from the pipe to the crest of the embankment).
- Slope instability of the downstream slope.
- Unraveling of the downstream face.
- Overtopping, e.g. due to settlement of the crest from suffusion and/or due to the formation of a sinkhole from a pipe in the embankment.

It should be noted that for Suffusion and global backward erosion no pipe is formed. The erosion of finer particles results in increased permeability, and potentially settlement but the matrix of the soil remains.

This event tree was developed jointly by UNSW, URS (now AECOM), USBR and USACE to prepare (Fell, et al., 2008). The description has been amended to better include backward erosion piping, suffusion and global backward erosion mechanisms and reference to levees.

4.1.4 Failure paths experience from SYMADREM France.
Contribution by T. Mallet (SYMADREM, France)

4.1.4.1 Context

The Rhône Delta covers an area of 1500 km². It is protected by three river levee systems (225 km) and a coastal levee system (50 km), managed by the *Syndicat Mixte Interrégional d'Aménagement des Digues du Delta du Rhône* and *Mer* (Symadrem), a public institution created in 1999 following the failure of the associations of riparian owners who had been managing the structures since the middle of the 19th century.

The levee systems were created after the floods of 1840 and 1856 (return periods estimated at 400 and 250 years respectively) replacing other even older structures, some of which date back to the 12th century. Due to their construction technique, which is compaction with manual tamping devices of 15 kg, not considering the optimum water content concept discovered in 1933 by Ralph Proctor and the "onion" effect caused by successive rising phases, the Rhône levees are highly exposed to failures by internal erosion (Mallet, Outalmit, & Fry, 2014). As part of the hazard studies required by French regulations, a analysis of observed failure mechanisms was carried out on the entire levees systems. The main results are presented below and can be found in more detail in (Mallet, Fry, Tourment, & Mériaux, 2019)

4.1.4.2 Statistics on recent and old events

Figure 4.7 presents peak flows, at the head of the delta, of maximum annual floods from 1830 to 2016. In red are the floods that initiated flooding of the protected zone by breach. Since 1840, nine floods have led to flooding: 1840, 1841, 1843, 1856, 1993, 1994, 2002, 2003 and 2016. The figure also indicates the analysed periods: the early period from 1840 to 1886 and the recent period from 1993 to 2016. The intermediate period from 1886 to 1993, corresponding to the hydrological “standby” of the Rhône, was not analysed for lack of sufficiently detailed archive documents to carry out a quality analysis. In addition to these floods leading to inundation of the protected land, six floods without inundation were also analysed. The analysis of Figure 4.7 shows that the probability of flooding per breach was:

- Less than 5% for floods with return periods of between 5 and 10 years;
- Between 5 and 50% for floods with a return period of between 10 and 20 years;
- Greater than 50% for events of 20 to 50 years;
- It is 100% for floods with return periods greater than 50 years.

These probabilities, derived from the observation of past floods, are considered a good indicator for crisis management. Of the 15 analysed floods: 57 breaches, 57 breaches in progress and 133 disorders were identified. Three breaches caused by water flowing back to the river were also recorded in 1840, which gives a total number of 117 breaches and breaches in progress in 176 years, which is consistent with the assessment made within the framework of the hazard studies (Mallet, et al., 2018).

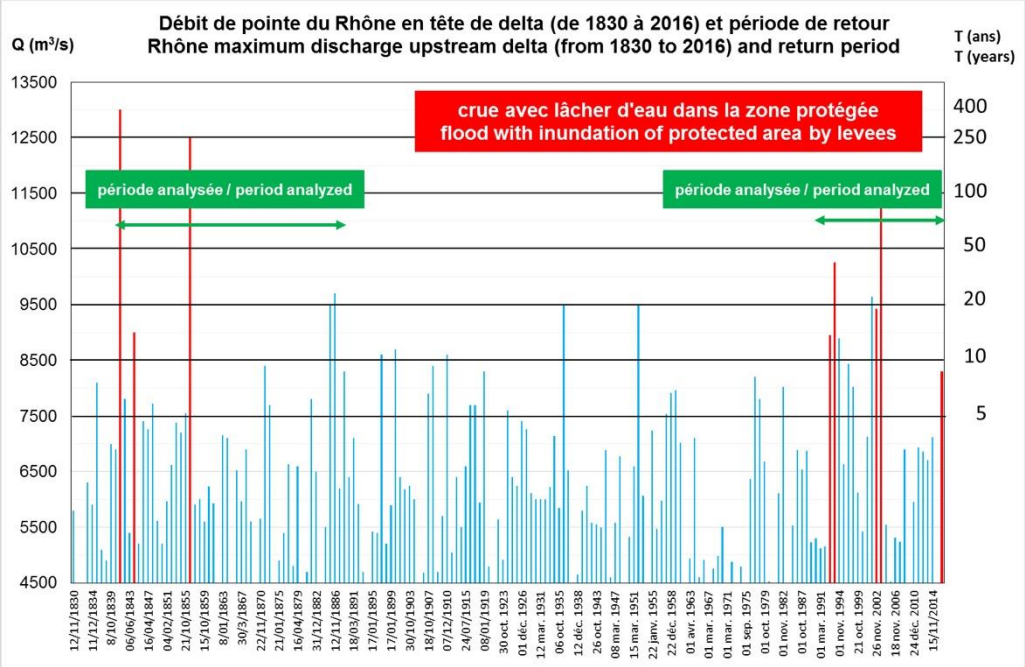

Figure 4.7 Flood discharges and inundation of the protected area (1830-2016).

Breaches are generally located on the Rhône and the upstream Petit Rhône, where levees are the highest (4.5 to 7 m) and hydraulic loads the highest in the past (3 to 6 m). Start of breaches are, for their part, rather localized on the Grand Rhône and the downstream Petit Rhône, where levees are lower (2 to 4.5 m) and the hydraulic loads have been lower in the past (1.5 to 2.5 m).

Table 4.1 provides an overview by breach initiator according to the period. The analysis of observed failure mechanisms of levees in the Rhône delta follows a similar trend to that of embankment dams with a higher proportion of accidents linked to internal erosion.

Table 4.1 Breaches and breach initiations by initiating failure mode.

period	*Breaches (57) by initiation cause*			*Breaches (57) and start of breaches (57) by initiation cause*		
	Overflow	*Internal erosion*	*External erosion, scouring*	*Overflow*	*Internal erosion*	*External erosion, scouring*
1840-1886	*36 %*	*64 %*	*0 %*	*19 %*	*73 %*	*8 %*
1993-2016	*25 % (0 % ?)*	*75 % (100 % ?)*	*0 %*	*17 %*	*83 %*	*0 %*
1840-2016	*33 %*	*67 %*	*0 %*	*18 %*	*76 %*	*6 %*
Dams (ICOLD, 2015)	*48 %*	*46 %*	*Sliding 6 %*			

There were 19 breaches caused by overflow throughout the period. From these 19 breaches, 16 occurred in 1840 before the general rising of the levees and 3 during the centennial flood of December 2003. For each of them, the water layer thickness at the crest of the levee during

overflow was thins, less than 10 cm, however with a fall height greater than 4 m. For these three breaches in 2003, certain heterogeneities were observed, after flooding, in the levee bodies. Internal erosion mechanisms cannot therefore be ruled out, which could give a total of 100% of breaches by internal erosion for the recent period. We also note two initiations of breaching by overflow in 2002 and 2003 over a line of 2 km downstream of the delta. These are analysed below.

4.1.4.3 Succinct analysis and lessons for risk analysis

Between 1993 and 2016, all breaches by internal erosion are due to concentrated leak erosion (Mallet, Outalmit, & Fry, 2014) except for one, for which the initiator remains to be confirmed. Between 1840 and 1886, the designation by the engineers of the time of "breach by seepage" leaves some doubt on the possibility of backward erosion, particularly at the place of former beds. Nevertheless, considering recent experience and the assessment of breach probability by backward erosion (Mallet & Fry, 2016), concentrated leak erosion seems to be the preferred mode of breaching by internal erosion in the past too. The study also showed that scour could be a source of damage, even the start of a breach when the flood was long, for example the 1856 flood, but without leading to a full breach.

The forensic analysis of recent breaches by concentrated leak erosion showed that, in all cases, the critical stress (characterizing the erosion threshold) of the materials was less than 10 Pa. The Erosion Rate indexes (characterizing the erosion kinetics) were in the order of 3, between 2.7 and 3.2. On the other hand, a case of large leaks in rabbit burrows was observed which did not lead to a breach when the critical stress was of the order of 50 Pa. The initiating gradients, when the breach process started in badger or rabbit burrows, all ranged from 0.01 to 0.05. They were slightly higher than 0.1 for breaches caused by pipe erosion along the crossing structures. (Mallet, Outalmit, & Fry, 2014) provides a quantitative assessment of the probability of breach by concentrated leak erosion. The analysis also showed that the parameters "water loads measured from the protected side" and "freeboard / height (R / H)" were strongly correlated with each other and played a key role in the breaching process (Mallet, et al., 2018) and (Mallet, Fry, Tourment, & Mériaux, 2019).

Regarding overflow, the study showed that with a fall height of less than 1.5 m and dense vegetation at the foot of the structure making it possible to slow down the waterflow velocity, the breaching process by overflow had not gone to its end with water layer thickness on the levee crest less than 20 cm and overflow times of several tens of hours. In contrast, with fall heights of 4 m, the overflow breaching process was completed with less than 10 cm water layer thickness at the crest of the levee during a few hours.

4.1.4.4 Analysis of the breaching process and lessons learned for risk analysis

The study in to the observed mechanisms showed that the initiation of a failure mode did not systematically lead to a breach and that breaches were a process with several steps described in (ICOLD, 2015) and quantified in (Mallet, Outalmit, & Fry, 2014), (Mallet & Fry, 2016) and (Mallet, et al., 2018). Table 4.2 presents respectively for the floods of November 2002, with a return period 20 years, duration of flood 15 days and of December 2003, with a return period of 100 years, duration of flood 3 days, the number of disorders (DES.), emergency interventions (URG.), breaches in progress (DP.BR.) and breaches (BR.) per breach initiator.. In the flood of November 2002, out of the 33 identified damages, only one led to a start of

breach and another to a breach. In the flood of December 2003, out of the 67 damages identified, 2 gave rise to starts of breaches and 4 to breaches. ,

Table 4.2 Disorders, breaches in progress and breaches by failure initiation mode, DES = number of disorders, URG = emergency inventions, DP.BR = breaches in progress, BR = number of breaches.

Initiation cause	*November 2002 flood*				*December 2003 flood*			
	DES.	*URG.*	*DP.BR.*	*BR.*	*DES.*	*URG.*	*DP.BR.*	*BR.*
overflow	*6*	*5*	*1*	*0*	*13*	*4*	*4*	*3*
concentrated leak erosion in burrow	*11*	*9*	*1*	*1*	*12*	*5*	*0*	*0*
concentrated leak erosion along a crossing pipe	*1*	*1*	*0*	*0*	*6*	*4*	*1*	*0*
contact erosion (ancient breach)	*3*	*1*	*0*	*0*	*8*	*0*	*0*	*0*
internal erosion-other	*0*	*0*	*0*	*0*	*1*	*0*	*1*	*1*
scour	*4*	*0*	*0*	*0*	*11*	*1*	*0*	*0*
land side sliding	*1*	*0*	*0*	*0*	*0*	*0*	*0*	*0*
water side sliding	*1*	*1*	*0*	*0*	*1*	*0*	*0*	*0*
functional failure (pipe)	*4*	*4*	*0*	*0*	9	2	0	0
Total	*31*	*21*	*2*	*1*	61	16	6	4

These statistics, crossed with those of 1993 and 1994 (Mallet, Outalmit, & Fry, 2014) make it possible to assess, according to the breach initiator, the possible evolution of an initial damage toward a breach in progress, then as a breach. They also make it possible to measure the impact of emergency interventions. For these two floods, the success of the emergency interventions on: localized overflows, even in the event of a rapid rise of water level; visible animals burrows; functional failures of through hydraulic structures; concentrated leak erosions along pipes. Conversely, emergency interventions were not possible when the burrows were hidden. In this scenario described in detail and evaluated in (Mallet, Outalmit, & Fry, 2014), partially plugged burrows appear suddenly after hydraulic fracturing of the plug. The hydraulic gradient is then significantly greater than the critical gradient and the erosion kinetics too fast to consider an emergency intervention. The very present scour and contact erosion hardly required any emergency interventions, given their very slow erosion kinetics. It is the same for sliding.

The accidentological study of the structures and of the consequences of their ruin on the protected area made it possible to determine for the risk analysis associated with the embankment structures, 11 breach scenarios involving one or more failure modes and 1 functional failure scenario (Mallet, et al., 2018). It also made it possible to establish event trees (see Figure 4.8) for each of the scenarios, taking into account not only the initiation phases characterized by the appearance of damage but also the other stages, which are continuation and progression (Mallet, et al., 2018). These event trees also integrated the phases of damage detection and emergency intervention, which made it possible to avoid, during the floods of

2002 and 2003 and more recently in 2014 and 2016, the initiation or extension of breaches. The assessment of breach scenarios was carried out using a probabilistic method based on feedback from experience.

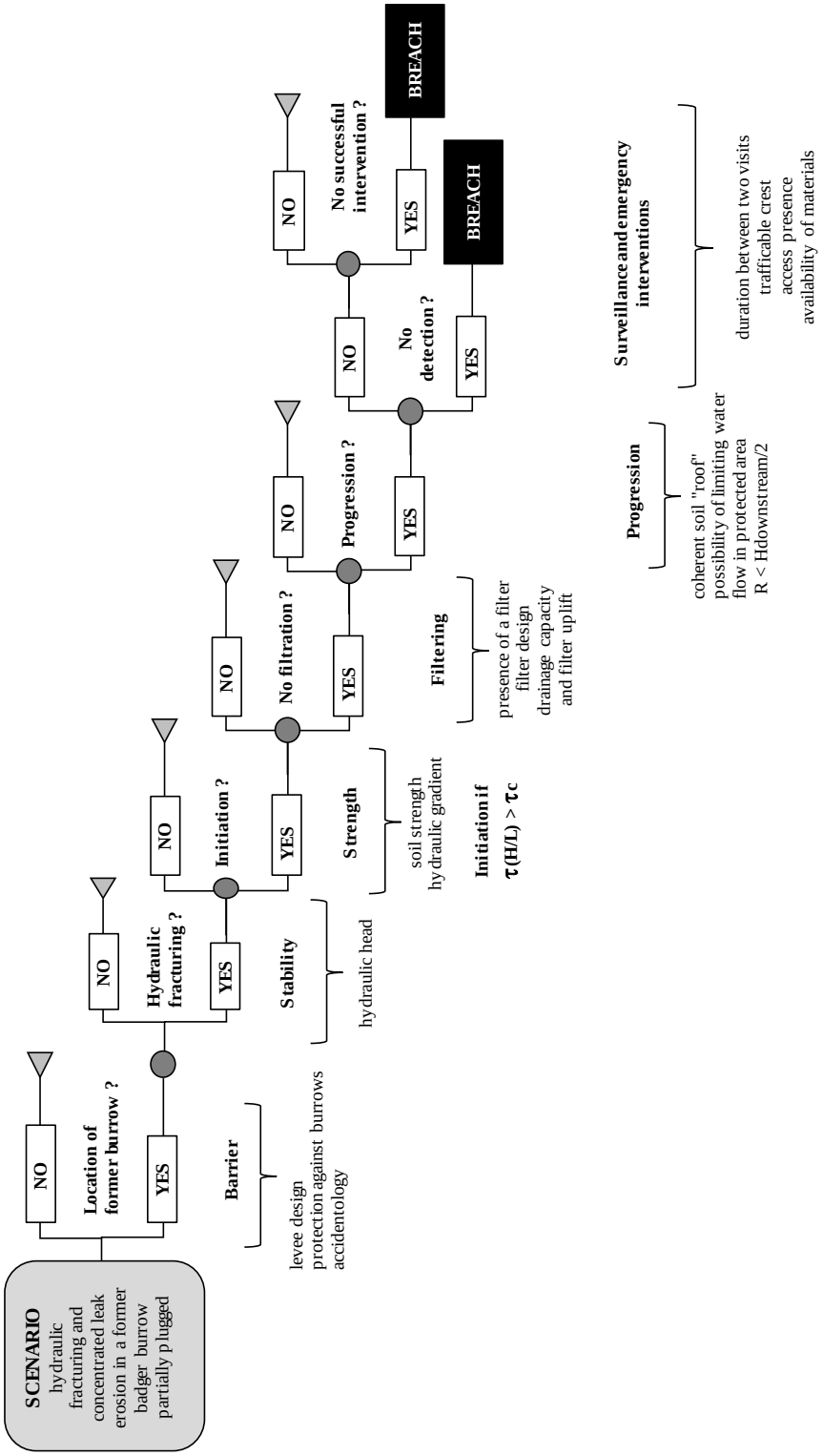

Figure 4.8 Example of an event tree for breach by internal erosion in badger burrow (Mallet et al., 2018).

4.1.4.5 *Probabilistic evaluation*

According to event tree, the probability of breach due to a hole by badger is expressed as:

$P_{breach} = P_{loc}.P_{frac}.P_{ini}.P_{non\ filtration}.P_{progression}.(P_{non\ detection} + (1\text{-}P_{non\ detection}).P_{non\ intervention})$

Where:

- $P_{location}$: probability that a location crosses a hole with an initial fracture;
- $P_{fracturing}$: probability of hydraulic fracturing a partially plugged burrow;
- $P_{initiation}$: probability of initiation of pipe flow with erosion ($\tau > \tau_c$);
- $P_{non\ filtration}$: probability that passage of the eroded particles isn't impeded in some way;
- $P_{progression}$: probability that the process continues without stabilization;
- $P_{non\ detection}$: probability that the pipe is not detected during safety patrol;
- $P_{non\ intervention}$: probability that emergency intervention can't be carried out.

Probabilities are frequential probability or subjective probability (Mallet, Outalmit, & Fry, 2014), (Mallet & Fry, 2016) and (Mallet, et al., 2018).

Eleven failure paths are studied by Symadrem, comprising seven internal erosion failure paths, which are illustrated below. Pictures are issued from Mallet 2019.

Failure path 1: Breach by concentrated leak erosion in a former badger burrow partially plugged, not visible and unknown, after hydraulic fracturing

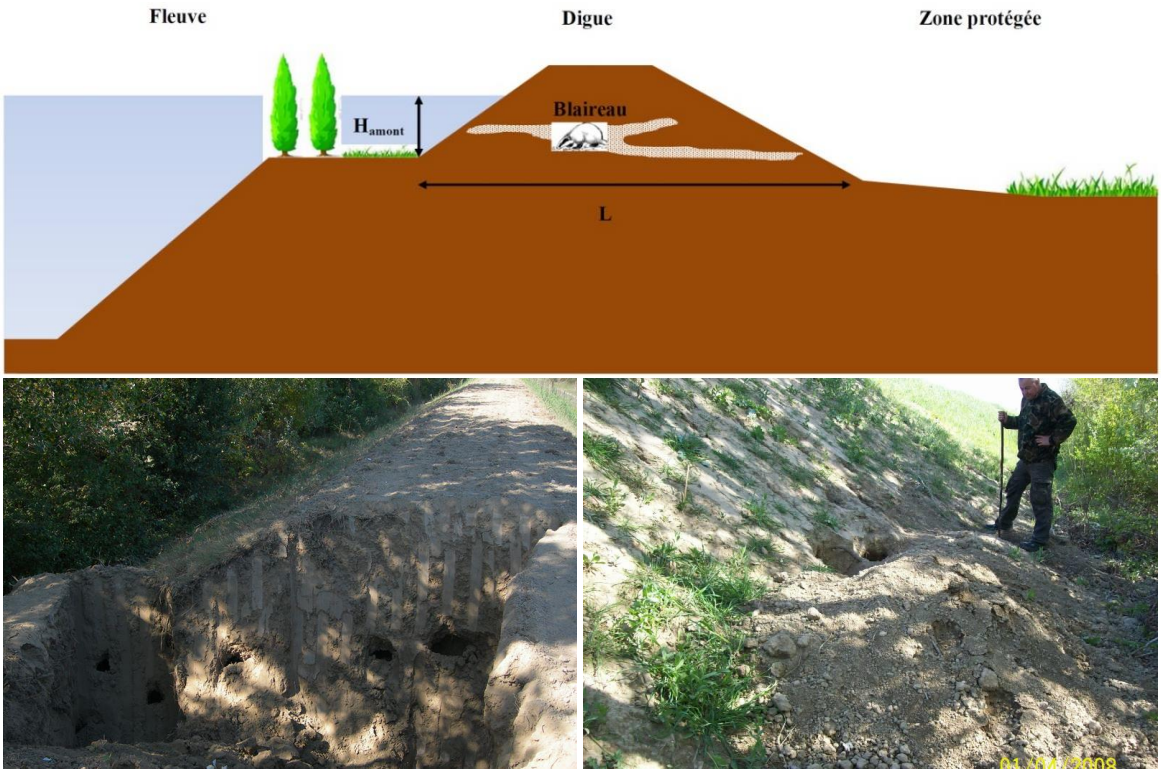

Figure 4.9 Scenario n°1: Breach by concentrated leak erosion in a former badger burrow partially plugged, not visible and unknown, after hydraulic fracturing.

Failure path 2: Breach by concentrated leak erosion in a hole along a crossing structure.

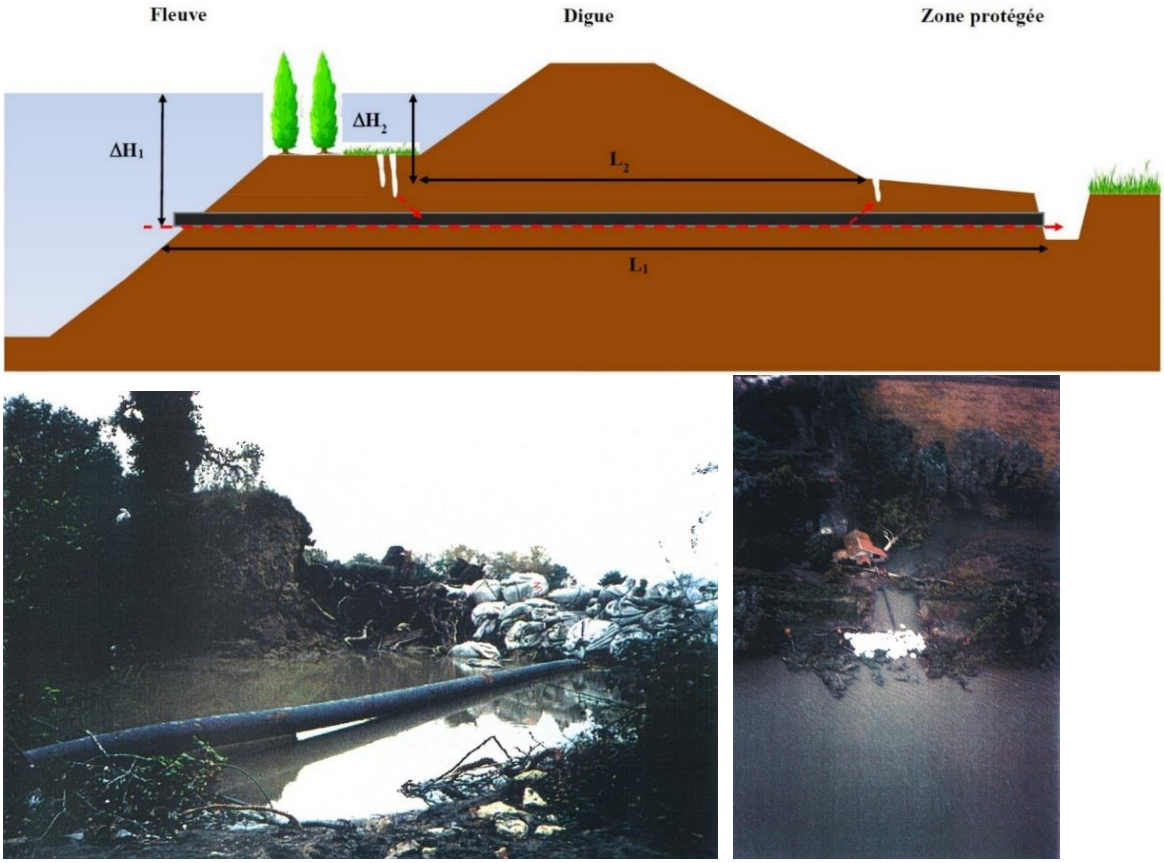

Figure 4.10 Scenario n°2: Breach by concentrated leak erosion in a hole along a crossing structure.

Failure path 3: Breach by concentrated leak erosion in a root of dead tree.

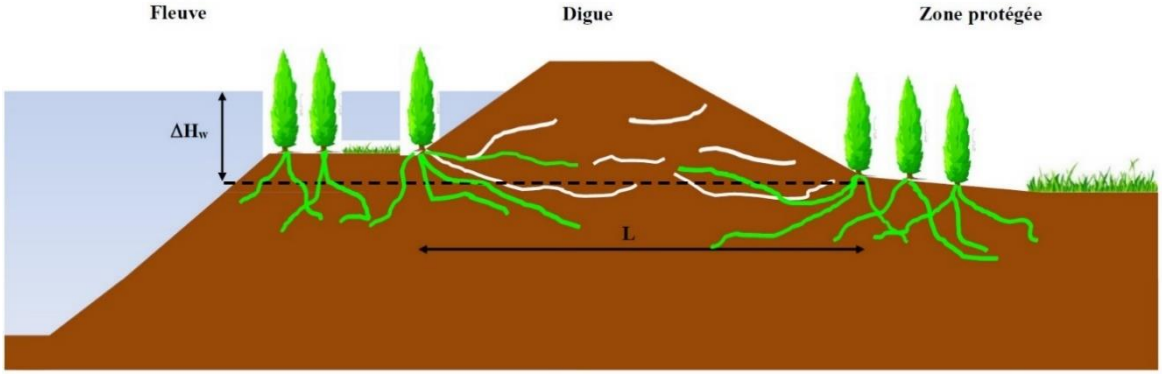

Figure 4.11 Scenario 3: Breach by concentrated leak erosion in a root of dead tree.

Failure path 4: Breach by concentrated leak erosion in a crossing crack along a former transition insufficiently treated.

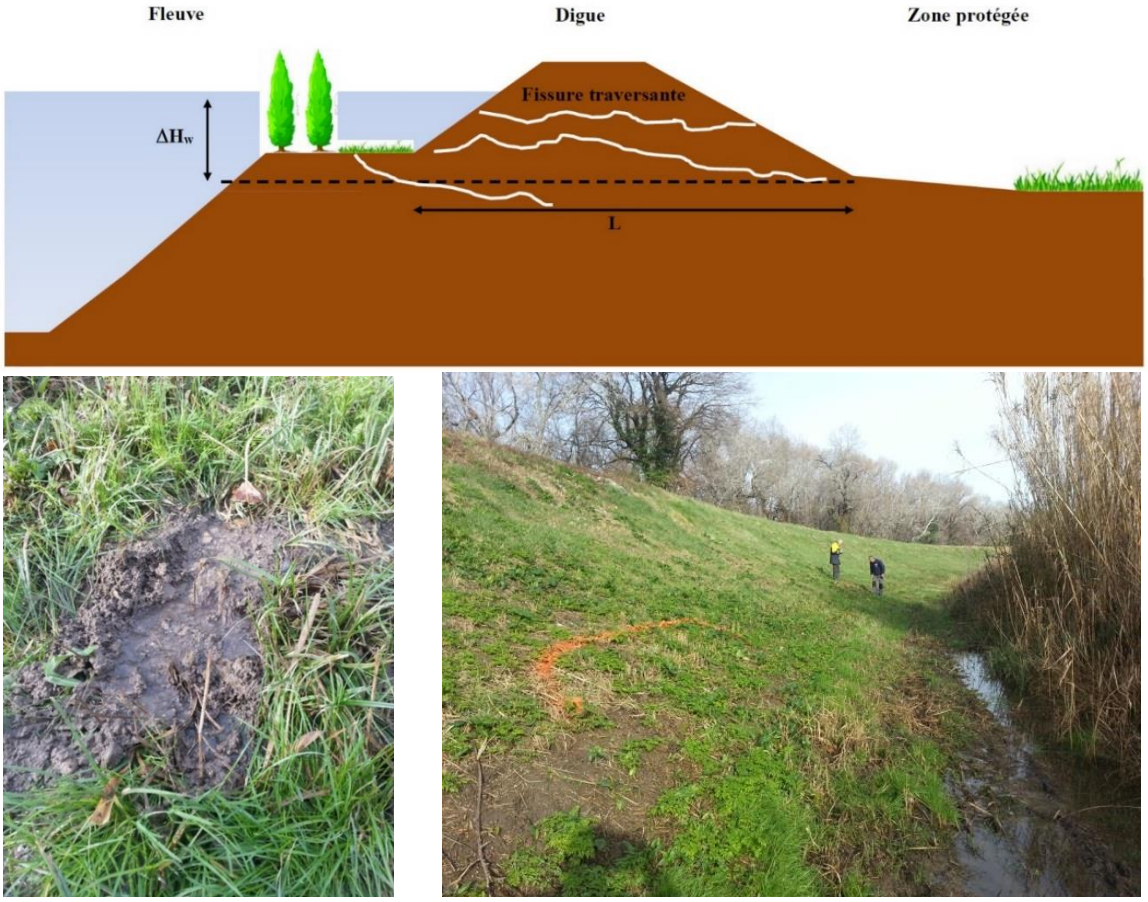

Figure 4.12 Scenario n°4: Breach by concentrated leak erosion in a crossing crack along a former transition insufficiently treated.

Failure path 5: Backward erosion in a sand layer after uplift the silty blanket overlying the sandy soil strata.

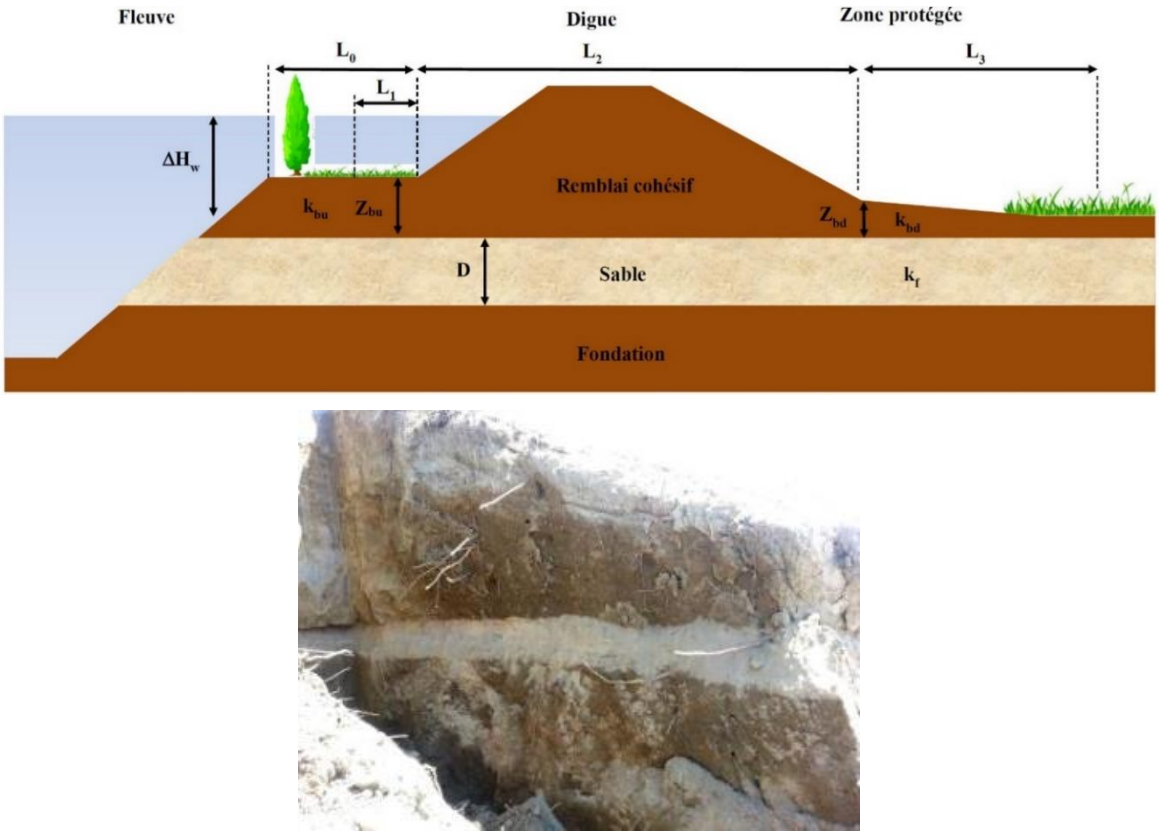

Figure 4.13 Scenario n°5: Backward erosion in a sand layer after uplift the silty blanket overlying the sandy soil strata.

Failure path 6: Contact erosion between gravel and silt (case of breaches repaired in emergency situations with permeable materials).

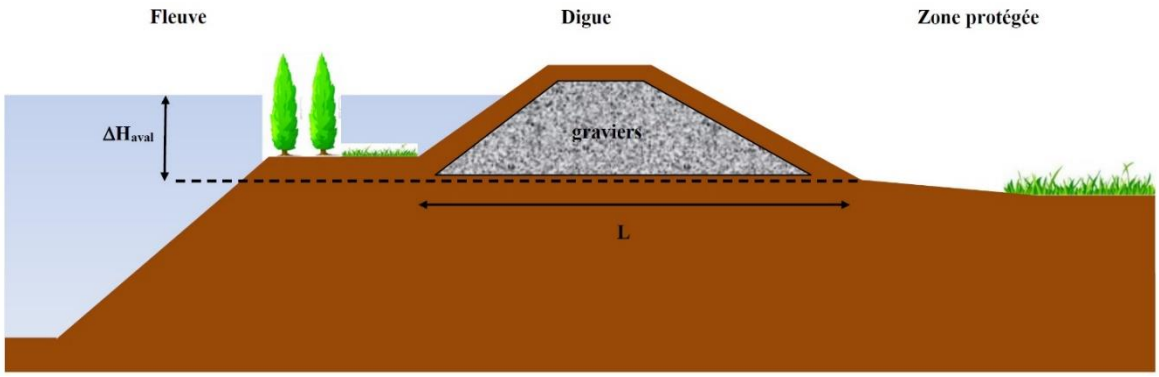

Figure 4.14 Scenario n°6: Contact erosion between gravel and silt (case of breaches repaired in emergency situations with permeable materials).

Failure path 7: Suffusion in gravel of an ancient pavement layer. It should be noted that levees were ancient ways of communication before their general raising in the 19th century.

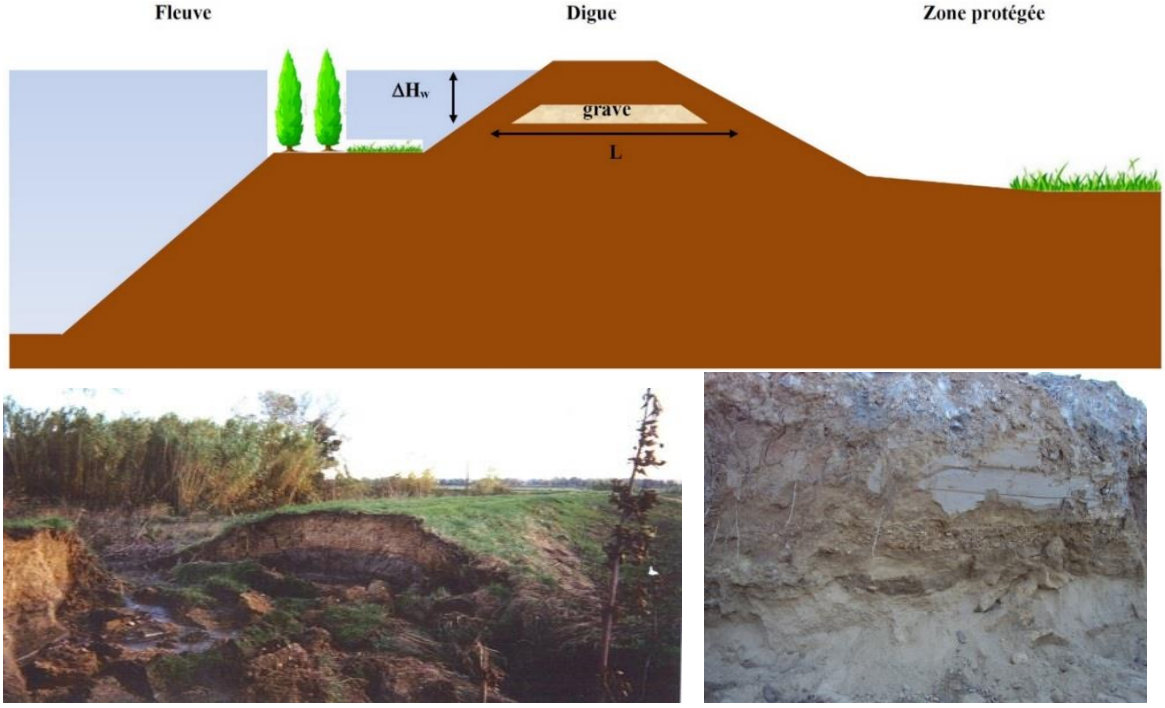

Figure 4.15 Scenario n°7: Suffusion in gravel of a ancient pavement layer (because levees were ancient ways of communication before their general raising in the 19th century).

The figure below illustrates for a geometric profile and a given design (old levee in the example without any particular component), the evolution of the conditional probability of each of the stages of the breach scenario studied, depending on the intensity of the flood.

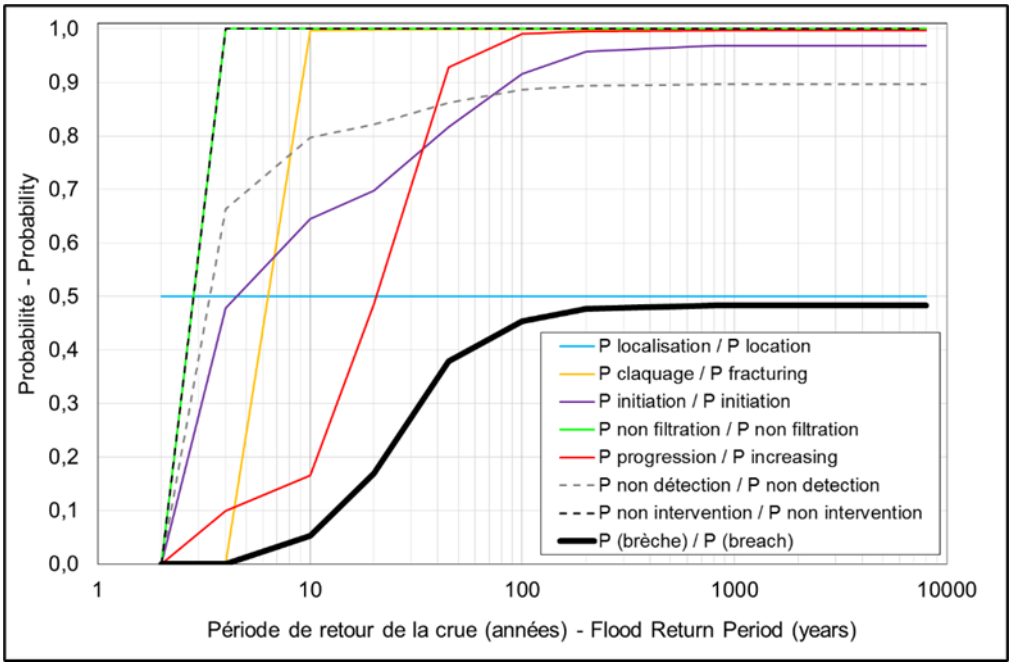

Figure 4.16 Conditional probabilities (stages and scenario) according to flood intensity (Mallet, et al., 2018).

The following figure illustrates the conditional probabilities of each breach scenario studied, as a function of the intensity of the flood, and the overall probability of breach integrating all these scenarios.

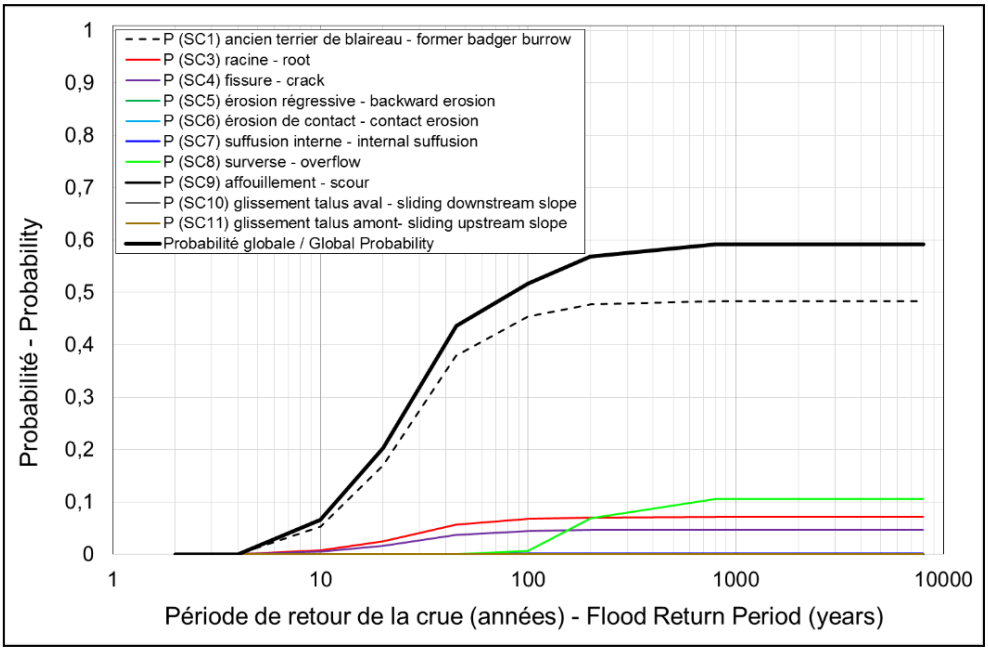

Figure 4.17 Conditional probabilities (scenarios and global) according to flood intensity (Mallet, et al., 2018).

4.1.5 Internal erosion and overtopping example from Czech Republic

Contribution by J. Říha

The example below shows an event tree analysis for both internal erosion and overtopping.

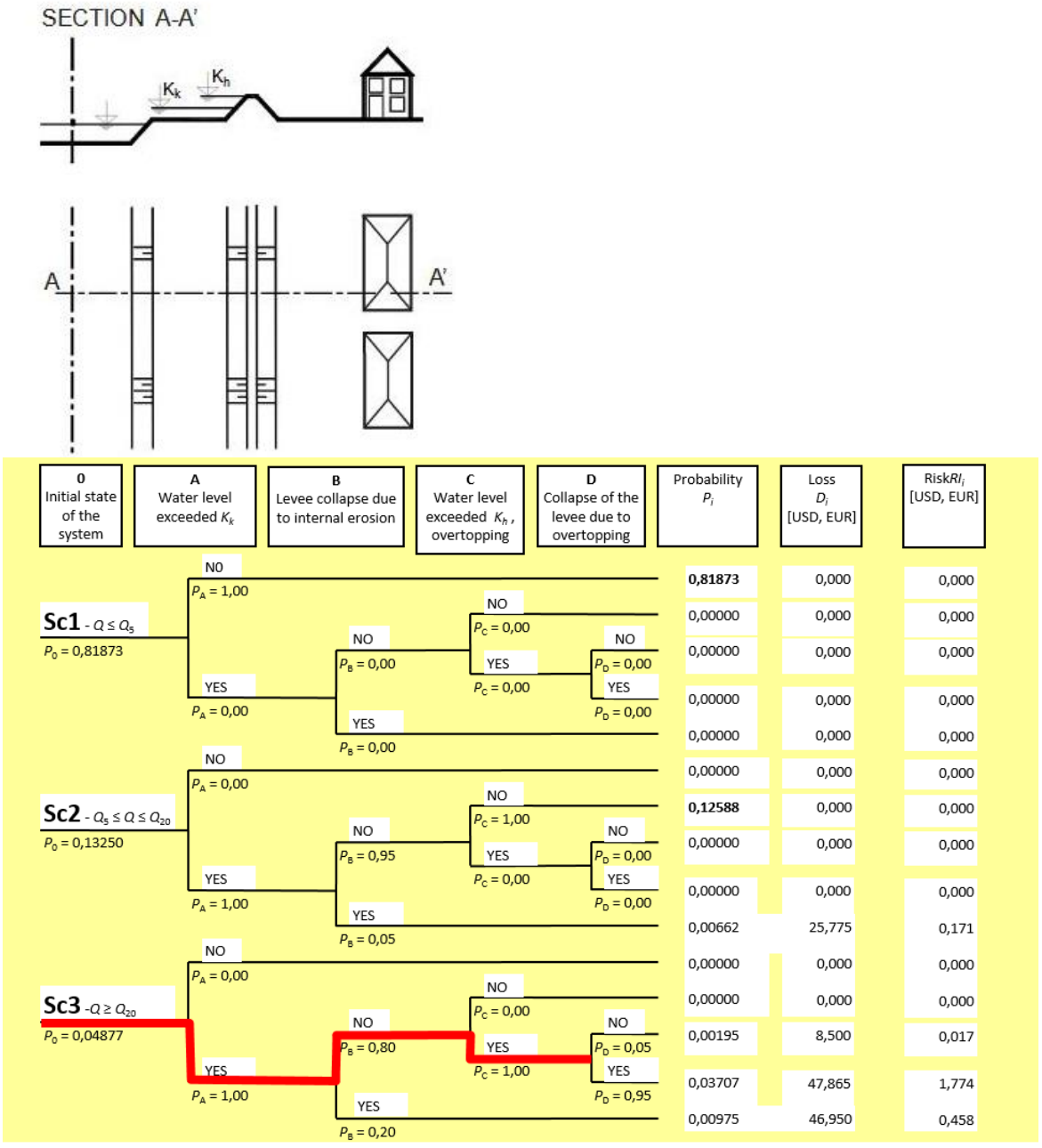

Figure 4.18 General event tree for levee failure due to internal erosion and overtopping from Czech Republic.

Comments to the event tree:

1. Initial state, 0 in Figure 4.18 - the probability of the event is based on the probability of the critical level for internal erosion and overtopping corresponding to the return period of the flood discharge. Both processes and final extent of levee damage depend on the duration of the flood and therefore are time dependent. The estimate is possible based on conditional probability of the flood volume at given peak discharge. Here the shape of flood hydrograph

plays significant role as illustrated below (Alhasan, Duchan, & Říha, 2019) that paper shows how the probabilities along the marked path may be estimated.

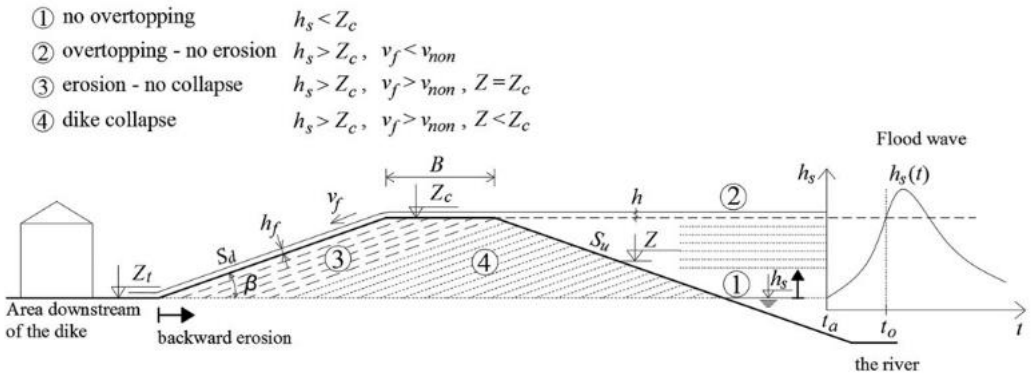

Figure 4.19 Failure of a levee due to overtopping (Alhasan, Duchan, & Říha, 2019).

2. The evaluation of individual paths (probability *P* of the events - 0, A, B, C, D in Figure 4.18) should be done using available data, mathematical and stochastic modelling of the phenomena:

   0 - Hydrological data - probability distribution of the discharges in the river.

   A - Hydraulic modelling of the flow in the river - Q(h) - dependence.

   B - Groundwater flow modelling and internal erosion process modelling (Říha, Kotaška, & Petrula, Dam Break Modeling in a Cascade of Small Earthen Dams: Case Study of the Cizina River in the Czech Republic, 2020). Here the time effect is significant.

   C - Hydraulic modelling of the flow in the river - Q(h) - dependence.

   D - Modelling of overtopping and surface erosion of the levee (Julínek, Duchan, & Říha, 2020) and (Říha, Kotaška, & Petrula, 2020).

3. The economic losses *D* are estimated as follows:

- The flood routing behind the levee preferable using 2D models. The inflow to the protected area may be natural /rainfall, local streams), seepage water, overtopping, levee damage or collapse, etc.
- Determining flood arrival time, local water depth and velocities for individual scenarios (sub-events).
- Determining percentual extent of the damage on the elements located at the flood plane (houses, agricultural land, industry, ...) using damage curves.
- Using census data about the property in the floodplain for the estimate of the loss for individual scenarios (sub-events).

4. The partial risks for individual scenarios (sub-events - *i*) is determined as $RI_i = D_i * P_i$.

5. Total risk is determined as follows:

$$RI_R = E(D) = \sum_{i=1}^{n} D_i \cdot P_i$$

6. The models mentioned above (hydraulic, seepage, internal and surface erosion) may be calibrated using documented case histories (Říha, 2007) and (Říha & Jandora, 2007).

4.1.6 Example backward erosion piping failure path from the Netherlands.

Contribution by Dr. E. Rosenbrand (Deltares, Netherlands)

An example of a failure path for backward erosion piping from the Netherlands is given by Figure 4.20. This path assumes a subsurface scenario of a granular aquifer covered by a clay layer, i.e. a subsurface scenario that is susceptible to backward erosion piping.

There are different versions of the backward erosion failure path. In simplified versions some steps are combined to facilitate analysis. The steps in the failure path can be described as:

1. A high-water event, e.g. a high-water level in the river.
2. Rising pore water pressures in the foundation below the blanket.
    - The increase in pore water pressures is strongly affected by the hydraulic conductivity of the granular basis. Also, the presence of a floodplane between the river and the levee can have an important damping effect. Especially if this floodplane is overlain by a less permeable cover layer, the increase of pore water pressure in the foundation can be strongly reduced. Other factors that affect the rise of pore water pressures in the foundation are the leakage length, which describes the distance over which the pore water pressure dissipates on the landward side and the geohydrology on the landward side. If the landward side has a thin and permeable blanket layer, pore water pressures will not be able to increase as much as when the blanket is thick and impermeable.
3. Uplift and cracking of the cover layer.
    - In the analysis generally the assumption is made that if the pore water pressures are high enough to cause uplift, the blanket will also crack. Whether or not uplift occurs depends on the weight (thickness and unit weight) of the blanket as well as the pore water pressure in the aquifer. The cracking of the blanket will also be affected by the strength and thickness of the blanket, but this is currently not included in assessing the limit state.
4. Heave, involves the transport of grains from the aquifer to the surface by flow, causing a sand boil.
    - This is affected by the flow rate in the sand boil, and by the weight of the grains.
5. Pipe formation progresses just below the cover layer in the upstream direction.
    - The cohesive cover layer forms a roof over the pipe. This mechanism is described in the Netherlands using the Sellmeijer model (Sellmeijer J. B., 1988) (Sellmeijer, de la Cruz, van Beek, & Knoeff, 2011). This model predicts the head drop above which a pipe will progress upstream. Important parameters are the permeability of the aquifer, the thickness of the aquifer, the grainsize of the aquifer and the seepage length.
      If there is a blanket layer and a sand boil at the landward side, the head drop in the sand boil, due to suspended sediment, also can provide additional resistance.
6. Hydraulic shortcut; the pipe contacts the upstream water body, and flow in the pipe increases dramatically.
    - This step is not assessed explicitly in the typical assessments. The shortcut may occur when the pipe contacts the outer water body, e.g. in the river. In the case of a cohesive cover on the floodplain a pipe could possibly make a shortcut if there is a crack or hole in this cover layer. The thickness and quality of the cover layer in the floodplain will affect whether this occurs.

7. The next steps include widening and deepening of the pipe, reduction of crest height and breaching are often captured in one step as little information is available regarding these processes.
8. Remediation measures are visualized in the path shown below but may be applied at any step before.

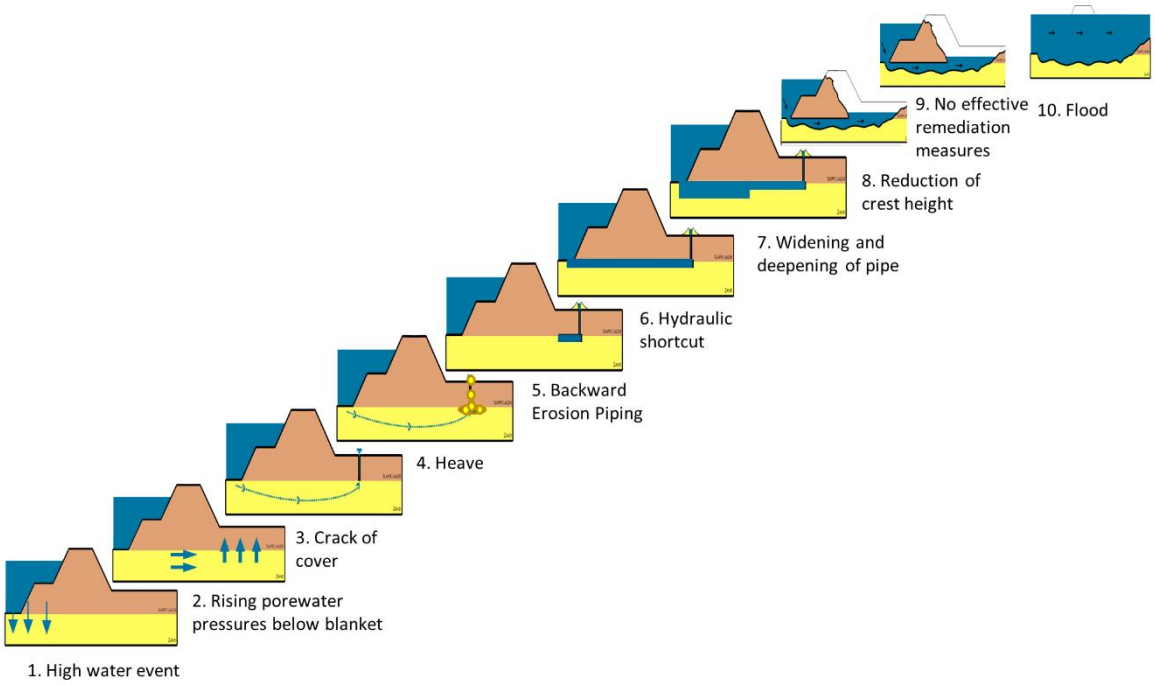

Figure 4.20 Example of a failure path for backward erosion piping, modified from (Rosenbrand, Knoeff, Hijma, & Van Onselen, 2020).

4.2 Examples of Failure trees/paths involving slope sliding or slope instability

Slope sliding is described as one of the prevalent forms of instability in the International Levee Handbook (CIRIA, French Ministry of Ecology, and USACE, 2013), and described as:

> *"a 3D phenomenon in which a certain volume of soil moves down the slope under the influence of gravity and/or external actions. The sliding mass is bounded above by the surface of the slope, and below by a surface of sliding characterized by a discontinuity in strain and velocity field. It is in fact a transitional zone generally sufficiently thin to be considered as a surface as regards to the sling soil volume."*

This section contains examples of failure paths involving slope instability or slope sliding.

4.2.1 Example of failure path for flooding due to outer slope instability from the Netherlands

Contribution by A.W. van der Meer MSc (Deltares, Geotechnical Risk and Reliability)

Most slope instabilities of embankments do not lead to flooding. Consecutive mechanisms are needed to cause flooding. The following study present the incorporation of those consecutive mechanisms in the determination of the probability of flooding due to outer slope instability. The study (Van der Meer, Teixeira, Rozing, & Kanning, 2021), funded by the Dutch Flood Protection Program (HWBP), is about outer slope instability. Similar approaches as the ones described below are now being used in different levee reinforcement projects in The Netherlands. The considered failure path starts with a high-water level event. Induced by the high-water level, the pore water pressures inside the levee increase. When the water level drops, the pore water pressures in the levee also decrease but with a time lag. The situation with high pore water pressures in the levee and a low water level is unfavorable for outer slope stability. In case of an instability there is yet no flooding, since the water level has just dropped. If the created damage is not repaired before the consecutive high-water level event and the damaged levee is insufficient to withstand the loading during this consecutive high-water level event, there will be flooding. The mechanisms erosion by wave attack, wave overtopping, and overflow are considered as dominant for the damaged levee during the consecutive high-water level event. The sequence of the events is visualized in Figure 4.21. The failure path is captured in three events: Event A, Event B and Event C.

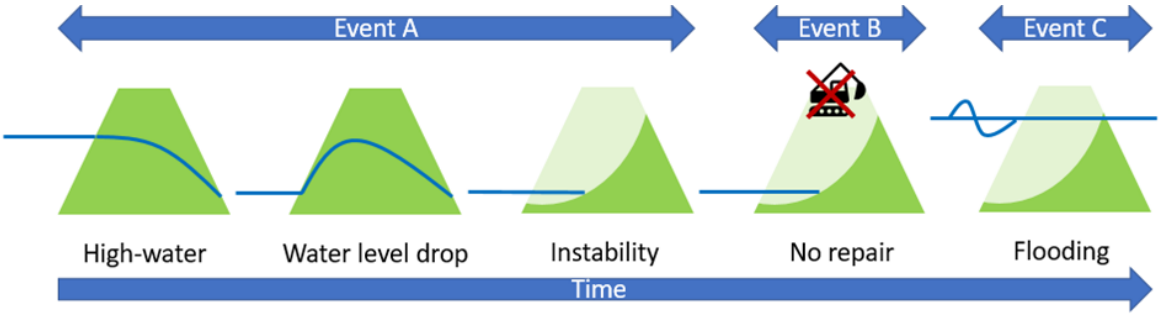

Figure 4.21 Events leading to flooding initiated by outer slope instability (Van der Meer, Teixeira, Rozing, & Kanning, 2021).

To quantify the probability of flooding for each of the three events a limit state function is defined. A limit state function, $Z = f(X)$, defines a failure criterion. Failure occurs when the result of the limit state function is smaller than zero, $Z < 0$. For stability, Event A, the limit state is calculated with a stability model (D-Stability) coupled to a groundwater flow model (D-Geo

Flow). The limit state is a function of the soil strength parameters, permeability of the levee and as boundary condition the water level development in time. The stochastic soil strength parameters and permeability are derived from lab and field measurements. The limit state of repair, Event B, is simply the time required to take emergency measures minus the time there is before the consecutive high-water. The repair time is obtained from consultations with several levee managers. The limit state for flooding during the consecutive high-water level event, Event C, is based on conservative and simplified erosion, overtopping and overflow equations. The use of simplified equations makes a detailed description of the damage unnecessary. The stochastic variables in the third limit state function are the water level and wave height. The hydraulic conditions for the three limit state functions (water level development, wave conditions, interarrival time of consecutive high-water level events) and their correlations are derived from measured water level data and hydraulic models. Having the three limit state functions and the correlations between the stochastic variables, the probability of flooding can simply be obtained with a Monte Carlo Importance Sampling Simulation or a Surrogate Model.

4.2.2 Example of slope instability for the inner slope of a levee or embankment from the Netherlands

Contribution by Deltares, Netherlands.

The figure below illustrates several parallel paths by which slope instability can lead to breaching of a levee (Deltares, 2016).

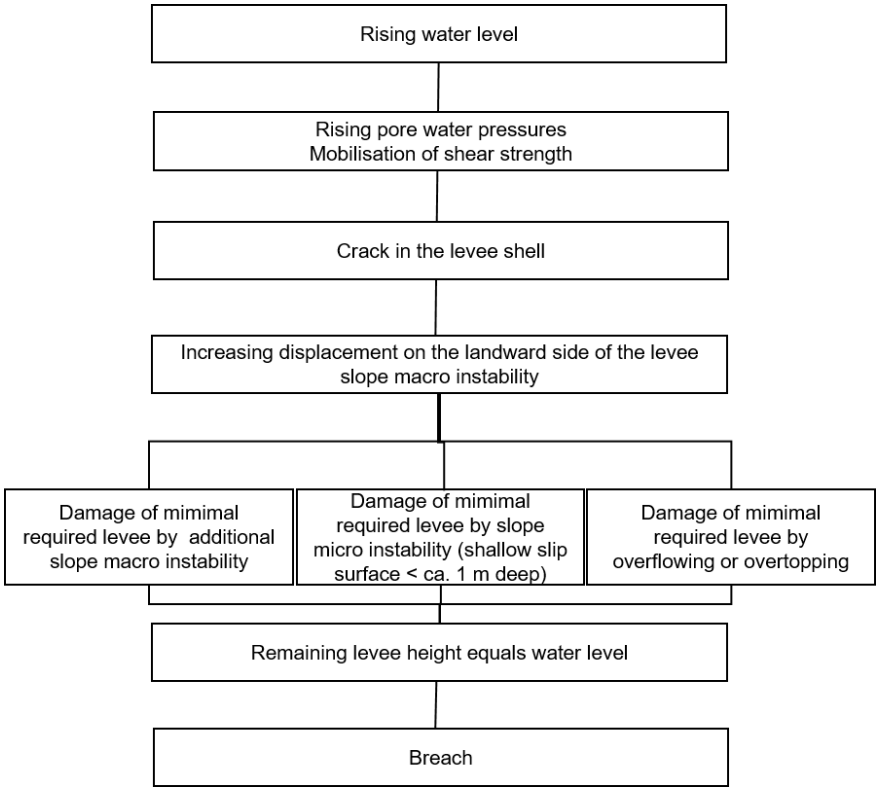

Figure 4.22 Example of a failure path for slope macro instability; sliding surface with a depth larger than ca. 1 m of the inner slope, as used in the Netherlands for assessment and design. This path is a modification of failure path in (Deltares, 2016). Assessment calculations are made for the nodes 'Increasing displacement on the landward side of the levee, slope macro instability'. The extent of damage after the first slope instability will also depend on the extent of the first slope instability. If the first sliding surface is relatively smaller, the follow-up mechanisms will also likely be less severe.

4.2.3 Pipe line failure in combination with hydraulic loading and slope instability from the Netherlands

Contribution by A.W. van der Meer MSc (Deltares, Geotechnical Risk and Reliability)

Pipeline failure can cause large erosion craters or leaking pipelines can increase the pore water pressures in a levee. Pipelines following the same trajectory as a levee or crossing a levee perpendicular can thus significantly impact the probability of flooding. An integral failure analysis of pipelines in flood defences is presented in (Van der Meer, Schweckendiek, Kruse, & Schelfhout, 2019). The assessment framework is based on an event tree with several scenarios or paths resulting in the failure of the flood defence and subsequent flooding of the hinterland. The general framework used is illustrated in Figure 4.23.

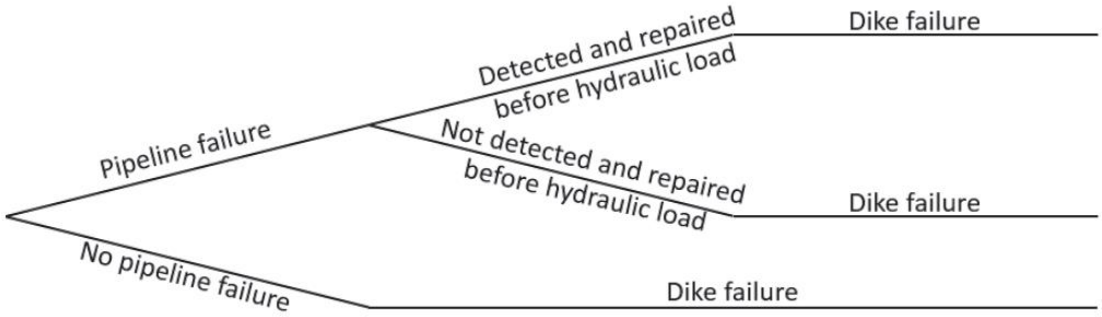

Figure 4.23 Generic approach for consecutive events leading to flooding (Van der Meer et al. 2019). The first node in the event tree is the possibility of failure of the pipeline (and alternatively no failure of the pipeline). The second is the possibility that the damage of pipeline failure (e.g. an erosion crater) is detected and repaired before a flood wave arrives. The last node is the probability of failure of the levee during this flood wave. Note that the levee can also fail when there is no failure of the pipeline or when the damage of pipeline failure is repaired before a flood wave arrives.

4.2.4 Example of instabilities (collapse or sliding) following scouring from France

Contribution by R. Tourment (INRAE, France)

The following examples (see Figure 4.24) present the consequence of scouring on the stability of the water side of a levee. In these partial failure paths, the presented scenario can be followed by more mechanisms potentially leading to a breach (internal erosion, more instabilities, …).

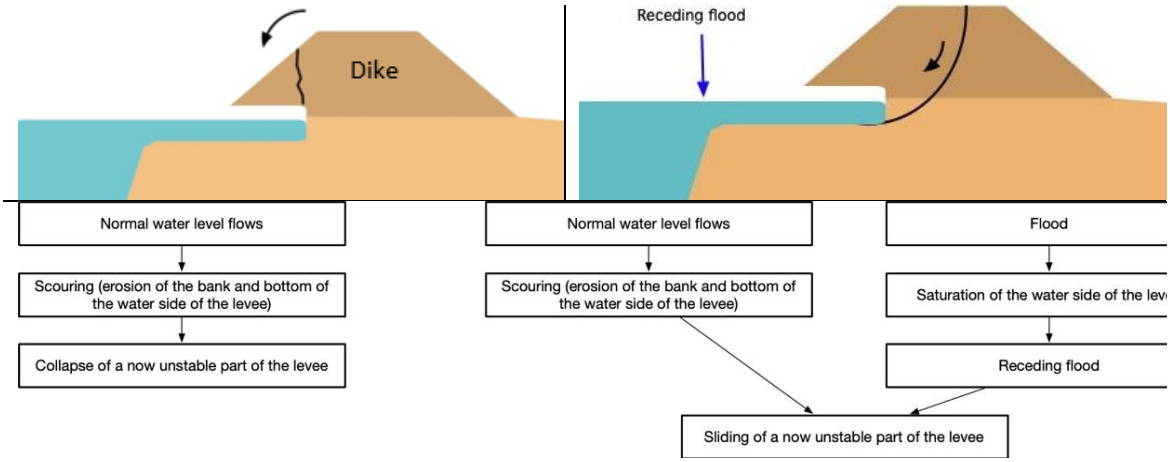

Figure 4.24 Instabilities initiated by scouring (Rémy Tourment).

4.3 Examples of Failure trees/paths involving overtopping

4.3.1 Conceptual Framework for Flood Overtopping Failure of Levee from the United States of America
Contribution by M. Sharp

Wave Overtopping
When the water surface elevation is below the levee top elevation, wave overtopping of levees may be a concern along coastal areas, lakes, wide inundation areas, etc. Typically, a significant surface area would need to be present to allow winds to develop waves that would be directed towards the levee and overtop it. For wave overtopping typically the wind and wave direction and levee slope and the local bathometry is a critical component for determining how the wave runs up the levee leading to overtopping.

Event Tree for Wave Overtopping
The example event tree described in this section is relatively simple and is typical for what would be considered for an overtopping potential failure mode. Each branch consists of five events –the pool loading, vegetation or riprap removal, headcut initiation, headcut or erosion advancing, and finally breach. In cases where debris plugging, gate failure, or wave overtopping is a concern, additional events can be added to account for the likelihood of these conditions developing. The erosion and breaching process can be subdivided into a sequence of necessary steps:

- Erosion of the surface of the downstream slope, which may consist of vegetation, riprap, or bare soil.
- Concentrated erosion on the downstream slope causing a deepening of the erosion channel until one or more headcuts are formed on the downstream slope (for conservatism, physically-based dam breach models such as WinDAM C assume that a headcut is formed at the top of the slope/downstream edge of the dam crest).
- Advancement of headcuts upstream, usually accompanied by consolidation of multiple headcuts.
- When the most upstream headcut advances through the upstream edge of the dam crest, breach is initiated, and the breach opening begins to enlarge. (After this point, intervention to save the levee is no longer possible).
- Headcuts continue to advance upstream, enlarging the breach and releasing water.
- The breach widens as long as hydraulic stresses at the sides of the breach opening are sufficient to exceed the erosion threshold of the soil.

For wave overwash, an additional node will be needed for the likelihood of waves forming sufficient height for erosion to initiate and of sufficient duration for the potential failure mode to lead to failure. Typically, in evaluation of this potential failure mode only one conditional event is typically considered beyond the loading (which considers starting reservoir water surface elevation and flood loadings for various return periods). A determination is made as to whether the levee will breach for the various loading combinations.

4.3.2 Conceptual Framework for Flood Overtopping of Levee Floodwalls from the United States of America

Contribution by M. Sharp

Floodwall Performance

Overtopping of a floodwall without the wall failing is not really a “failure” of the wall as it is simply a function of what level of protection the wall provided; thus, the wall performed its intended function but was simply not constructed high enough to contain the flood event. Additionally, floodwalls that are overtopped and subsequently failed likely performed their intended function since they held for water elevations up to the top of the wall, but if the failure occurs after overtopping then impacts can be more severe. Having floodwalls resilient to overtopping can reduce the risks associated with overtopping events for some flood protection projects.

Depending upon the erosion resistance of the land side soils, failure can occur quickly following overtopping or it could sustain substantial overtopping without failing. If the soil has little erosion resistance, it is possible that damaging land side scour and subsequent wall failure could occur simply due to wave overwash. There are several factors that are important to consider when evaluating overtopping risks including the exposed height of the wall, duration of the event, and type of soils on the land side face of the wall. Some walls have been designed to be more overtopping resilient by adding scour protection on the land side and transition zones between levee embankment and wall sections.

Event Tree for Levee Floodwall

An example event tree for a risk analyses of a levee floodwall is shown in Figure 4.25. The event tree presented is related to failure of an I-wall. Branches associated with the seepage/piping under either a T-wall or I-wall are not depicted for clarity. It is important to note that exceeding the limit state for global instability or excessive moment/shear does not necessarily lead to breaching of the floodwall. There are usually additional resisting forces, such as side friction between monoliths, which are not considered as part of simplified 2D analysis. These additional resisting forces should be considered as part of a risk analysis, however, if they are likely to exist. Analytical computations from a Monte Carlo risk analysis model can be used to help statistically estimate probabilities and probability ranges for branches associated with limit state exceedance. Elicitation-based approaches are usually used for estimating branch probabilities for branches following the limit state branches.

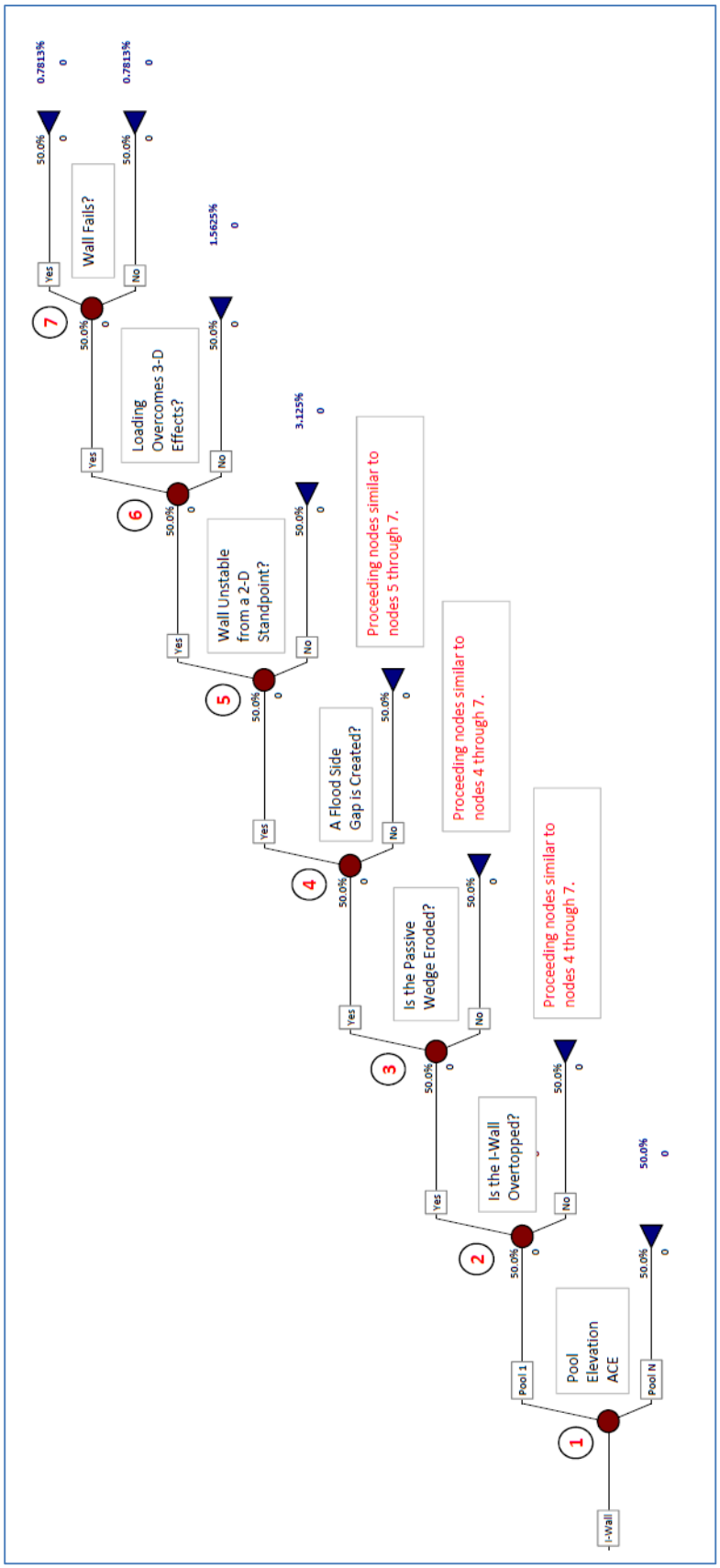

Figure 4.25 Example event tree for failure of an I-wall.

4.4 Example of Failure trees/paths involving revetments damage from the Netherlands

Contributions by Deltares, Netherlands

Damage of revetments can be an initiator of failure as this allows the erosion of underlying material and subsequently of the embankment body. The following examples show various failure paths that have been constructed for analysis of different types of revetment (Deltares, 2018).

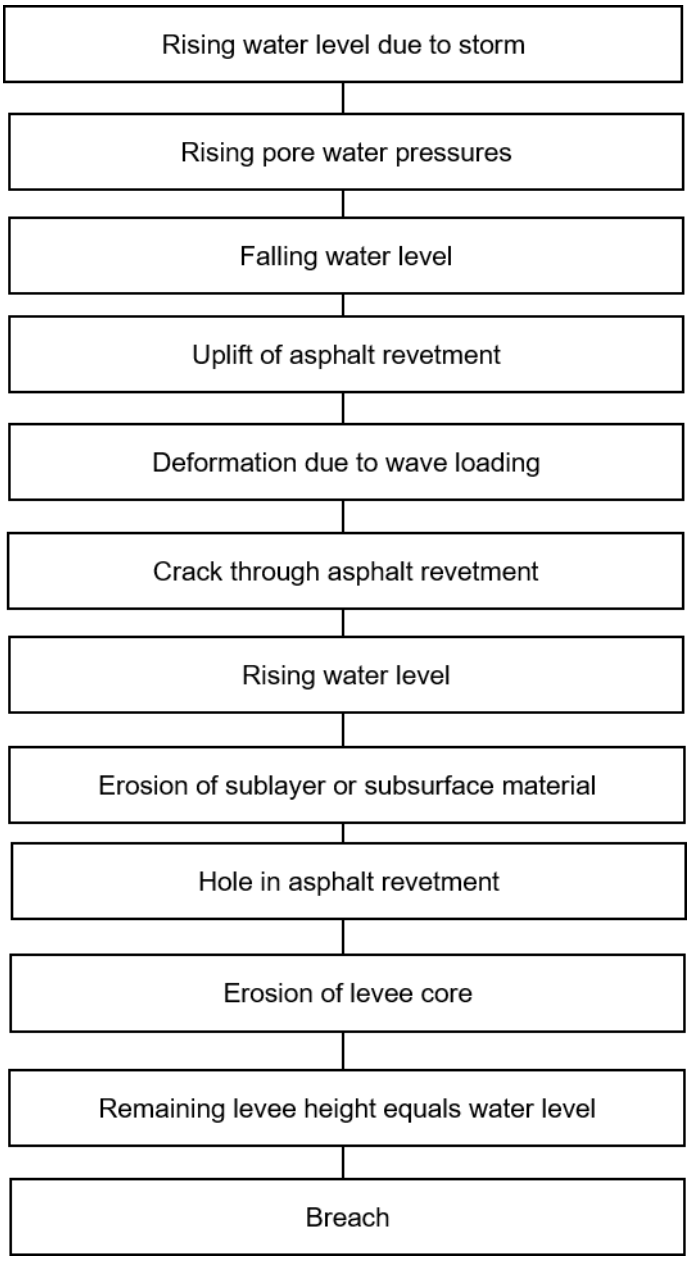

Figure 4.26 Failure path for asphalt revetment due to uplift of the revetment on the outer slope, modification of failure path in Deltares (2018).

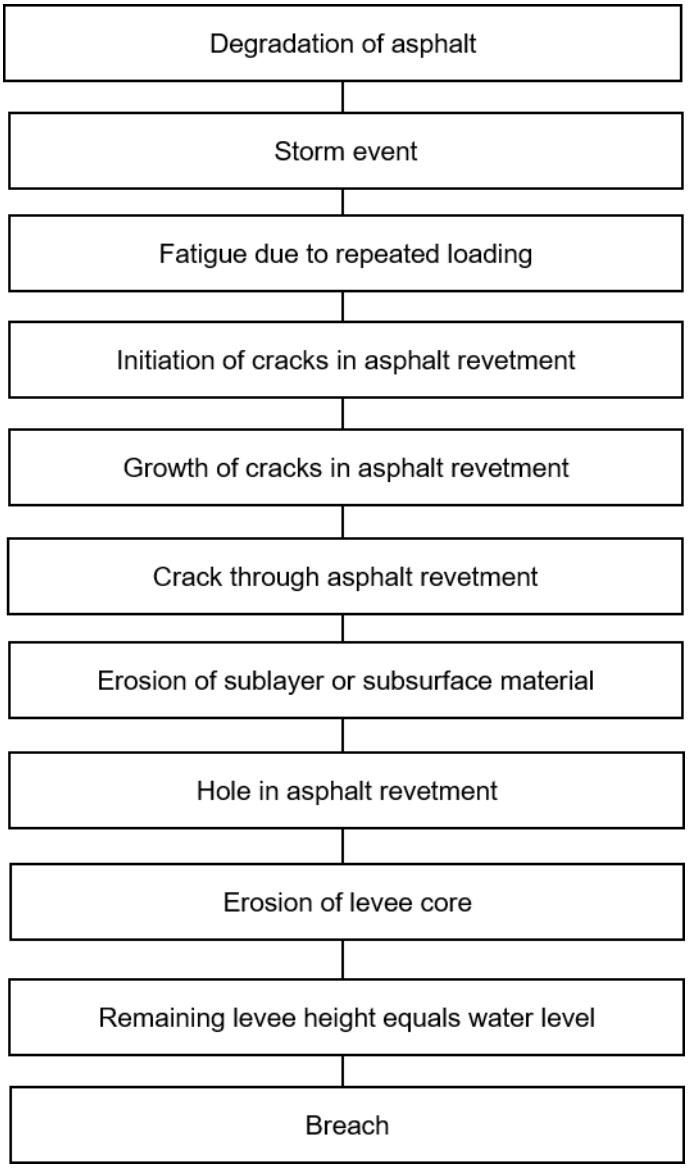

Figure 4.27 Failure path for asphalt revetment due to wave loading on the outer slope, modification of failure path in Deltares (2018).

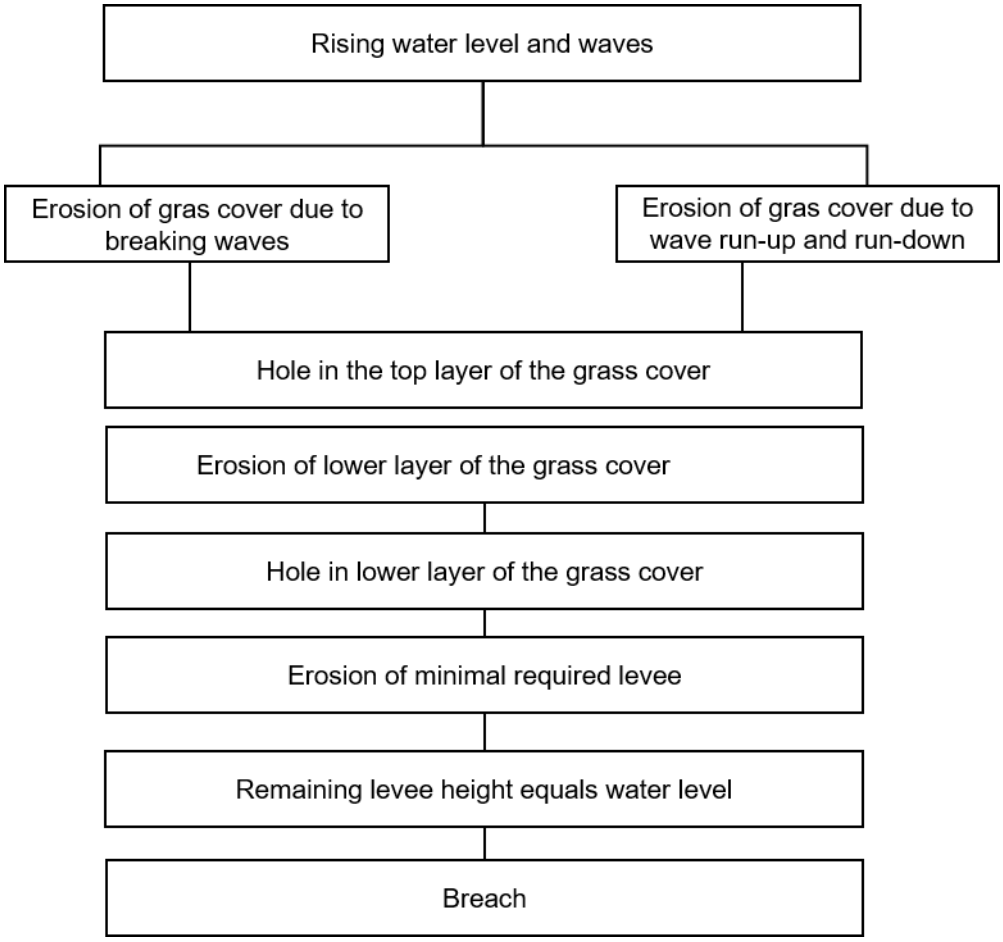

Figure 4.28 Failure path for grass cover by erosion due to wave action on the outer slope, modification of failure path in Deltares (2018).

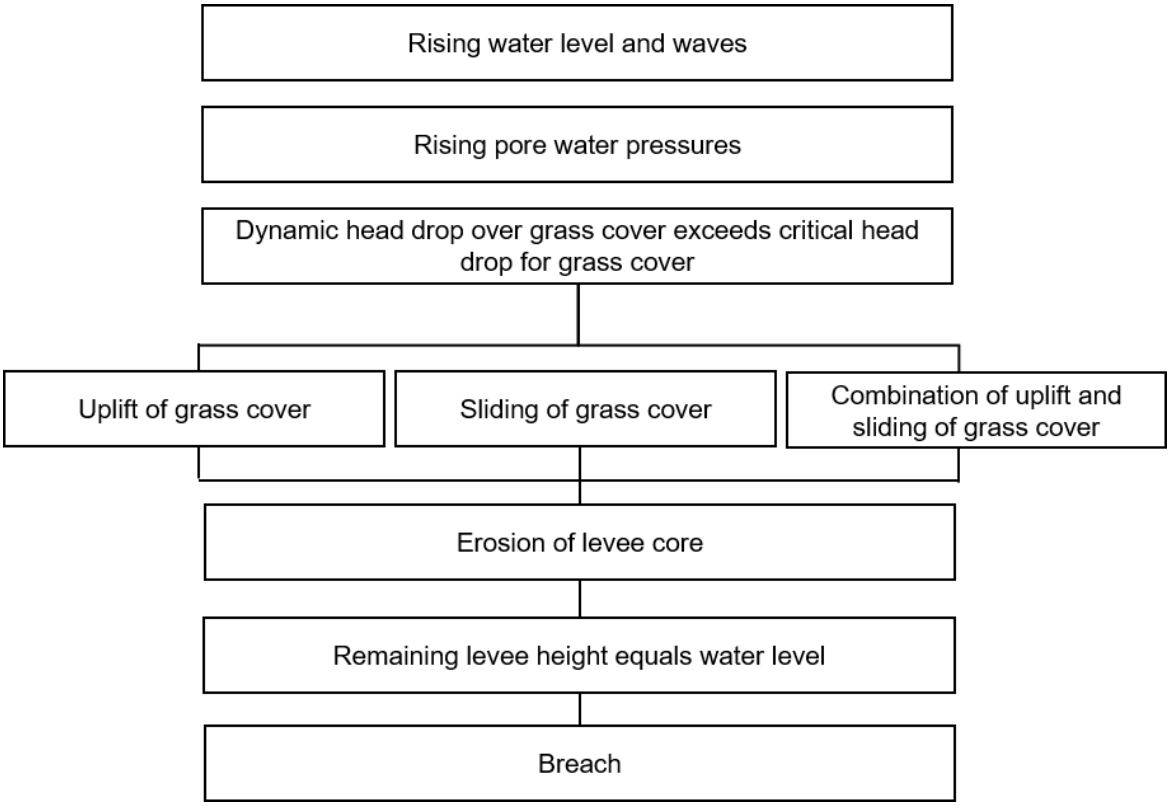

Figure 4.29 Failure path for grass cover due to high pore pressures on the outer slope, modification of failure path in Deltares (2018).

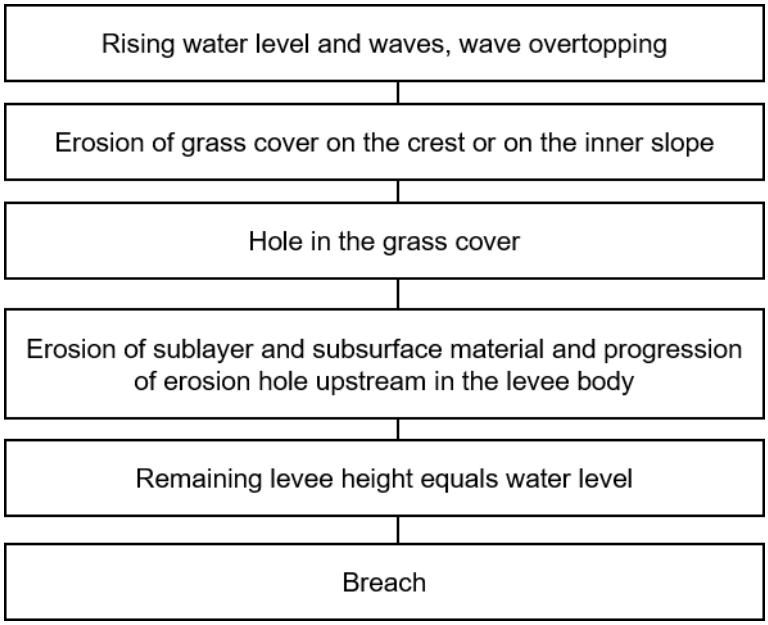

Figure 4.30 Failure path for grass cover by erosion due to overtopping on the inner slope, modification of failure path in Deltares (2018).

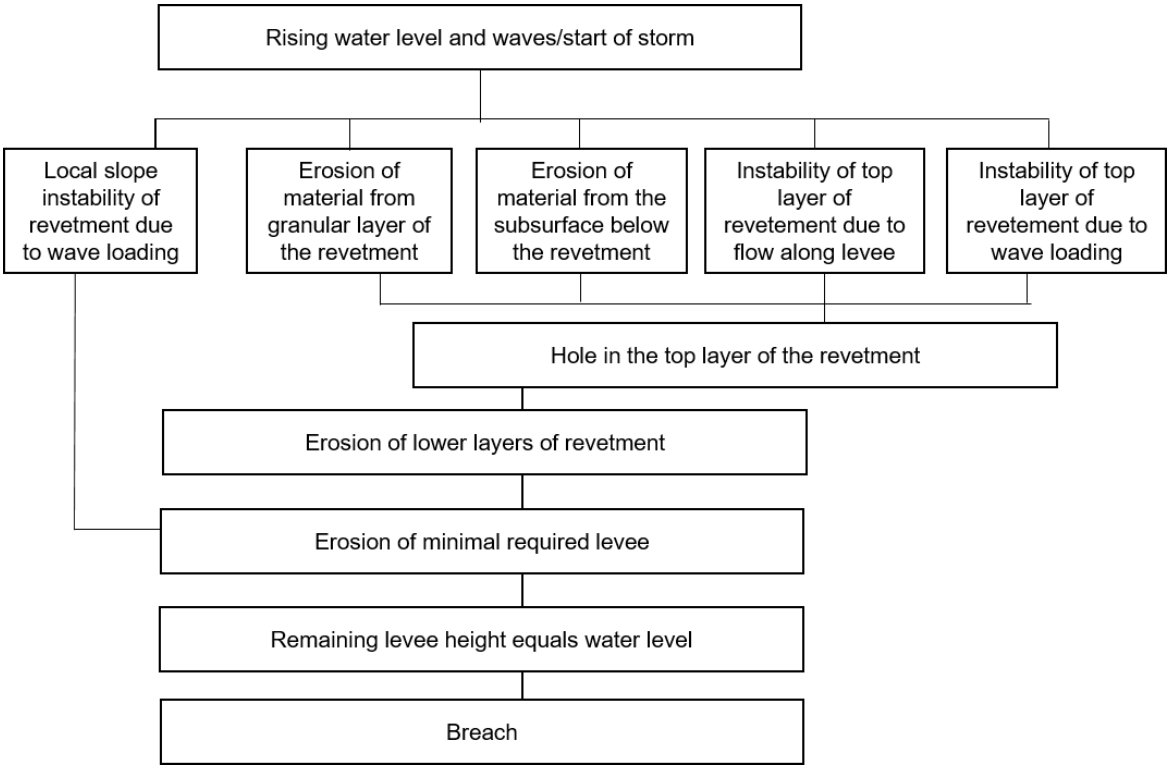

Figure 4.31 Failure path for stone revetment (revetment consisting of top layer of stone, granular layer, geotextile and lower layer usually consisting of clay but can also be a broadly graded material), modification of failure path in Deltares (2018).

5 References

Alhasan, Z., Duchan, D., & Říha, J. (2019). Influence of Surface Lining Type on the Probability of Dike Breaching Due to Overtopping. *Journal of Flood Risk Management, 17*, 1–13. Retrieved from https://doi.org/10.1111/jfr3.12534

Benedek, J. (1932). A strange dyke failure. *Vízügyi Közlemények*, 254-255.

Bezuijen, A., Kruse, G., & Van, M. (2005). Failure of peat Dikes in the netherlands. *16th Int. Conf. On Soil Mechanics and geotechnical Engineering. 3*, pp. 1857-1860. Osaka: Millpress.

CIRIA, French Ministry of Ecology, and USACE. (2013). *The International Levee Handbook.* London. Retrieved from www.ciria.org

Deltares. (2016). *WBI - Onzekerheden Overzicht van Belasting- En Sterkteonzekerheden in Het Wettelijk Beoordelingsinstrumentarium.*

Deniaud, Y., van Hemert, H., McVicker, J., Bernard, A., Beullac, B., Tourment, R., . . . Simm, J. (2013). *Functions, forms and failure of levees.* CIRIA.

Dunbar, J., Torrey, V., & Wakeley, L. (1999). *A Case History of Embankment Failure: Geological and Geotechnical Aspects of the Celotex Levee Failure, New Orleans, Louisiana. Technical Report GL-99-11.* Vicksburg, MS, USA: Waterways Experiment Station, US Corps of Engineers.

Fannin, R., Slangen, A., Mehdizadeh, A., Disfani, M., Arulrajah, A., & Evans, R. (2015). Discussion: On the distinct phenomena of suffusion and suffosion. *Géotechnique Letters 5*, 129-130.

Fehér, Á. (1973). *Improvement of river dyke stability.* VITUKI research report.

Fell, R., Foster, M., Davidson, R., Cyganiewicz, J., Sills, G., & Vroman, N. (2008). *A Unified Method for Estimating Probabilities of Failure of Embankment Dams by Internal Erosion and Piping.* University of New South Wales, The School of Civil and Environmental Engineering. Sydney: UNICIV Report R 446. Retrieved from www.engineering.unsw.edu.au/civil-engineering/uniciv-reports

Foster, M. (1999). *PhD Thesis: The probability of failure of embankment dams by internal erosion and piping.* School of Civil and Environmental Engineering. Sydney: The University of New South Wales.

Foster, M., & Fell, R. (1999). *A framework for estimating the probability of failure of embankment dams by piping using event tree methods.* The University of New South Wales, School of Civil and Environmental Engineering. Sidney: UNICIV Report No. R-377. Retrieved from www.engineering.unsw.edu.au/civil-engineering/uniciv-reports

Foster, M., & Fell, R. (2001). Assessing embankment dams, filters who do not satisfy design criteria. *Geotechnical and Geoenvironmental Engineering*.

Galli, L. (1955). Seepage phenomena along flood protection dams . *Vízügyi Közlemények*, 1-2.

Garai, J. (2016). Hydraulic failure by heave and piping. *Eighth International Conference on Scour and Erosion (ICSE-8)* (pp. 427-431). London: Taylor & Francis Group.

GeoDelft. (2003a). *Rapport CO-123456/123.* Hilversum.: GeoDelft report CO-123456/890 for AKG.

GeoDelft. (2003b). *Rapport CO-123456/123.* Delft: GeoDelft report CO-123456/890 for Schieland.

Horváth, E. (2001). A tiszasasi buzgár. *Hidrológiai közlöny, 81*(3), 177-188.

ICOLD. (2015). *Internal erosion of existing dams, levees and dikes, and their foundations bulletin n°164 – Volume 1.* Internal erosion processes and engineering assessment.

ICOLD. (2019). *Presentations from ICOLD Internal Erosion Workshop on Friday, June 14.* Ottawa. Retrieved from

https://www.dropbox.com/sh/edmgxdgr2cjdd6y/AAC3MzUDpQD2l_XPPvOPv_u3a?dl=0

Imre, E. (1995). Characterization of dispersive and piping soils. *XI. ECSMFE*, (pp. 49-55). Copenhague.

Imre, E., & Rétháti, L. (1991). *Complex geotechnical examination of river dykes.* OTKA research project.

Imre, E., & Telekes, G. (2002). Seepage in river dykes. *3rd International Conference on Unsaturated Soils*, (pp. 799-804). Recife.

Imre, E., Lörincz, J., Szendefy, J., Trang, P. Q., Nagy, L., Singh, V. P., & Fityus, S. (2012). Case Studies and Benchmark Examples for the Use of Grading Entropy in Geotechnics. *Entropy, 14*(6), 1079-1102.

Imre, E., Lorincz, J., Trang, P., Barreto, D., Goudarzy, M., Rahemi, N., . . . Schanz, T. (2019). A note on seismic induced liquefaction. *VII ECSMGE*, (pp. 979-988).

Imre, E., Nagy, L., Lörincz, J., Rahemi, N., Schanz, T., Singh, V., & Fityus, S. (2015). Some comments on the entropy-based criteria for piping. *Entropy, 17*(4), 2281--2303.

Jefferies, M., & Been, K. (2016). Soil liquefaction, a critical state approach, 2nd edition. *Taylor and Francis*.

Julínek, T., Duchan, D., & Říha, J. (2020). Mapping of Uplift Hazard Due to Rising Groundwater Level during Floods. *Journal of Flood Risk Management, 13*(4), 1–13. Retrieved from https://doi.org/10.1111/jfr3.12601

Koenders, M., & Sellmeijer, J. (1992). Mathematical model for piping. *Journal of Geotech. Eng., 118*(6), 943-946.

Lampl, H. (1959). Buzgárképződés és talajtörés. *Vízügyi Közlemények, 41*(1), 25-49.

Lőrincz, J. (1993). On particle migration with the help of grading entropy. *Filters in Geotechnical and Hydraulic Engineering*, 63-65.

Mallet, T., & Fry, J. (2016). Probability of failure of an embankment by backward erosion using the formulas of Sellmeijer and Hoffmans. *ICOLD Johannesburg International Symposium.*

Mallet, T., Dast, C., Requi, M., Chardès, C., Castagnet, A., & Fry, J. (2018). Etude de dangers du système d'endiguement rive gauche du delta du Rhône. *ICOLD Vienna Congress.*

Mallet, T., Fry, J., Tourment, R., & Mériaux, P. (2019). Accidentologie des digues du delta du Rhône de 1840 à nos jours. *Digues maritimes et fluviales de protection contre les inondations – 3ème colloque national.* Aix-en-Provence.

Mallet, T., Outalmit, K., & Fry, J. (2014). Probability of failure of an embankment by internal erosion using the Hole Erosion Test. *ICOLD BALI International Symposium*.

Mastbergen, D., Beinssen, K., & Nédélec, Y. (2019). Watching the beach steadily disappearing: the evolution of understanding of Retrogressive Breach Failures. *Journal of Marine Science and Engineering, 7*(10), 368. doi:10.3390/jmse7100368

Mallet, T. (2019). Internal Erosion Workshop. ICOLD Ottawa

Mastbergen, D., Van den Ham, G., Cartigny, M., Koelewijn, A., de Kleine, M., Clare, M., . . . Vellinga, A. (2016). Multiple flow slide experiment in the Westerschelde Estuary, The Netherlands. In G. Lamarche, J. Mountjoy, S. Bull, T. Hubble, S. Krastel, E. Lane, . . . S. Woelz, *Submarine Mass Movements and Their Consequences, Advances in Natural and Technological Hazards Research* (Vol. 41, pp. 241-249). Springer. Retrieved from http://dx.doi.org/10.1007/978-3-319-20979-1_24

Ministerie van Verkeer en Waterstaat. (2007). *Voorschrift Toetsen op Veiligheid Primaire Waterkeringen.*

Morris, M., Benahmed, N., Philippe, P., Royet, P., Tourment, R., van den Ham, G., . . . Van, M. (2012). FloodProBE report WP 3: Reliability of Urban Flood Defences - D3.1 Guidance on improved performance of urban flood defences. Retrieved from http://www.floodprobe.eu/document-details.asp?ID=869

Nagy, L. (2014). Buzgárok az árvízvédelemben. *Országos Vízügyi Föigazgatóság*, 234.

NF EN 61508 . (2002). *Sécurité fonctionnelle des systemes électriques/électroniques/électroniques programmables relatifs a la sécurité.*

Říha, J. (2007). Two Examples of the Failures of the Inundation Levees. *The content of this paper is the part of the research supported by the Grant Agency of the Czech Republic, project No. 103/05/2391*.

Říha, J., & Jandora, J. (2007). The Failure of the Inundation Levee of Cep Sand Pit. *The content of this paper is a part of the research supported by the Grant Agency of the Czech Republic, project No. 103/05/2391*.

Říha, J., Kotaška, S., & Petrula, L. (2020). Dam Break Modeling in a Cascade of Small Earthen Dams: Case Study of the Cizina River in the Czech Republic. *Water, 12*(8). Retrieved from https://doi.org/10.3390/w12082309

Rosenbrand, E., Knoeff, J., Hijma, M., & Van Onselen, C. (2020). *Gebiedsspecifieke Faalpaden Voor Piping (Concept).*

Sellmeijer, H., de la Cruz, J. L., van Beek, V., & Knoeff, H. (2011). Fine-tuning of the backward erosion piping model through small-scale, medium-scale and IJkdijk experiments. *European Journal of Environmental and Civil Engineering, 15*(8), 1139-1154.

Sellmeijer, J. B. (1988). On the mechanism of piping under impervious structures.

Silvis, F., & De Groot, M. (1995). Flow slides in the Netherlands: experience and engineering practice. *Canadian Geotechnical Journal, 32*, 1086-1092.

Szepessy, J. (1983). Tunnel erosion and liquefaction of granular and plastic soils in river dikes. *Hidrológiai Közlöny*.

Szepessy, J., & Fehér, Á. (1981). *Research report on Hosszúfok breach.*

Szepessy, J., Bogárdi, I., & Vastagh, G. (1973). *Literature review about river dyke failures.* VITUKI research report.

Szilvássy, Z., & Vágó, I. (1967). Helyszíni tapasztalatok, elméleti megállapítások az 1965 évi szigetközi árvédekezésről. *Hidrológiai. Közlöny*, 3.

The 1965 flood. (n.d.). *Vízügyi Közlemények special issue*.

Torrey, V., Dunbar, J., & Peterson, R. (1988). *Retrogressive Failures in Sand Deposits of the Mississippi River Report 1: Field Investigations, Laboratory Studies, and Analysis of Hypothesized Failure Mechanism. Report 2: Empirical Evidence in Support of the Hypothesized Failure Mechanism and Developm.* Vicksburg, MS, USA: Waterways Experiment Station Corps of Engineers.

Tourment, R., Benahmed, N., Nicaise, S., Mériaux, P., Salmi, A., & Rougé, M. (2018). Lessons learned on the damage on the levees of the Agly river. Analysis of the sand-boils phenomena. *26th ICOLD Congress.* Vienna.

Tourment, R., Beullac, B., Berthelier, E., Boulay, A., Maurin, J., & Queffelean, Y. (2019). *Inondations-Analyse de risque des systèmes de protection-Application aux études de dangers.* Lavoisier.

Tourment, R., Mallet, T., Patouillard, S., & Salmi, A. (2022). Accidents and incidents on fluvial levees on the Loire, Rhône and Agly rivers, and lessons learned. *27th ICOLD Congress.* Marseille.

Tourment, R., Rulliere, A., Poulain, D., Sutter, M., Chevalier, C., Deniaud, Y., . . . Mallet, T. (2021). *Recueil de méthodes de confortement et réparations des digues de protection en remblai.*

Tournier, J., Radchenko, V., Marley, M., Tschernutter, P., Viotti, C., Dimitrov, N., . . . Hori, T. (2015). *Internal erosion of existing dams, levees, and dikes, and their foundations* (Vol. 1). CIGB ICOLD.

Van den Ham, G., De Groot, M., & Mastbergen, D. (2014). A Semi-empirical Method to Assess Flow-slide Probability. In *Submarine mass movements and their consequences,*

Advances in Natural and Technological Hazards Research (pp. 213--223). Springer. doi:10.1007/978-3-319-00972-8 19

Van der Meer, A., Schweckendiek, T., Kruse, H., & Schelfhout, H. (2019). Integral Failure Analysis of Pipelines. *Proceedings of the 7th International Symposium on Geotechnical Safety and Risk (ISGSR)*, (pp. 978–81). Taiwan. Retrieved from https://doi.org/10.3850/978-981-11-2725-0

Van der Meer, A., Teixeira, A., Rozing, A. P., & Kanning, W. (2021). Probability of flooding due to instability of the outer slope of a levee. *18th International Probabilistic Workshop, IPW 2020* (pp. 1-11). Guimaraes: Springer Science and Business Media Deutschland GmbH.

Van der Wal, M. (2020). Bank Protection Structures along the Brahmaputra-Jamuna River, a Study of Flow Slides. *Water*. Retrieved from https://doi.org/10.3390/w12092588

Van Dijk, W., Mastbergen, D., Van den Ham, G., Leuven, J., & Kleinhans, M. (2016). Location and probability of shoal margin collapses in a sandy estuary. *Earth Surface Processes and Landforms, 43*(11), 2342 – 2357.

van Esch, J., & Van, M. (2007). Geo-hydrologic design procedure for peat dikes under drying conditions. *Proc. 10th Int. Symp. Of Numerical Models in Geomechanics* (pp. 603-609). London: Taylor francis.

Van, M., Zwanenburg, C., van Esch, J., Sharp, M., & Mosher, R. (2008). Horizontal Translational Failures of Levees due to Water Filled gaps. *proceedings of 6th International Conference on Case Histories in Geotechnical Engineering.*

Yoshimine, M., Robertson, P., & Wride, C. (1999). Undrained shear strength of clean sands to trigger flow liquefaction. *Canadian Geotechnical Journal, 36*(5), 891–906.

Yoshimine, M., Robertson, P., & Wride, C. (2001). Undrained shear strength of clean sands to trigger flow liquefaction: Reply to Discussion. *Canadian Geotechnical Journal, 38*(3), 654–657.

Zwanenburg, C., López-Acosta, N. P., Tourment, R., Tarantino, A., Pozzato, A., & Pinto, A. (2018). Lessons Learned from Dike Failures in Recent Decades. *International Journal of Geoengineering Case Histories, 4*(3), 203-229. doi:10.4417/IJGCH-04-03-04

Glossary

Action	The term *action* means external phenomena that can cause movement or deformation of a structure. It includes the concepts of force and moment used in general mechanics. As stated in Eurocode 0 (EN 1990:2002), the term *action* means: a) the set of forces (loads) applied to the structure (direct action); b) the set of imposed deformations or accelerations caused for example by temperature changes, moisture variation, uneven settlement or earthquakes (indirect action). Actions can be permanent, variable or accidental. This term should not be confused with the term “effects of actions” ("sollicitation" in French) (Tourment & Beullac, 2019).
Breach	Significant structural impairment to, or collapse of, the levee resulting from hydraulic or other actions during a flood and leading to the transmission of water through the levee. An opening through the body of the levee (from one side to the other); such that the levee no longer fulfils its function (Tourment & Beullac, 2019). Any loss of material such that water could or does pass through the structure (ILH).
Damage	Significant structural impairment (but insufficient to cause a breach) resulting from hydraulic or other actions, most commonly during a flood. Damage should be repaired as soon as possible to mitigate the risk of breach during subsequent flood events.
Deterioration	A gradual decline in the condition, serviceability or strength of a levee or components of a levee by processes such as weathering, erosion or animal activity. The impact of deterioration can usually be mitigated by regular and appropriate maintenance. The process of degradation of the condition of, or the defective behaviour of, a structure (or component) from the point of view of its safety and performance (ICOLD, 1983).

Effects of Actions	*Effects of actions* is a general term that denotes internal forces, moments, stresses, and strains in structural members plus the deflection and rotation of the whole structure. [EN 1990 §1.5.3.2] In structural engineering, *effects of actions* are a function of the actions applied to a structure and that structure's dimensions, but not of material strength. Designers should verify that a composite structure should be able to resist both the direct actions and the effect of the actions. Beyond certain thresholds of resistance of the structure, *actions* can cause damage or deterioration (Tourment & Beullac, 2019).
Event	An unusual or severe incident or occurrence leading to a significant increase in loading on a structure such as an abnormal action (e.g. an excessively heavy vehicle) or an extreme environmental load (e.g. flood, earthquake, etc.).
Failure	Loss of the ability of a functional unit to perform a required function or to function as intended (NF EN 61508 , 2002). Impairment or cessation of the ability of a system to perform its required function(s) with the performance defined in the technical specifications.
Failure of a levee	In the context of this report the term failure of the levee is reserved for failure of the levee to retain water, resulting in flooding of the protected area. This differs from the exceedance of the limit state for a specific mechanism, which may indicate failure of a component of the levee whereas the levee itself still fulfils the function of retaining water.
Failure path	In this report, a failure path is considered as an entire sequence of events by which an initial event, the high-water loading, leads to flooding of the protected area. A failure path consists of a sequence of events and mechanisms.
Failure tree	Different mechanisms may occur simultaneously in time and influence each other. The term failure tree, which indicates the presence of branches, describes such situations. A failure tree may also be used to show different parallel failure paths which might or might not occur. Failure trees are usually used as part of the design process (to verify the design for each identifiable individual mechanism) or to assess the overall risk of failure of a structure (through the combination of risks associated with individual possible mechanisms or failure paths).
Flaw	An observable or quantifiable sign of deterioration in the condition of a structure or one of its components.
Initiating event	For levee systems, generally a flood or storm event that will cause retained water levels to rise significantly so as to apply increased load to the levees (see also **Event**).

Mechanism	A physical process that can directly lead to degradation, damage or collapse of a structure. Examples of mechanisms leading to the deterioration of levees include external erosion, internal erosion, desiccation cracking, slope sliding and uplift.
Partial breach	Breach through only a part of the full height of the levee (upper part or through conduit) (Tourment, et al., 2019).
Performance	The ability of a structure (or system) to perform the functions for which it was designed.
Protected Area (from flooding)	The area of land (or water) protected from flooding by the presence of an effective levee system.
Scenario	A set of events reconstructed with the different mechanisms involved in a phenomenon such as a breach or a flooding. A scenario is constructed from a diagnosis (expert analysis) of an actual event or a prediction based on analysis (e.g. FMEA). (Tourment & Beullac, 2019).
Total breach	Breach through the full height of the levee. A *total breach* can include or can cause an erosion pit in the foundation or on the landward side of the levee. (Tourment & Beullac, 2019).